Cytochrome P450-derived eicosanoids, inflammation, and atherosclerotic cardiovascular disease

Katherine N. Theken

A dissertation submitted to the faculty of the University of North Carolina at Chapel Hill in partial fulfillment of the requirements for the degree of Doctor of Philosophy in Pharmaceutical Sciences in the Eshelman School of Pharmacy (Pharmacotherapy and Experimental Therapeutics)

Chapel Hill
2011

Approved by:

Adviser: Craig R. Lee

Adviser: J. Herbert Patterson

Adviser: Howard L. McLeod

Adviser: Samuel M. Poloyac

Adviser: Jo Ellen Rodgers

Abstract

Katherine N. Theken: Cytochrome P450-derived eicosanoids, inflammation, and atherosclerotic cardiovascular disease
(Under the direction of Craig R. Lee, J. Herbert Patterson, Howard L. McLeod, Samuel M. Poloyac, and Jo Ellen Rodgers)

Inflammation contributes to the pathogenesis of atherosclerosis from the initiation of plaque formation to progression to acute coronary syndrome clinical events. Due to the divergent effects of cytochrome P450 (CYP)-derived epoxyeicosatrienoic acids (EETs) and 20-hydroxyeicosatetraenoic acid (20-HETE) in the regulation of vascular tone and inflammation, alterations in the functional balance between the CYP epoxygenase and ω-hydroxylase pathways may contribute to the pathophysiology of cardiovascular disease. The objectives of the work described in this doctoral dissertation were to characterize the effect of inflammation, metabolic dysfunction, and cardiovascular disease on the functional balance between the CYP epoxygenase and ω-hydroxylase pathways, and explore the potential of modulating CYP-mediated eicosanoid metabolism as an anti-inflammatory therapeutic strategy for atherosclerotic cardiovascular disease. Acute activation of the innate immune response altered CYP-mediated eicosanoid metabolism in a tissue- and time-dependent manner. High fat diet feeding shifted the functional balance between the pathways in favor of the CYP ω-hydroxylase pathway, suggesting that dysregulation of CYP-mediated eicosanoid metabolism contributes to the pathophysiologic consequences of the metabolic syndrome. Enalapril treatment restored the functional balance between the pathways, implicating the renin-angiotensin system in mediating high fat diet-induced alterations in CYP-mediated eicosanoid metabolism. Although 20-HETE does not contribute to the acute inflammatory response to lipopolysaccharide, inhibition of the CYP ω-hydroxylase pathway may have

therapeutic utility for the treatment of chronic vascular inflammation. CYP epoxygenase and ω-hydroxylase pathway function differed between healthy volunteers and patients with established atherosclerosis, and several clinical factors were associated with plasma levels of CYP-derived eicosanoids. Functional genetic variation in the CYP epoxygenase and ω-hydroxylase pathways was associated with survival in patients following an acute coronary syndrome, suggesting that therapies that specifically modulate CYP-mediated eicosanoid metabolism may represent a novel treatment strategy for atherosclerotic cardiovascular disease.

Acknowledgements

Completion of this dissertation would not have been possible without the important contributions of many individuals. First, I would like to thank my adviser, Craig Lee, for his mentorship and advice, as well as my dissertation committee members, Herb Patterson, Howard McLeod, Sam Poloyac, and Jo Ellen Rodgers, for their guidance. I am grateful to have had the opportunity to work with you all throughout my graduate training.

I would also like to thank my lab mates, Yangmei Deng, Bob Schuck, Alison Kannon, and Akin Oni-Orisan, for their help in designing and completing the experiments, as well as for commiserating with me when the results did not turn out as hypothesized. Special thanks to Tricia Miller at the University of Pittsburgh for performing many of the microsomal incubations, tissue extractions, and UPLC-MS/MS analyses that were integral to the preclinical studies, and to the drug development fellows, Almasa Bass, Kyle Ellis, Bryant Tran, and Savannah Steele, who were instrumental in recruiting the subjects for the case-control analysis of plasma eicosanoids. I would also like to thank our collaborators at NIEHS, Darryl Zeldin, Matt Edin, and Fred Lih, for their help with the HPLC analysis of plasma eicosanoid levels, and our collaborators for the analysis in the INFORM cohort, John Spertus, Sharon Cresci, and Philip Jones.

I am grateful for the support of my fellow graduate students, especially Christina Won and LaToya Griffin. I could not have asked for better friends with whom to share the joys and frustrations of graduate school. I would also like to acknowledge the Eshelman School of Pharmacy and the Division of Pharmacotherapy and Experimental

Therapeutics, especially Kathy Maboll and Amber Allen for their administrative support, as well as the financial support of the American Foundation for Pharmaceutical Education.

I would like to express my deepest gratitude to my family, especially my parents, Stephen and Angela Francis. Without your love and support, I would not have become the person I am today.

Most especially of all, I would like to thank my husband, Andrew, who while I was working on my Ph.D. in Pharmaceutical Sciences, more than earned his in Patience, Encouragement, and Understanding. Thank you for being my companion on this journey, my shoulder to cry on, and my greatest champion. I love you.

Table of Contents

List of Tables

List of Figures

List of Abbreviations

ACE	angiotensin converting enzyme
ACS	acute coronary syndrome
ARB	angiotensin receptor blocker
ANOVA	analysis of variance
BHT	butylated hydroxytoluene
BMI	body mass index
CABG	coronary artery bypass graft
CAD	coronary artery disease
cDNA	complementary DNA
CI	confidence interval
CTRC	Clinical and Translational Research Center
CVD	cardiovascular disease
CYP	cytochrome P450
DBP	diastolic blood pressure
DHET	dihydroxyeicosatrienoic acid
DHOME	dihydroxyoctadecenoic acid
DTT	dithiothreitol

EDTA	ethylenediaminetetraacetic acid
EET	epoxyeicosatrienoic acid
EpOME	epoxyoctadecenoic acid
HDL	high density lipoprotein
20-HEDGE	N-[20-hydroxyeicosa-6(Z),15(Z)-dienoyl]glycine
HESI	heated electrospray ionization
HET0016	N-hydroxy-N'-(4-n-butyl-2-methylphenyl) formamidine
20-HETE	20-hydroxyeicosatetraenoic acid
HPLC	high performance liquid chromatography
HR	hazard ratio
HV	healthy volunteers
HW	Hardy-Weinberg
IQR	interquartile range
LBBB	left bundle branch block
LDL	low density lipoprotein
LPS	lipopolysaccharide
MI	myocardial infarction
MS	mass spectrometry

NADPH	nicotinamide adenine dinucleotide phosphate
NF-κB	nuclear factor-κB
PCI	percutaneous coronary intervention
PI3K	phosphatidylinositol 3-kinase
PPAR	peroxisome proliferator-activated receptor
PXR	pregnane X receptor
qRT-PCR	quantitative real time polymerase chain reaction
SE	standard error
sEH	soluble epoxide hydrolase
SEM	standard error of the mean
SRM	selective reaction monitoring
Stat-1	signal transducer and activator of transcription-1
TNF-α	tumor necrosis factor-α
UPLC	ultra performance liquid chromatography
WT	wild-type

Chapter I: Introduction

Cardiovascular disease (CVD) is the leading cause of morbidity and mortality in the United States, accounting for more than 810,000 deaths in 2007. Nearly half of these deaths are attributable to coronary artery disease (CAD) and acute coronary syndromes (ACS) associated with progressive atherosclerosis [1]. Despite advances in the diagnosis, prevention, and treatment of atherosclerotic CVD, it remains a significant public health concern, and novel therapies are needed to improve outcomes.

Inflammation is integral to the development and progression of atherosclerotic CVD. Cellular adhesion molecules (CAMs) (i.e. E-selectin), chemokines (i.e. monocyte chemoattractant protein-1 (MCP-1)), and cytokines (i.e. interleukin-6 (IL-6), tumor necrosis factor-α (TNF-α)), have been detected in atherosclerotic lesions of humans and experimental animals [2]. Moreover, animals deficient in these pro-inflammatory mediators are resistant to lesion development [2]. In patients, elevated plasma levels of inflammatory biomarkers, including C-reactive protein (CRP) [3], E-selectin [4], MCP-1 [5,6], and TNF-α [7], have been associated with poor outcomes. Consequently, novel pharmacologic agents that specifically modulate vascular inflammation may offer therapeutic potential for the treatment of atherosclerotic CVD.

Cytochrome P450-mediated arachidonic acid metabolism

The role of cytochrome P450 (CYP) enzymes in drug metabolism is well-recognized; however, various CYPs also metabolize numerous endogenous substrates, including steroids, hormones, and fatty acids, to biologically active mediators. One such example is the oxidative metabolism of arachidonic acid to epoxyeicosatrienoic acids

(EETs) and hydroxyeicosatetraenoic acids (HETEs). Olefin epoxidation of arachidonic acid to four EET regioisomers (5,6-, 8,9-, 11,12-, 14,15-EET) is primarily catalyzed by CYP2J and CYP2C isoforms. Soluble epoxide hydrolase (sEH) rapidly hydrolyzes EETs to the corresponding dihydroxyeicosatrienoic acids (DHETs), which, in general, are much less biologically active. In contrast, CYP4A and CYP4F isoforms catalyze the ω-hydroxylation of arachidonic acid to 20-HETE [8,9,10] (Figure 1.1).

EETs function as endothelium-derived hyperpolarizing factors and are vasodilatory via activation of calcium-sensitive potassium (BK_{Ca++}) channels [11,12]. Potentiation of the CYP epoxygenase pathway, via enhanced CYP-mediated EET biosynthesis or inhibition of sEH-mediated EET hydrolysis, lowers blood pressure in rodent models of hypertension [13,14,15,16], and improves functional recovery following myocardial ischemia/reperfusion injury [17,18,19]. In contrast to EETs, 20-HETE is a potent vasoconstrictor [20], and promotes hypertension and endothelial dysfunction in rodents [21,22,23,24]. Furthermore, inhibition of 20-HETE formation is cardioprotective [25,26,27,28] and neuroprotective [29] following ischemic injury.

Accumulating evidence suggests that the CYP epoxygenase and ω-hydroxylase pathways are involved in the regulation of inflammation. EETs possess potent anti-inflammatory properties by attenuating cytokine-induced leukocyte adhesion to the vascular wall via inhibition of nuclear factor-κB (NF-κB) activation [30], a well-characterized initiating event of pro-inflammatory signaling and atherosclerotic lesion development [31]. EETs also activate peroxisome proliferator-activated receptor-α (PPAR-α)) [32] and PPAR-γ [33], transcription factors which inhibit NF-κB activation. Conversely, 20-HETE induces expression of CAMs and cytokines via NF-κB activation, thereby promoting inflammation [34]. 20-HETE also stimulates production of reactive oxygen species in endothelial cells via activation of NADPH oxidase [35] and promotes endothelial nitric oxide synthase uncoupling [36,37]. These observations suggest that

modulating CYP-mediated eicosanoid metabolism may be a novel anti-inflammatory therapeutic strategy, but the functional role of the CYP epoxygenase and ω-hydroxylase pathways in the regulation of vascular inflammation *in vivo* has not been investigated.

CYP expression and metabolic activity in the presence of inflammation and metabolic dysfunction

It is well-established that acute inflammatory stimuli alter hepatic CYP expression *in vitro* and *in vivo*. Cytokines suppress hepatic CYP expression via a pretranslational mechanism, thereby decreasing xenobiotic metabolism and clearance in preclinical models and humans [38,39,40]. In human hepatocyte culture, direct administration of IL-6, interleukin-1β (IL-1β), and TNF-α significantly decreases CYP1A2, CYP2C, CYP2E1, and CYP3A mRNA and metabolic activity [41]. Similarly, systemic lipopolysaccharide (LPS) treatment induces cytokine expression and significantly suppresses hepatic CYP2A, CYP2C, CYP2E, and CYP3A expression in rodents *in vivo* [42,43]. Although the effect of inflammation has not been rigorously characterized in extrahepatic tissues, studies to date suggest that pulmonary CYP2C and CYP2J expression and activity are suppressed in rat models of sepsis [44] and *Pseudomonas* pneumonia [45,46].

In contrast to other CYPs, CYP4A and CYP4F isoforms can be induced in the presence of inflammation, although the effects are isoform- and tissue-specific. In rats, systemic administration of LPS significantly induced hepatic [42] and renal [47] CYP4A expression. However, LPS treatment suppressed hepatic *Cyp4a*, but significantly induced renal *Cyp4a10* in mice [43]. Direct cytokine administration and systemic LPS treatment significantly induced *CYP4F5* mRNA expression in cultured rat hepatocytes [48] and in rat liver tissue [49], respectively. In contrast, hepatic *CYP4F4* expression was suppressed by LPS treatment *in vivo*, and no alterations in renal *CYP4F* expression were observed [49]. Pulmonary *CYP4A* mRNA expression was markedly induced in a

rat model of sepsis [44] and in mice following systemic IL-1β administration [50]. Similarly, pulmonary CYP4F expression was induced in the presence of inflammation secondary to traumatic brain injury in rats [51].

CYP expression and metabolic activity is also altered in preclinical models of obesity and metabolic syndrome. Hepatic CYP2C is suppressed in obese Zucker rats [52] and in high fat diet-fed mice [53], while *db/db* mice exhibit higher hepatic *Cyp2c29* mRNA levels and metabolic activity [54,55], relative to lean controls. In kidney, CYP epoxygenase expression and metabolic activity was suppressed in high fat diet-fed rats [56,57], obese Zucker rats [58,59] and heme oxygenase-2-deficient mice [60]. In contrast, hepatic CYP4A expression was significantly higher in both obese Zucker rats [61] and *db/db* mice [54,55], relative to lean controls. Hepatic Cyp4a protein expression was induced in mice continuously fed a high fat diet [62], but renal tubular CYP ω-hydroxylase expression and metabolic activity were suppressed in high fat diet-fed rats [56,57]. Collectively, these studies demonstrate that inflammation and metabolic dysfunction alter CYP expression and metabolic activity. However, the effects of these stimuli on CYP epoxygenase and ω-hydroxylase pathway function have not been rigorously characterized.

CYP-mediated eicosanoid metabolism in humans

Although numerous preclinical studies have demonstrated that CYP-mediated eicosanoid metabolism is important in the maintenance of cardiovascular homeostasis following a pathologic insult, few studies have directly assessed CYP epoxygenase and ω-hydroxylase pathway function in humans. One small study found that plasma 20-HETE concentrations correlated with plasma renin activity and were significantly higher in individuals with renovascular disease, compared to healthy controls. Plasma EET levels tended to be lower in renovascular disease patients, but this finding was not

statistically significant [63]. Urinary 20-HETE levels have been shown to correlate with body mass index [64,65], and higher plasma and urinary 20-HETE concentrations have been reported in individuals with metabolic syndrome compared to healthy controls [66]. These studies suggest that CYP-mediated eicosanoid metabolism may be altered in the presence of cardiovascular and metabolic disease in humans, but CYP epoxygenase and ω-hydroxylase pathway function in CAD patients has not been characterized.

Pharmacologic agents that specifically modulate CYP-mediated eicosanoid metabolism are not approved for use in humans; thus, the therapeutic utility of directly manipulating the CYP epoxygenase and ω-hydroxylase pathways in patients with atherosclerotic CVD has not been investigated. Epidemiologic studies have been conducted to initially characterize the relationship between functional genetic variants in the CYP epoxygenases (*CYP2J2*, *CYP2C8*), sEH (*EPHX2*), and the CYP ω-hydroxylases (*CYP4A11*, *CYP4F2*) and cardiovascular disease susceptibility in humans. A *CYP2J2* proximal promoter polymorphism (*-50G>T*), which decreases *CYP2J2* mRNA expression and plasma EET levels, has been associated with significantly greater risk of CAD [67] and prevalent myocardial infarction (MI) [68]. Genetic variation in *CYP2J2* and *CYP2C8* has also been shown to influence risk of incident CAD events [69]. The *EPHX2* Arg287Gln variant has been associated with coronary artery calcification [70], an established measure of subclinical atherosclerotic burden. Another *EPHX2* variant, Lys55Arg, has been associated with higher apparent sEH activity *in vivo* and increased risk of incident CAD [71] and ischemic stroke [72]. Nonsynonymous polymorphisms in *CYP4A11* (Phe434Ser) and *CYP4F2* (Val433Met) have been associated with increased risk of hypertension [73,74,75,76,77,78], and the CYP4F2 Val433Met polymorphism has been associated with ischemic stroke [79]. However, the relationship between genetic variation in *CYP4A11* and *CYP4F2* and CAD has not been evaluated to date. These results suggest that alterations in CYP-mediated eicosanoid metabolism may influence

cardiovascular disease risk in humans, but some inconsistent relationships have been observed across studies. Of note, all studies to date have evaluated the relationship between these polymorphisms and CVD susceptibility. Because the CYP epoxygenase pathway is believed to function as a reserve system to nitric oxide, functional genetic variants in the CYP epoxygenases or *EPHX2* may be most influential in individuals with endothelial dysfunction, a key process in the pathophysiology of CVD that has been ascribed to impaired nitric oxide biosynthesis [80]. Moreover, numerous preclinical studies have demonstrated that the CYP epoxygenase and ω-hydroxylase pathways are important in the maintenance of cardiovascular homeostasis following pathologic insult [8,9,10]. Therefore, the clinical impact of polymorphisms that result in altered EET or 20-HETE levels may be most pronounced in individuals with underlying atherosclerotic CVD. However, the relationship between genetic variation in the CYP epoxygenase and ω-hydroxylase pathways and prognosis in patients with established CAD has not been evaluated to date.

Perspective

Atherosclerotic CVD is a leading cause of death in the United States, and novel therapies are needed to decrease morbidity and mortality. Inflammation contributes to the pathogenesis of atherosclerosis from the initiation of plaque formation to progression to ACS clinical events. Due to the divergent effects of CYP-derived EETs and 20-HETE in the regulation of vascular tone and inflammation, alterations in the functional balance between the CYP epoxygenase and ω-hydroxylase pathways may contribute to the pathophysiology of cardiovascular disease. However, studies investigating the effects of inflammation and metabolic dysfunction on CYP-mediated eicosanoid metabolism remain necessary. Moreover, EETs and 20-HETE regulate inflammation *in vitro,* but additional studies are necessary to demonstrate that potentiation of the CYP

epoxygenase pathway and/or inhibition of the CYP ω-hydroxylase pathway attenuates vascular inflammation *in vivo*. Few studies have evaluated CYP epoxygenase and ω-hydroxylase pathway function in humans, and CYP-mediated eicosanoid metabolism has not been characterized in CAD patients. Furthermore, additional studies are needed to evaluate the association between genetic variation in the CYP epoxygenase and ω-hydroxylase pathways and CVD prognosis, and potentially identify subsets of the population who will most benefit from therapies that modulate these pathways.

Specific Aims

Aim #1: Characterize the effect of acute inflammation and high fat diet-induced metabolic dysfunction on the expression and function of the CYP epoxygenase and ω-hydroxylase pathways *in vivo*.

Hypothesis: Acute inflammation and metabolic dysfunction will result in lower levels of EETs and higher levels of 20-HETE due to suppression of CYP epoxygenase (CYP2J, CYP2C) and induction of CYP ω-hydroxylase (CYP4A, CYP4F) expression via a pretranslational mechanism.

Aim #2: Determine the therapeutic effect of pharmacologic inhibition of the CYP ω-hydroxylase pathway on acute vascular inflammation *in vivo*.

Hypothesis: Inhibition of CYP-mediated 20-HETE biosynthesis or the putative 20-HETE receptor will attenuate the acute inflammatory response to LPS *in vivo* by inhibiting NF-κB activation.

Aim #3: Evaluate the contribution of phenotypic and genotypic variation in the CYP epoxygenase and ω-hydroxylase pathways to the pathogenesis of cardiovascular disease in humans.

Hypothesis: Patients with established atherosclerotic CVD will have lower levels of EETs and higher levels of 20-HETE in plasma compared to healthy controls. Genetic variation in the CYP epoxygenase and ω-hydroxylase pathways will be associated with 5-year survival in patients with acute coronary syndromes.

Figure 1.1: The CYP epoxygenase and ω-hydroxylase pathways

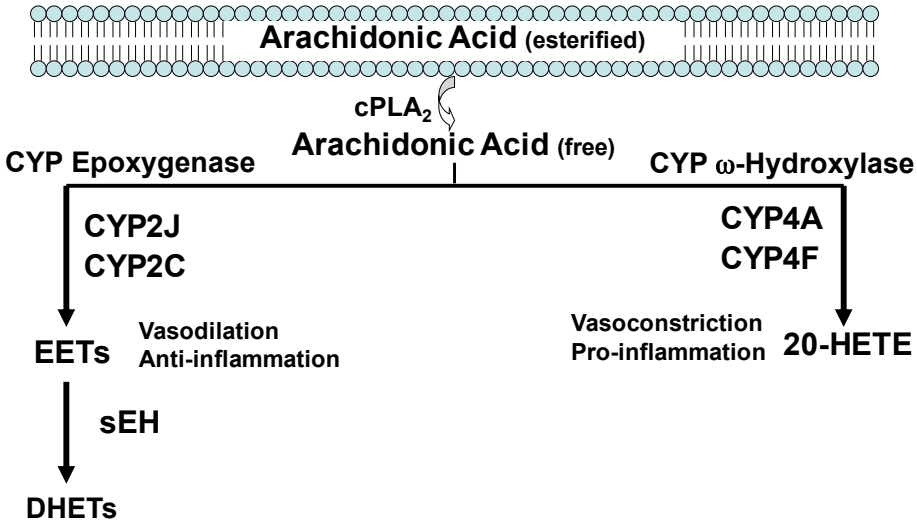

References

1. Roger VL, Go AS, Lloyd-Jones DM, Adams RJ, Berry JD, et al. (2011) Heart disease and stroke statistics--2011 update: a report from the American Heart Association. Circulation 123: e18-e209.

2. Libby P, Ridker PM, Maseri A (2002) Inflammation and atherosclerosis. Circulation 105: 1135-1143.

3. Libby P, Ridker PM (2004) Inflammation and atherosclerosis: role of C-reactive protein in risk assessment. Am J Med 116 Suppl 6A: 9S-16S.

4. Kavsak PA, Ko DT, Newman AM, Palomaki GE, Lustig V, et al. (2008) "Upstream markers" provide for early identification of patients at high risk for myocardial necrosis and adverse outcomes. Clin Chim Acta 387: 133-138.

5. de Lemos JA, Morrow DA, Sabatine MS, Murphy SA, Gibson CM, et al. (2003) Association between plasma levels of monocyte chemoattractant protein-1 and long-term clinical outcomes in patients with acute coronary syndromes. Circulation 107: 690-695.

6. Kavsak PA, Ko DT, Newman AM, Palomaki GE, Lustig V, et al. (2007) Risk stratification for heart failure and death in an acute coronary syndrome population using inflammatory cytokines and N-terminal pro-brain natriuretic peptide. Clin Chem 53: 2112-2118.

7. Ridker PM, Rifai N, Pfeffer M, Sacks F, Lepage S, et al. (2000) Elevation of tumor necrosis factor-alpha and increased risk of recurrent coronary events after myocardial infarction. Circulation 101: 2149-2153.

8. Roman RJ (2002) P-450 metabolites of arachidonic acid in the control of cardiovascular function. Physiol Rev 82: 131-185.

9. Zeldin DC (2001) Epoxygenase pathways of arachidonic acid metabolism. J Biol Chem 276: 36059-36062.

10. Deng Y, Theken KN, Lee CR (2010) Cytochrome P450 epoxygenases, soluble epoxide hydrolase, and the regulation of cardiovascular inflammation. J Mol Cell Cardiol 48: 331-341.

11. Campbell WB, Gebremedhin D, Pratt PF, Harder DR (1996) Identification of epoxyeicosatrienoic acids as endothelium-derived hyperpolarizing factors. Circ Res 78: 415-423.

12. Fisslthaler B, Popp R, Kiss L, Potente M, Harder DR, et al. (1999) Cytochrome P450 2C is an EDHF synthase in coronary arteries. Nature 401: 493-497.

13. Sinal CJ, Miyata M, Tohkin M, Nagata K, Bend JR, et al. (2000) Targeted disruption of soluble epoxide hydrolase reveals a role in blood pressure regulation. J Biol Chem 275: 40504-40510.

14. Imig JD, Zhao X, Capdevila JH, Morisseau C, Hammock BD (2002) Soluble epoxide hydrolase inhibition lowers arterial blood pressure in angiotensin II hypertension. Hypertension 39: 690-694.

15. Imig JD, Zhao X, Zaharis CZ, Olearczyk JJ, Pollock DM, et al. (2005) An orally active epoxide hydrolase inhibitor lowers blood pressure and provides renal protection in salt-sensitive hypertension. Hypertension 46: 975-981.

16. Lee CR, Imig JD, Edin ML, Foley J, DeGraff LM, et al. (2010) Endothelial expression of human cytochrome P450 epoxygenases lowers blood pressure and attenuates hypertension-induced renal injury in mice. FASEB J 24: 3770-3781.

17. Seubert J, Yang B, Bradbury JA, Graves J, Degraff LM, et al. (2004) Enhanced postischemic functional recovery in CYP2J2 transgenic hearts involves mitochondrial ATP-sensitive K+ channels and p42/p44 MAPK pathway. Circ Res 95: 506-514.

18. Seubert JM, Sinal CJ, Graves J, DeGraff LM, Bradbury JA, et al. (2006) Role of soluble epoxide hydrolase in postischemic recovery of heart contractile function. Circ Res 99: 442-450.

19. Motoki A, Merkel MJ, Packwood WH, Cao Z, Liu L, et al. (2008) Soluble epoxide hydrolase inhibition and gene deletion are protective against myocardial ischemia-reperfusion injury in vivo. Am J Physiol Heart Circ Physiol 295: H2128-2134.

20. Zou AP, Fleming JT, Falck JR, Jacobs ER, Gebremedhin D, et al. (1996) 20-HETE is an endogenous inhibitor of the large-conductance Ca(2+)-activated K+ channel in renal arterioles. Am J Physiol 270: R228-237.

21. Holla VR, Adas F, Imig JD, Zhao X, Price E, Jr., et al. (2001) Alterations in the regulation of androgen-sensitive Cyp 4a monooxygenases cause hypertension. Proc Natl Acad Sci U S A 98: 5211-5216.

22. Wang JS, Singh H, Zhang F, Ishizuka T, Deng H, et al. (2006) Endothelial dysfunction and hypertension in rats transduced with CYP4A2 adenovirus. Circ Res 98: 962-969.

23. Sodhi K, Wu CC, Cheng J, Gotlinger K, Inoue K, et al. (2010) CYP4A2-induced hypertension is 20-hydroxyeicosatetraenoic acid- and angiotensin II-dependent. Hypertension 56: 871-878.

24. Wu CC, Cheng J, Zhang FF, Gotlinger KH, Kelkar M, et al. (2011) Androgen-dependent hypertension is mediated by 20-hydroxy-5,8,11,14-eicosatetraenoic acid-induced vascular dysfunction: role of inhibitor of kappaB Kinase. Hypertension 57: 788-794.

25. Nithipatikom K, Gross ER, Endsley MP, Moore JM, Isbell MA, et al. (2004) Inhibition of cytochrome P450omega-hydroxylase: a novel endogenous cardioprotective pathway. Circ Res 95: e65-71.

26. Gross ER, Nithipatikom K, Hsu AK, Peart JN, Falck JR, et al. (2004) Cytochrome P450 omega-hydroxylase inhibition reduces infarct size during reperfusion via the sarcolemmal KATP channel. J Mol Cell Cardiol 37: 1245-1249.

27. Lv X, Wan J, Yang J, Cheng H, Li Y, et al. (2008) Cytochrome P450 omega-hydroxylase inhibition reduces cardiomyocyte apoptosis via activation of ERK1/2 signaling in rat myocardial ischemia-reperfusion. Eur J Pharmacol 596: 118-126.

28. Yousif MH, Benter IF, Roman RJ (2009) Cytochrome P450 metabolites of arachidonic acid play a role in the enhanced cardiac dysfunction in diabetic rats following ischaemic reperfusion injury. Auton Autacoid Pharmacol 29: 33-41.

29. Poloyac SM, Zhang Y, Bies RR, Kochanek PM, Graham SH (2006) Protective effect of the 20-HETE inhibitor HET0016 on brain damage after temporary focal ischemia. J Cereb Blood Flow Metab 26: 1551-1561.

30. Node K, Huo Y, Ruan X, Yang B, Spiecker M, et al. (1999) Anti-inflammatory properties of cytochrome P450 epoxygenase-derived eicosanoids. Science 285: 1276-1279.

31. de Winther MP, Kanters E, Kraal G, Hofker MH (2005) Nuclear factor kappaB signaling in atherogenesis. Arterioscler Thromb Vasc Biol 25: 904-914.

32. Cowart LA, Wei S, Hsu MH, Johnson EF, Krishna MU, et al. (2002) The CYP4A isoforms hydroxylate epoxyeicosatrienoic acids to form high affinity peroxisome proliferator-activated receptor ligands. J Biol Chem 277: 35105-35112.

33. Liu Y, Zhang Y, Schmelzer K, Lee TS, Fang X, et al. (2005) The antiinflammatory effect of laminar flow: the role of PPARgamma, epoxyeicosatrienoic acids, and soluble epoxide hydrolase. Proc Natl Acad Sci U S A 102: 16747-16752.

34. Ishizuka T, Cheng J, Singh H, Vitto MD, Manthati VL, et al. (2008) 20-Hydroxyeicosatetraenoic acid stimulates nuclear factor-kappaB activation and the production of inflammatory cytokines in human endothelial cells. J Pharmacol Exp Ther 324: 103-110.

35. Medhora M, Chen Y, Gruenloh S, Harland D, Bodiga S, et al. (2008) 20-HETE increases superoxide production and activates NAPDH oxidase in pulmonary artery endothelial cells. Am J Physiol Lung Cell Mol Physiol 294: L902-911.

36. Cheng J, Wu CC, Gotlinger KH, Zhang F, Falck JR, et al. (2010) 20-hydroxy-5,8,11,14-eicosatetraenoic acid mediates endothelial dysfunction via IkappaB kinase-dependent endothelial nitric-oxide synthase uncoupling. J Pharmacol Exp Ther 332: 57-65.

37. Cheng J, Ou JS, Singh H, Falck JR, Narsimhaswamy D, et al. (2008) 20-hydroxyeicosatetraenoic acid causes endothelial dysfunction via eNOS uncoupling. Am J Physiol Heart Circ Physiol 294: H1018-1026.

38. Morgan ET (2001) Regulation of cytochrome p450 by inflammatory mediators: why and how? Drug Metab Dispos 29: 207-212.

39. Morgan ET, Goralski KB, Piquette-Miller M, Renton KW, Robertson GR, et al. (2008) Regulation of drug-metabolizing enzymes and transporters in infection, inflammation, and cancer. Drug Metab Dispos 36: 205-216.

40. Riddick DS, Lee C, Bhathena A, Timsit YE, Cheng PY, et al. (2004) Transcriptional suppression of cytochrome P450 genes by endogenous and exogenous chemicals. Drug Metab Dispos 32: 367-375.

41. Abdel-Razzak Z, Loyer P, Fautrel A, Gautier JC, Corcos L, et al. (1993) Cytokines down-regulate expression of major cytochrome P-450 enzymes in adult human hepatocytes in primary culture. Mol Pharmacol 44: 707-715.

42. Sewer MB, Koop DR, Morgan ET (1996) Endotoxemia in rats is associated with induction of the P4504A subfamily and suppression of several other forms of cytochrome P450. Drug Metab Dispos 24: 401-407.

43. Barclay TB, Peters JM, Sewer MB, Ferrari L, Gonzalez FJ, et al. (1999) Modulation of cytochrome P-450 gene expression in endotoxemic mice is tissue specific and peroxisome proliferator-activated receptor-alpha dependent. J Pharmacol Exp Ther 290: 1250-1257.

44. Cui X, Wu R, Zhou M, Simms HH, Wang P (2004) Differential expression of cytochrome P450 isoforms in the lungs of septic animals. Crit Care Med 32: 1186-1191.

45. Yaghi A, Bradbury JA, Zeldin DC, Mehta S, Bend JR, et al. (2003) Pulmonary cytochrome P-450 2J4 is reduced in a rat model of acute Pseudomonas pneumonia. Am J Physiol Lung Cell Mol Physiol 285: L1099-1105.

46. Yaghi A, Bend JR, Webb CD, Zeldin DC, Weicker S, et al. (2004) Excess nitric oxide decreases cytochrome P-450 2J4 content and P-450-dependent arachidonic acid metabolism in lungs of rats with acute pneumonia. Am J Physiol Lung Cell Mol Physiol 286: L1260-1267.

47. Sewer MB, Koop DR, Morgan ET (1997) Differential inductive and suppressive effects of endotoxin and particulate irritants on hepatic and renal cytochrome P-450 expression. J Pharmacol Exp Ther 280: 1445-1454.

48. Kalsotra A, Anakk S, Brommer CL, Kikuta Y, Morgan ET, et al. (2007) Catalytic characterization and cytokine mediated regulation of cytochrome P450 4Fs in rat hepatocytes. Arch Biochem Biophys 461: 104-112.

49. Kalsotra A, Cui X, Antonovic L, Robida AM, Morgan ET, et al. (2003) Inflammatory prompts produce isoform-specific changes in the expression of leukotriene B(4) omega-hydroxylases in rat liver and kidney. FEBS Lett 555: 236-242.

50. Le Bouquin R, Lugnier A, Frossard N, Pons F (2004) Expression of cytochrome P450 4A mRNA in mouse lung: effect of clofibrate and interleukin-1beta. Fundam Clin Pharmacol 18: 181-186.

51. Kalsotra A, Zhao J, Anakk S, Dash PK, Strobel HW (2007) Brain trauma leads to enhanced lung inflammation and injury: evidence for role of P4504Fs in resolution. J Cereb Blood Flow Metab 27: 963-974.

52. Bandyopadhyay AM, Chaudhary I, Robertson LW, Gemzik B, Parkinson A, et al. (1993) Expression of a male-specific cytochrome P450 isozyme (CYP2C11) in fa/fa Zucker rats: effect of phenobarbital treatment. Arch Biochem Biophys 307: 386-390.

53. Yoshinari K, Takagi S, Yoshimasa T, Sugatani J, Miwa M (2006) Hepatic CYP3A expression is attenuated in obese mice fed a high-fat diet. Pharm Res 23: 1188-1200.

54. Yoshinari K, Takagi S, Sugatani J, Miwa M (2006) Changes in the expression of cytochromes P450 and nuclear receptors in the liver of genetically diabetic db/db mice. Biol Pharm Bull 29: 1634-1638.

55. Lam JL, Jiang Y, Zhang T, Zhang EY, Smith BJ (2010) Expression and functional analysis of hepatic cytochromes P450, nuclear receptors, and membrane transporters in 10- and 25-week-old db/db mice. Drug Metab Dispos 38: 2252-2258.

56. Wang MH, Smith A, Zhou Y, Chang HH, Lin S, et al. (2003) Downregulation of renal CYP-derived eicosanoid synthesis in rats with diet-induced hypertension. Hypertension 42: 594-599.

57. Zhou Y, Lin S, Chang HH, Du J, Dong Z, et al. (2005) Gender differences of renal CYP-derived eicosanoid synthesis in rats fed a high-fat diet. Am J Hypertens 18: 530-537.

58. Zhao X, Dey A, Romanko OP, Stepp DW, Wang MH, et al. (2005) Decreased epoxygenase and increased epoxide hydrolase expression in the mesenteric artery of obese Zucker rats. Am J Physiol Regul Integr Comp Physiol 288: R188-196.

59. Zhao X, Quigley JE, Yuan J, Wang MH, Zhou Y, et al. (2006) PPAR-alpha activator fenofibrate increases renal CYP-derived eicosanoid synthesis and improves endothelial dilator function in obese Zucker rats. Am J Physiol Heart Circ Physiol 290: H2187-2195.

60. Sodhi K, Inoue K, Gotlinger KH, Canestraro M, Vanella L, et al. (2009) Epoxyeicosatrienoic acid agonist rescues the metabolic syndrome phenotype of HO-2-null mice. J Pharmacol Exp Ther 331: 906-916.

61. Enriquez A, Leclercq I, Farrell GC, Robertson G (1999) Altered expression of hepatic CYP2E1 and CYP4A in obese, diabetic ob/ob mice, and fa/fa Zucker rats. Biochem Biophys Res Commun 255: 300-306.

62. Deng QG, She H, Cheng JH, French SW, Koop DR, et al. (2005) Steatohepatitis induced by intragastric overfeeding in mice. Hepatology 42: 905-914.

63. Minuz P, Jiang H, Fava C, Turolo L, Tacconelli S, et al. (2008) Altered release of cytochrome p450 metabolites of arachidonic acid in renovascular disease. Hypertension 51: 1379-1385.

64. Laffer CL, Laniado-Schwartzman M, Nasjletti A, Elijovich F (2004) 20-HETE and circulating insulin in essential hypertension with obesity. Hypertension 43: 388-392.

65. Ward NC, Rivera J, Hodgson J, Puddey IB, Beilin LJ, et al. (2004) Urinary 20-hydroxyeicosatetraenoic acid is associated with endothelial dysfunction in humans. Circulation 110: 438-443.

66. Tsai IJ, Croft KD, Mori TA, Falck JR, Beilin LJ, et al. (2009) 20-HETE and F2-isoprostanes in the metabolic syndrome: the effect of weight reduction. Free Radic Biol Med 46: 263-270.

67. Spiecker M, Darius H, Hankeln T, Soufi M, Sattler AM, et al. (2004) Risk of coronary artery disease associated with polymorphism of the cytochrome P450 epoxygenase CYP2J2. Circulation 110: 2132-2136.

68. Liu PY, Li YH, Chao TH, Wu HL, Lin LJ, et al. (2006) Synergistic effect of cytochrome P450 epoxygenase CYP2J2*7 polymorphism with smoking on the onset of premature myocardial infarction. Atherosclerosis.

69. Lee CR, North KE, Bray MS, Couper DJ, Heiss G, et al. (2007) CYP2J2 and CYP2C8 polymorphisms and coronary heart disease risk: the Atherosclerosis Risk in Communities (ARIC) study. Pharmacogenet Genomics 17: 349-358.

70. Fornage M, Boerwinkle E, Doris PA, Jacobs D, Liu K, et al. (2004) Polymorphism of the soluble epoxide hydrolase is associated with coronary artery calcification in African-American subjects: The Coronary Artery Risk Development in Young Adults (CARDIA) study. Circulation 109: 335-339.

71. Lee CR, North KE, Bray MS, Fornage M, Seubert JM, et al. (2006) Genetic variation in soluble epoxide hydrolase (EPHX2) and risk of coronary heart disease: The Atherosclerosis Risk in Communities (ARIC) study. Hum Mol Genet 15: 1640-1649.

72. Fava C, Montagnana M, Danese E, Almgren P, Hedblad B, et al. (2010) Homozygosity for the EPHX2 K55R polymorphism increases the long-term risk of ischemic stroke in men: a study in Swedes. Pharmacogenet Genomics 20: 94-103.

73. Fu Z, Nakayama T, Sato N, Izumi Y, Kasamaki Y, et al. (2008) A haplotype of the CYP4A11 gene associated with essential hypertension in Japanese men. J Hypertens 26: 453-461.

74. Gainer JV, Bellamine A, Dawson EP, Womble KE, Grant SW, et al. (2005) Functional variant of CYP4A11 20-hydroxyeicosatetraenoic acid synthase is associated with essential hypertension. Circulation 111: 63-69.

75. Gainer JV, Lipkowitz MS, Yu C, Waterman MR, Dawson EP, et al. (2008) Association of a CYP4A11 variant and blood pressure in black men. J Am Soc Nephrol 19: 1606-1612.

76. Mayer B, Lieb W, Gotz A, Konig IR, Aherrahrou Z, et al. (2005) Association of the T8590C polymorphism of CYP4A11 with hypertension in the MONICA Augsburg echocardiographic substudy. Hypertension 46: 766-771.

77. Mayer B, Lieb W, Gotz A, Konig IR, Kauschen LF, et al. (2006) Association of a functional polymorphism in the CYP4A11 gene with systolic blood pressure in survivors of myocardial infarction. J Hypertens 24: 1965-1970.

78. Ward NC, Tsai IJ, Barden A, van Bockxmeer FM, Puddey IB, et al. (2008) A single nucleotide polymorphism in the CYP4F2 but not CYP4A11 gene is associated with increased 20-HETE excretion and blood pressure. Hypertension 51: 1393-1398.

79. Fava C, Montagnana M, Almgren P, Rosberg L, Lippi G, et al. (2008) The V433M variant of the CYP4F2 is associated with ischemic stroke in male Swedes beyond its effect on blood pressure. Hypertension 52: 373-380.

80. Kawashima S, Yokoyama M (2004) Dysfunction of endothelial nitric oxide synthase and atherosclerosis. Arterioscler Thromb Vasc Biol 24: 998-1005.

Chapter II: Activation of the acute inflammatory response alters cytochrome P450 expression and eicosanoid metabolism

In addition to their role in xenobiotic metabolism, cytochromes P450 (CYP) metabolize numerous endogenous substrates, including steroids, hormones, and fatty acids, to biologically active mediators [1]. One such example is the oxidative metabolism of arachidonic acid to epoxyeicosatrienoic acids (EETs) and hydroxyeicosatetraenoic acids (HETEs). Olefin epoxidation of arachidonic acid to four EET regioisomers (5,6-EET, 8,9-EET, 11,12-EET, 14,15-EET) is primarily catalyzed by CYP2C and CYP2J isoforms [2]. Soluble epoxide hydrolase (sEH, *Ephx2*) rapidly hydrolyzes EETs to dihydroxyeicosatrienoic acids (DHETs), which, in general, are less biologically active. In contrast, ω-hydroxylation of arachidonic acid by CYP4A and CYP4F isoforms produces 20-HETE [1].

EETs and 20-HETE regulate numerous biological processes, including vascular tone, angiogenesis, and the response to ischemia/reperfusion injury [1,2,3]. Accumulating evidence has demonstrated that the CYP epoxygenase and ω-hydroxylase pathways also regulate inflammation. The EETs possess potent anti-inflammatory properties by attenuating cytokine-induced nuclear factor-κB (NF-κB) activation and leukocyte adhesion to the vascular wall [4]. Conversely, 20-HETE activates NF-κB signaling and induces expression of cellular adhesion molecules and cytokines, thereby promoting inflammation [5].

Due to the divergent effects of the CYP epoxygenase and ω-hydroxylase pathways in the regulation of inflammation, alterations in the functional balance between these parallel pathways may contribute to the pathogenesis and progression of

inflammatory diseases, such as sepsis, cancer, and cardiovascular disease. Although it is well-established that acute inflammatory stimuli suppress hepatic CYP expression via a pretranslational mechanism, thereby decreasing xenobiotic metabolism and clearance in preclinical models and humans [6,7,8], the effect on CYP-mediated eicosanoid metabolism in hepatic and extra-hepatic tissue has not been rigorously evaluated. Moreover, the biological properties of the CYP epoxygenase and ω-hydroxylase pathways *in vivo* are most commonly investigated in mouse models; however, the relative expression and function of each pathway across tissues in mice has not been well described to date. Therefore, we sought to characterize the (1) relative expression and metabolic activity of the CYP epoxygenase and ω-hydroxylase pathways across liver, kidney, lung, and heart in mice, and (2) impact of acute inflammation induced by systemic lipopolysaccharide (LPS) administration on CYP epoxygenase and ω-hydroxylase expression and metabolic activity in each tissue.

Methods

Reagents

All reagents were purchased from Fisher Scientific (Pittsburgh, PA, USA) unless otherwise noted.

Experimental Protocol

Male C57Bl/6 mice (4-5 months of age) were treated with *E. coli* LPS (1 mg/kg; serotype O111:B4, 1,000,000 EU/mg; Sigma, St. Louis, MO) or endotoxin-free saline by intraperitoneal injection and were euthanized by CO_2 inhalation 3, 6, 24, or 48 hours after treatment. Liver, kidney, lung, heart and aorta were harvested and flash frozen in liquid nitrogen. Blood was collected in heparinized tubes, and plasma was separated by centrifugation. Tissue and plasma were stored at -80ºC pending analysis. All studies were in accordance with principles outlined in the *NIH Guide for the Care and Use of*

Laboratory Animals and were approved by the Institutional Animal Care and Use Committee at the University of North Carolina at Chapel Hill.

RNA isolation, reverse transcription, and qRT-PCR

Total RNA was isolated from whole tissue homogenates using the RNeasy Miniprep Kit (QIAGEN, Valencia, CA) per the manufacturer's instructions. Total RNA was reverse transcribed to cDNA using the ABI High Capacity cDNA Reverse Transcription Kit (Applied Biosystems, Foster City, CA) with a reaction temperature of 25ºC for 10 minutes then 37ºC for 120 minutes. Expression of murine *Cyp2c29*, *Cyp2c44*, *Cyp2j5*, *Cyp2j9*, *Cyp4a12a*, *Cyp4a12b*, *Cyp4f13*, *Cyp4f16*, *Ephx2*, and *GAPDH* were quantified by quantitative RT-PCR using commercially available Taqman® Assays on Demand (Applied Biosystems) (Table 2.1). CYP isoforms were selected based on known epoxygenase or ω-hydroxylase activity and/or expression in several of the tissues examined in an initial expression screen [9,10,11,12,13,14]. The metabolic activity of murine Cyp4f isoforms has not been characterized, but these isoforms were included as CYP4F isoforms in other species have been shown to catalyze 20-HETE formation [15,16,17]. Each reaction was carried out in a 20 µL volume with 50 ng cDNA, 20X Assay on Demand, and 2X Taqman® Universal PCR Master Mix. All reactions were performed in triplicate using the ABI Prism 7300 Sequence Detection System. The cycling conditions were as follows: 2 minutes at 50ºC, 10 minutes at 95ºC, and 40 cycles of 15 seconds at 95ºC followed by 60 seconds at 60ºC. The efficiency of each RT-PCR probe was calculated over a range of cDNA amounts (1-100 ng), as previously described [18], and was equivalent for all probes (data not shown). CYP mRNA levels were normalized to *GAPDH* and expressed relative to the saline-treated controls using the $2^{-\Delta\Delta Ct}$ method [19].

Microsome isolation

Microsomal fractions from liver, kidney, lung, and heart were isolated as previously described [20]. Briefly, frozen tissue was homogenized in 0.25 M sucrose/10mM Tris-HCl buffer (pH 7.5) containing protease inhibitors. Liver and kidney homogenates were prepared from individual mice. Lung and heart homogenates were prepared from tissue pooled from 2-4 mice, due to the tissue size and low levels of CYP expression. Homogenates were centrifuged at 4ºC at 2570 x *g* for 20 minutes, then at 10300 x *g* for 20 minutes to remove cellular debris. The supernatants were then centrifuged at 100000 x *g* at 4ºC for 90 minutes. The resulting microsomal pellets were resuspended in 50 mM Tris/1 mM DTT/1 mM EDTA buffer (pH 7.5) containing 20% glycerol. Protein concentrations were quantified using the Bio-Rad protein assay (Bio-Rad, Hercules, CA), per the manufacturer's instructions.

Microsomal incubations

Incubations contained 300 µg (liver, kidney) or 350 µg (lung, heart) microsomal protein and 50 µM (liver, kidney, heart) or 150 µM (lung) arachidonic acid in a 1 mL volume of 0.12 M potassium phosphate incubation buffer containing 5 mM magnesium chloride, as previously described [21]. In the presence of these saturating substrate concentrations, formation rates reflect the amount of metabolically active protein [21]. The limited amount of tissue precluded assessment of CYP epoxygenase and ω-hydroxylase activity in aorta. Reactions were initiated by the addition of 1 mM NADPH and were carried out at 37ºC for 20 minutes (liver, kidney) or 60 minutes (lung, heart). In lung and heart incubations, an additional 1 mM NADPH was added after 30 minutes. Incubations were carried out at saturating concentrations of substrate, and metabolite formation was linear with respect to incubation time and microsomal protein, as determined from preliminary incubations. The reactions were stopped by placing the samples on ice, and 12.5 ng 20-HETE-d6 was added as an internal standard. Due to

high metabolite formation, liver incubations were diluted 20-fold in incubation buffer prior to addition of internal standard. Metabolites were extracted with diethyl ether, evaporated to dryness under nitrogen gas, and reconstituted in 80% methanol in deionized water for analysis.

Immunoblotting

Immunoblotting was performed as previously described [20]. Briefly, hepatic microsomes (20µg) were separated by electrophoresis using 4-12% NuPAGE Bis-Tris gels (Invitrogen, Carlsbad, CA) and were transferred to nitrocellulose membranes. Membranes were blocked with 5% non-fat milk in Tris-buffered saline (TBS) for 2 hours at room temperature. Membranes were incubated with anti-CYP2C (1:2000 in 5% non-fat milk; kindly provided Dr. Darryl Zeldin, NIH/NIEHS, Research Triangle Park, NC, USA), anti-CYP2J2 pep3 (1:2000 in 5% non-fat milk; kindly provided by Dr. Darryl Zeldin), anti-CYP4A1/2/3 (1:2000 in 5% non-fat milk; Santa Cruz Biotechnology, Santa Cruz, CA), anti-CYP4F2 (1:2000 in 5% BSA, Fitzgerald, Concord, MA), or anti-β-actin (1:1000 in 3% milk, Cell Signaling Technology, Danvers, MA) at 4ºC overnight. The anti-CYP2C antibody was developed against a CYP2C-specific peptide (RGKLPPGPTPLPII) and recognizes multiple murine CYP2C isoforms [22]. The anti-CYP2J2pep3 antibody was developed against a polypeptide (RESMPYTNAVIHEVQRMGNIIPLN) of human CYP2J2 and cross-reacts with murine CYP2J isoforms [23]. The anti-CYP4A1/2/3 and anti-CYP4F2 antibodies are commercially available polyclonal antibodies that recognize rat CYP4A isoforms and human CYP4F2, respectively. After washing in 0.05% Tween 20-TBS, membranes were incubated with the appropriate horseradish peroxidase-conjugated secondary antibody (1:5000 in 5% non-fat milk; Santa Cruz Biotechnology) for 1.5 hours at room temperature. Immunoreactive bands were detected by chemiluminescence using SuperSignal chemiluminescent substrate (Pierce, Rockford,

IL) and visualized with a VersaDoc Imager (Bio-Rad). Densitometry of each immunoreactive band was evaluated using Quantity One software (v.4.4, Bio-Rad).

Plasma Extractions

Plasma (125-200μL) was diluted in 0.12 M potassium phosphate buffer containing 0.113 mM butylated hydroxytoluene, and 12.5 ng 20-HETE-d6 was added as an internal standard. Samples were loaded onto Oasis HLB (30 mg) SPE cartridges (Waters, Milford, MA) that were conditioned and equilibrated with 1 mL of methanol and 1 mL of water, respectively. Columns were washed with three 1 mL volumes of 5% methanol and were eluted with 100% methanol. Extracts were dried under nitrogen gas at 37 °C and reconstituted in 125 μL of 80:20 methanol:deionized water.

UPLC-MS/MS

Arachidonic acid metabolites (14,15-EET, 11,12-EET, 8,9-EET, 14,15-DHET, 11,12-DHET, 8,9-DHET, 5,6-DHET, and 20-HETE) in microsomal incubations and plasma were quantified by UPLC-MS/MS as previously described [24]. Analytes were separated on a UPLC BEH C-18, 1.7 μm (2.1 mm x 100 mm) reversed-phase column (Waters, Milford, MA) protected by a guard column (2.1 mm x 5 mm; Waters). Mobile phases consisted of 0.005% acetic acid/5% acetonitrile in deionized water (A) and 0.005% acetic acid in acetonitrile (B) at an initial mixture of 65% A and 35% B. Mobile phase B increased from 35% to 70% in a linear gradient over 4 minutes, then increased to 95% over 0.5 minute where it remained for 0.3 minute. This was followed by a linear return to the initial conditions over 0.1 minute with a 1.5 minute pre-equilibration period prior to the next sample run.

Mass spectrometric analysis was performed with a TSQ Quantum Ultra (Thermo Fisher Scientific, San Jose, CA) triple quadrupole mass spectrometer coupled with heated electrospray ionization (HESI) operated in negative selective reaction monitoring

(SRM) mode. Unit resolutions at both Q1 and Q3 were set at 0.70 full width at half maximum. Quantitation by SRM analysis on EETs, DHETs, and HETEs was performed by monitoring their *m/z* transitions. Parameters were optimized to obtain the highest $[M-H]^-$ ion abundance and were as follows: capillary temperature 400ºC, spray voltage 3000V, and a source collision-induced dissociation set at 0V. Sheath gas, auxiliary gas, and ion sweep gas pressures were set at 65, 55, and 3, respectively. Scan time was set at 0.01 seconds and collision gas pressure was set at 1.3 mTorr. Analytical data was acquired and analyzed using Xcaliber software version 2.0.6 (ThermoFinnigan, San Jose, CA). Metabolite concentrations were calculated from a standard curve and expressed as formation rates (pmol/mg protein/min).

Statistical analysis

All data are expressed as mean ± standard error of the mean (SEM). The sum formation rate of all EET and DHET regioisomers was calculated and used as an index of total CYP epoxygenase metabolic activity. The functional balance between the CYP ω-hydroxylase and epoxygenase pathways was assessed by the ratio of 20-HETE to total EET+DHET formation. Because the data were not normally distributed, mRNA and protein levels were transformed to ranks and metabolite formation rates were log-transformed prior to statistical analysis. Data from saline-treated mice at each time point were pooled to create a single control group for statistical comparisons. Data were analyzed by one-way ANOVA followed by post-hoc Dunnett's test for comparison to the pooled saline control group. The relationship between CYP mRNA and protein levels and EET+DHET or 20-HETE formation was evaluated by Spearman rank correlation. Statistical analysis was performed using SAS software (v.9.1.3, SAS Institute, Cary, NC). $P<0.05$ was considered statistically significant.

Results

Induction of cytokine expression

Systemic LPS administration induced tumor necrosis factor-α (TNF-α) expression in a time-dependent manner in all tissues examined, consistent with acute activation of the innate immune response (Figure 2.1). The most substantial increase was observed 3 and 6 hours after LPS administration. TNF-α expression decreased over time, but remained significantly elevated compared to saline-treated mice in most tissues at 48 hours.

Liver

All CYP isoforms examined were expressed at high levels in liver, with *Cyp2c29* and *Cyp4a12a* being the most abundant CYP epoxygenase and ω-hydroxylase, respectively (Figure 2.2A). Hepatic *Cyp2c29* (0.06±0.02), *Cyp2c44* (0.18±0.03), and *Cyp2j5* (0.34±0.06) mRNA levels were markedly suppressed 24 hours after LPS administration (Figure 2.2B), with partial (*Cyp2c29*: 0.62±0.16; *Cyp2c44*: 0.69±0.22) or full (*Cyp2j5*: 1.00±0.25) restoration of expression to basal levels at 48 hours. Hepatic CYP2C and CYP2J protein expression was also significantly suppressed 24 hours after LPS administration (Figure 2.3, $P<0.05$ versus saline). At 48 hours, CYP2C remained significantly suppressed, but CYP2J expression recovered to near-basal levels. Hepatic *Cyp4a12a* (0.47±0.06), *Cyp4a12b* (0.67±0.06), and *Cyp4f13* (0.59±0.08) mRNA levels were also significantly suppressed, but to a lesser degree, 24 hours after LPS administration, and returned to basal levels by 48 hours (*Cyp4a12a*: 0.79±0.22; *Cyp4a12b*: 1.21±0.37; *Cyp4f13*: 1.02±0.33). In contrast, *Cyp4f16* mRNA levels were significantly higher 24 (4.56±0.62) and 48 hours (2.82±0.81) after LPS administration compared to saline controls (Figure 2.2C). No significant alterations in CYP4A or CYP4F protein expression were observed (Figure 2.3).

Total hepatic CYP epoxygenase metabolic activity was significantly lower 24 (173.9±15.7 pmol/mg protein/min) and 48 (295.4±18.8 pmol/mg protein/min) hours after LPS administration, compared to the saline control group (458.2±24.0 pmol/mg protein/min), while no differences were observed at 3 and 6 hours (Figure 2.2D). Similar results were observed when each EET+DHET regioisomer was evaluated individually (Figure 2.4A). Total CYP epoxygenase metabolic activity was strongly correlated with hepatic *Cyp2c29* (r=0.74, P<0.001), *Cyp2c44* (r=0.65, P<0.001), and *Cyp2j5* (r=0.56, P<0.001) mRNA levels, as well as CYP2C (r=0.50, P=0.006) and CYP2J (r=0.37, P=0.056) protein levels. Compared to saline-treated mice (286.7±11.2 pmol/mg protein/min), 20-HETE formation was also significantly lower 24 hours (180.8±17.8 pmol/mg protein/min) after LPS administration, but returned to basal levels at 48 hours (305.5±11.7 pmol/mg protein/min) (Figure 2.2D). No significant differences in hepatic 20-HETE formation were observed 3 or 6 hours after LPS administration. 20-HETE formation was significantly correlated with hepatic *Cyp4a12b* mRNA levels (r=0.51, P=0.002).

Kidney

Cyp2j5 and *Cyp4a12a* were the most abundant CYP epoxygenase and ω-hydroxylase in kidney, respectively, while *Cyp2c29* mRNA was undetectable (Figure 2.5A). Renal *Cyp2c44* mRNA levels were significantly suppressed 3 (0.64±0.06), 6 (0.56±0.03), and 24 hours (0.26±0.03) after LPS administration, but returned to baseline at 48 hours (1.04±0.11). A similar profile was observed for *Cyp2j5*, but *Cyp2j5* was suppressed to a lesser degree (Figure 2.5B). *Cyp4a12a* expression was also significantly suppressed at 24 hours (0.63±0.06). In contrast, *Cyp4a12b* and *Cyp4f16* mRNA levels were significantly lower at 6 hours, but were significantly higher 24 and 48

hours after LPS administration (Figure 2.5C, P<0.05 versus saline). Significant changes in *Cyp4f13* mRNA levels were observed only at 24 hours.

Total CYP epoxygenase metabolic activity was significantly lower in kidney microsomes 24 hours (13.2±0.7 pmol/mg protein/min) after LPS administration, compared to the saline control group (18.7±1.6 pmol/mg protein/min). Formation of the 14,15- and 11,12-, but not the 8,9- or 5,6-, regioisomers was significantly lower 24 hours after LPS administration (Figure 2.4B). At 48 hours, total EET+DHET formation was returning to basal levels (14.7±1.4 pmol/mg protein/min; P=0.12 vs. saline) (Figure 2.5D). Similarly, renal 20-HETE formation was significantly lower in LPS-treated mice at 24 hours (15.3±1.9 pmol/mg protein/min), compared to saline (32.5±6.7 pmol/mg protein/min), but was recovering toward baseline at 48 hours (22.2±4.9 pmol/mg protein/min; P=0.45 vs. saline) (Figure 2.5D). No significant differences in renal EET+DHET, or 20-HETE formation were observed 3 or 6 hours after LPS administration. A significant correlation between total CYP epoxygenase and ω-hydroxylase metabolic activity, and renal *Cyp2j5* (r=0.42, P=0.012) and *Cyp4a12a* mRNA levels (r=0.55, P<0.001), respectively, was observed.

Lung

Cyp2j9 was the most abundant CYP epoxygenase isoform expressed in lung (Figure 2.6A). *Cyp2j9* and *Cyp2c44* mRNA levels were significantly lower in LPS-treated mice at 3, 6, 24, and 48 hours (Figure 2.6B, P<0.05 versus saline). *Cyp2j5* also appeared to be suppressed at 24 hours (0.20±0.05; P=0.11); however, due to substantial inter-animal variability, these differences were not statistically significant (Figure 2.6B). Following LPS administration, *Cyp4a12a*, *Cyp4a12b*, *Cyp4f13*, and *Cyp4f16* mRNA levels were significantly lower at almost every time point, although *Cyp4f16* returned to basal levels at 48 hours (Figure 2.6C).

Compared to saline-treated mice (54.1±5.2 pmol/mg protein/min), total CYP epoxygenase metabolic activity in lung microsomes was lower, but not statistically significant, 3 (35.8±3.0 pmol/mg protein/min, P=0.063), 6 (38.4±7.3 pmol/mg protein/min, P=0.171), and 24 (38.7±3.7 pmol/mg protein/min, P=0.094) hours after LPS treatment, while EET+DHET formation was significantly lower at the 48 hour time point (28.9±2.2 pmol/mg protein/min, P=0.008) (Figure 2.6D). Similar time-dependent changes in metabolism were observed for each regioisomer (Figure 2.4C). 20-HETE formation was significantly lower 6 (12.8±5.9 pmol/mg protein/min) and 24 (9.4±1.5 pmol/mg protein/min) hours after LPS administration, compared to the saline control group (23.1±1.4 pmol/mg protein/min), whereas no differences were observed at 3 or 48 hours (Figure 2.6D). No significant correlations between total CYP epoxygenase metabolic activity and *Cyp2c44*, *Cyp2j5*, or *Cyp2j9* mRNA levels were observed. However, 20-HETE formation significantly correlated with pulmonary *Cyp4a12a* (r=0.47, P=0.026), *Cyp4a12b* (r=0.46, P=0.030), and *Cyp4f13* (r=0.46, P=0.033) mRNA levels.

Heart/Aorta

Overall, myocardial CYP mRNA levels were low, with *Cyp4f13* and *Cyp4f16* being the most abundant isoforms. Of the CYP epoxygenases examined, only *Cyp2c44* was expressed at detectable levels (Figure 2.7A). The CYP expression profile in aorta was similar; however, *Cyp2c29* mRNA was expressed at detectable levels, and *Cyp2c44* and *Cyp4f13* mRNA levels were approximately 10-fold higher in aorta compared to heart (Table 2.1). Myocardial *Cyp2c44* mRNA levels were significantly lower 3 and 6 hours after LPS administration (Figure 2.7B, $P<0.05$ versus saline). Although it remained significantly suppressed at 24 hours (0.51±0.14), *Cyp2c44* appeared to be returning to basal levels, with full recovery observed at 48 hours (0.78 ±0.13). In aorta, *Cyp2c29* (0.38±0.12, P=0.128) and *Cyp2c44* (0.26±0.06, P=0.128) mRNA appeared to be

suppressed 24 hours after LPS administration, relative to saline-treated mice, but this difference was not statistically significant due to substantial inter-animal variability. In heart, both *Cyp4f13* and *Cyp4f16* mRNA levels were significantly lower in LPS-treated mice at 3 hours, but significantly higher at 24 and 48 hours (Figure 2.7C, $P<0.05$ versus saline). Similarly, *Cyp4f13* and *Cyp4f16* mRNA levels in aorta were significantly higher in LPS-treated mice at 24 (*Cyp4f13*: 1.48±0.12; *Cyp4f16*: 3.65±0.44; $P<0.05$ vs. saline) and 48 hours (*Cyp4f13*: 1.93±0.18; *Cyp4f16*: 3.30±0.61; $P<0.05$ vs. saline).

Total CYP epoxygenase metabolic activity (3.97±0.44 pmol/mg protein/min) was approximately 8-fold higher than CYP ω-hydroxylase activity (0.51±0.04 pmol/mg protein/min) in heart microsomes under basal conditions (Figure 2.7D). Compared to saline, no significant differences in EET+DHET or 20-HETE formation were observed 24 hours after LPS administration. Although EET+DHET formation appeared to be lower and 20-HETE formation appeared to be higher 48 hours after LPS administration, the limited sample size (N=2 incubations) at 48 hours precluded statistical comparisons.

Ephx2 expression

Ephx2 was abundantly expressed in all tissues examined. In liver, kidney, and lung, *Ephx2* mRNA levels were similar to the CYP isoforms examined. In contrast, *Ephx2* was approximately 100- and 10-fold more abundant than *Cyp4f13* in heart and aorta, respectively (Table 2.1). Tissue-specific alterations in *Ephx2* expression were observed following LPS administration (Figure 2.8). In liver, kidney, and lung, *Ephx2* expression was suppressed by 30-80% 6 to 48 hours following LPS administration, relative to saline control. In contrast, no differences were observed in heart, and *Ephx2* mRNA levels were significantly higher in aorta at 48 hours (2.57±0.49, $P<0.05$ vs. saline).

Functional balance between CYP epoxygenase and ω-hydroxylase pathways across tissues

Under basal conditions, hepatic EET+DHET formation was higher than 20-HETE formation, resulting in a 20-HETE: EET+DHET formation rate ratio of 0.64±0.03 in saline-treated mice (Figure 2.9A). A similar 20-HETE: EET+DHET formation rate ratio was observed in lung (0.45±0.06, Figure 2.9C) and heart (0.13±0.02, Figure 2.9D), indicative of higher CYP epoxygenase metabolic activity relative to CYP ω-hydroxylase metabolic activity. In contrast, the renal ratio of CYP ω-hydroxylase to CYP epoxygenase metabolic activity was 1.69±0.25 (Figure 2.9B), due to higher 20-HETE compared to EET+DHET formation under basal conditions in kidney.

Following LPS stimulation, the hepatic 20-HETE: EET+DHET formation rate ratio was significantly greater at 24 (1.02±0.06) and 48 (1.05±0.06) hours compared to saline-treated mice (Figure 2.9A). Although the ratio of CYP ω-hydroxylase to CYP epoxygenase metabolic activity in heart appeared higher 48 hours after LPS treatment (0.23±0.06), the limited sample size precluded formal statistical comparisons (Figure 2.9D). In contrast, the pulmonary 20-HETE: EET+DHET formation rate ratio was significantly lower at 24 hours (0.24±0.02) compared to saline-treated mice (Figure 2.9C). In kidney, no significant differences in the ratio of CYP ω-hydroxylase to CYP epoxygenase metabolic activity were observed after LPS treatment (Figure 2.9B), which remained greater than 1.0 at all time-points.

Compared to saline-treated mice, plasma 14,15-DHET levels were significantly higher 6 hours after LPS administration; however, no differences in DHET levels were observed at 3, 24 or 48 hours (Figure 2.4E). Plasma EETs and 20-HETE were below the limit of detection in the majority of mice (data not shown).

Discussion

Although it is well established that acute inflammatory stimuli suppress hepatic CYP expression and xenobiotic metabolism, the effect on CYP-mediated eicosanoid metabolism in hepatic and extra-hepatic tissues has not been characterized to date. To our knowledge, this is the first study demonstrating that acute activation of the innate immune response alters CYP epoxygenase and ω-hydroxylase metabolic activity in mice, through pretranslational regulation of CYP expression, and disrupts the functional balance between these parallel pathways in a tissue- and time-dependent manner. Collectively, these findings suggest that alteration of CYP-mediated eicosanoid metabolism is an important consequence of the acute inflammatory response *in vivo*.

Under basal conditions, CYP epoxygenase and ω-hydroxylase metabolic activity in liver was approximately 10-20-fold greater than kidney and lung, and 100-fold greater than heart. In contrast to the other tissues examined, CYP mRNA levels in heart and aorta were low, with *Cyp4f13* and *Cyp4f16* being the most abundant isoforms. Myocardial EET+DHET formation was approximately 8-fold higher than 20-HETE formation despite the high levels of *Cyp4f13* and *Cyp4f16*, suggesting that these isoforms play a minor role in 20-HETE biosynthesis.

Consistent with previous studies in human hepatocyte culture [25] and in rodents [26,27], hepatic CYP epoxygenase mRNA, protein, and metabolic activity was suppressed 24 hours after LPS treatment, with partial (CYP2C) or full (CYP2J) restoration to basal levels at 48 hours. The correlation between time-dependent changes in hepatic *Cyp2c29*, *Cyp2c44*, and *Cyp2j5* mRNA levels and epoxygenase metabolic activity support the hypothesis that inflammation-mediated alterations in CYP metabolism are mediated primarily via pretranslational regulation of CYP expression [7]. Although Cyp2c29, Cyp2c44, and Cyp2j5 catalyze the formation of individual EET

regioisomers in different proportions [9,10,11], the collective suppression of all EET+DHET regioisomers is consistent with the regioisomer profiles for these isoforms.

In contrast to the majority of CYPs, hepatic CYP4A and CYP4F isoforms may be induced by inflammation, although this appears to be isoform- and species-specific [26,27,28,29]. The temporal profiles of hepatic *Cyp4a12a*, *Cyp4a12b*, and *Cyp4f13* mRNA levels were similar to 20-HETE formation, which was also suppressed at 24 hours, but to a lesser degree than EET+DHET formation. The significantly higher 20-HETE:EET+DHET formation rate ratio at 24 and 48 hours suggests that following systemic activation of the innate immune response, the functional balance in liver is tipped in favor of the pro-inflammatory CYP ω-hydroxylase pathway.

Consistent with previous findings in rats [28], LPS suppressed renal *Cyp2c44* and *Cyp2j5* expression and epoxygenase metabolic activity, which correlated with *Cyp2j5* mRNA levels. This suggests a pretranslational mechanism and that Cyp2j5 is primarily responsible for renal EET formation. We observed lower *Cyp4a12a*, but higher *Cyp4a12b*, *Cyp4f13*, and *Cyp4f16* mRNA levels in kidney following LPS administration. Renal *Cyp4a10* mRNA levels were also higher 24 and 48 hours after LPS administration (data not shown), which is consistent with previous reports [26]. However, Cyp4a10 does not readily catalyze 20-HETE formation [13]. Renal CYP ω-hydroxylase activity was suppressed at 24 hours and significantly correlated with *Cyp4a12a* mRNA levels, suggesting that Cyp4a12a is primarily responsible for renal 20-HETE formation. In contrast to the other tissues examined, CYP ω-hydroxylase metabolic activity predominated under both basal and LPS-stimulated conditions, indicating that inhibition of 20-HETE biosynthesis may be a rational therapeutic strategy to attenuate renal inflammation.

In lung, our findings are consistent with studies demonstrating lower pulmonary CYP2C and CYP2J expression and epoxygenase metabolic activity in rat models of sepsis [30] and *Pseudomonas* pneumonia [31,32], providing further evidence that suppression of pulmonary EET formation is a key component of the pathological response to inflammation. Compared to basal conditions, 20-HETE formation and the 20-HETE:EET+DHET formation rate ratio were significantly lower 24 hours after LPS administration, suggesting that the functional balance was shifted in favor of the anti-inflammatory CYP epoxygenase pathway. Although this could serve as a compensatory mechanism to facilitate resolution of the inflammatory response, additional studies are necessary to dissect the role of CYP-mediated EET and 20-HETE biosynthesis in the regulation of pulmonary inflammation.

A recent study demonstrated that myocardial CYP epoxygenase activity was significantly suppressed, while CYP ω-hydroxylase activity was induced following LPS administration in rats [28]. Although we observed no significant changes in CYP epoxygenase or ω-hydroxylase metabolic activity, the low arachidonic acid-metabolizing capacity of mouse heart limited our sample size. Future studies remain necessary to characterize the effect of inflammation on myocardial CYP epoxygenase and ω-hydroxylase metabolic activity.

Plasma EETs and 20-HETE were below the limit of detection in the majority of mice, consistent with previous reports [33,34]. Plasma DHET levels appeared modestly elevated 6 hours after LPS administration, consistent with previous studies [33,34,35]; however, only 14,15-DHET was statistically significant. Importantly, the primary source of circulating EET, DHET, and 20-HETE levels in plasma has not been determined. A recent study demonstrated that LPS-induced elevations in plasma DHETs were attenuated in myeloperoxidase-deficient (*Mpo*$^{-/-}$) mice, suggesting that lipid peroxidation

by reactive oxygen species may serve as a CYP-independent source of circulating eicosanoids [33]. Furthermore, since EETs and 20-HETE circulate at levels <1.0 ng/mL, it has been hypothesized that these mediators act predominantly in a paracrine manner [1]. Our data demonstrate that systemic activation of the innate immune response significantly alters the formation of EETs and 20-HETE in tissue. Future studies characterizing the functional consequences of these local effects remain necessary.

It is believed that the primary mechanism by which CYP expression is down-regulated in response to LPS is cytokine-mediated suppression of gene transcription. However, identification of the specific nuclear receptors that mediate these effects has remained elusive [6,7,8]. For example, an initial study suggested that LPS-mediated alteration of hepatic and renal CYP expression was mediated by peroxisome proliferator-activated receptor-α (PPAR-α) [26]. However, subsequent experiments have demonstrated that LPS-mediated down-regulation of hepatic CYP expression is independent of PPAR-α, pregnane X receptor (PXR), and signal transducer and activator of transcription (Stat)-1 [36,37]. Although we did not directly investigate the mechanism by which LPS alters CYP expression and metabolic activity, the observed isoform- and tissue-specific response suggests that the mechanism is complex, and most likely involves multiple transcription factors that vary across isoforms and tissues. Moreover, the time-dependent changes observed further suggest a multi-factorial mechanism. In addition, multiple murine CYP isoforms catalyze EET and 20-HETE formation, further complicating the ability to identify a single factor that underlies the net impact of the inflammatory response on CYP-mediated eicosanoid metabolism in each tissue. Future studies remain necessary to dissect these complex mechanisms.

CYP-derived EETs possess anti-inflammatory properties via inhibition of NF-κB activation [4], while 20-HETE activates NF-κB signaling and elicits pro-inflammatory effects [5]. These opposing effects on the regulation of inflammation suggest that

inflammation-induced alterations in the functional balance between these parallel pathways may contribute to the pathologic consequences of the inflammatory response. A limitation of the current work is that we did not directly demonstrate that potentiation of the CYP epoxygenase pathway and/or inhibition of the CYP ω-hydroxylase pathway attenuates the acute inflammatory response to LPS in each tissue. However, our findings provide an important foundation to guide future studies evaluating these therapeutic strategies, particularly in tissues where inflammatory stimuli tip the functional balance in favor of CYP-mediated 20-HETE biosynthesis, such as liver. Indeed, the liver is the predominant source of cytokine production and drives the systemic inflammatory response, as observed during sepsis, via subsequent activation of extra-hepatic inflammation and multi-organ dysfunction [38]. Inhibition of sEH-mediated EET hydrolysis has potent anti-inflammatory effects, including attenuation of endotoxemia-induced hypotension and mortality [34,39,40]. In contrast, a recent study demonstrated that LPS-induced hepatic inflammation was not attenuated in *Ephx2*$^{-/-}$ mice or by sEH inhibition [35]. Although the mechanisms underlying these conflicting findings remain unclear, our data suggest that dual inhibition of 20-HETE biosynthesis and sEH-mediated EET hydrolysis may be a more effective means to attenuate hepatic inflammation. Future studies remain necessary to evaluate these therapeutic strategies in disease models of local and systemic inflammation.

In conclusion, our findings demonstrate that acute activation of the inflammatory response with LPS alters CYP epoxygenase and ω-hydroxylase expression and metabolic activity in a tissue-, isoform-, and time-dependent manner. These results highlight the relative differences in CYP-mediated eicosanoid metabolism across tissues under basal and inflammatory conditions, and lay an important foundation to guide future studies that seek to determine whether therapeutic restoration of the functional balance

between the CYP epoxygenase and ω-hydroxylase pathways is an effective anti-inflammatory strategy *in vivo*.

Table 2.1: Basal CYP mRNA levels relative to *GAPDH* across tissues.

	Liver	Kidney	Lung	Heart	Aorta
Cyp2c29 Mm00725580_s1	0.89 ± 0.10	N.D.	N.D.	N.D.	0.0002 ± 0.0001
Cyp2c44 Mm01197184_m1	0.16 ± 0.01	0.007 ± 0.0003	0.0009 ± $8.3x10^{-5}$	$1.3x10^{-5}$ ± $4.2x10^{-6}$	$7.4x10^{-5}$ ± $3.9x10^{-5}$
Cyp2c50 Mm00663066_gH	0.17 ± 0.03	N.D.	N.D.	N.D.	$3x10^{-5}$ ± $2x10^{-5}$
Cyp2c55 Mm00472168_m1	0.004 ± 0.0002	$1.6x10^{-5}$ ± $1.2x10^{-5}$	N.D.	N.D.	N.D.
Cyp2j5 Mm00487292_m1	0.28 ± 0.03	0.35 ± 0.01	0.0003 ± $7.7x10^{-5}$	N.D.	N.D.
Cyp2j9 Mm00466423_m1	0.0003 ± $2.3x10^{-5}$	0.0006 ± $7.5x10^{-5}$	0.017 ± 0.001	0.0009 ± 0.0002	0.0009 ± $8.4x10^{-5}$
Cyp4a10 Mm02601690_gH	0.04 ± 0.02	0.06 ± 0.01	N.D.	N.D.	$1.3x10^{-5}$ ± $8.6x10^{-6}$
Cyp4a12a Mm00514494_m1	0.21 ± 0.02	0.05 ± 0.002	0.007 ± 0.002	N.D.	N.D.
Cyp4a12b Mm00655431_gH	0.05 ± 0.009	0.003 ± 0.0002	0.005 ± 0.001	N.D.	N.D.
Cyp4f13 Mm00504576_m1	0.02 ± 0.001	0.006 ± 0.0003	0.02 ± 0.0007	0.0003 ± $2.2x10^{-5}$	0.003 ± 0.0002
Cyp4f16 Mm00775893_m1	0.0002 ± $2.9x10^{-5}$	0.0007 ± $4.5x10^{-5}$	0.007 ± 0.0009	0.0002 ± $2.3x10^{-5}$	0.0003 ± $2x10^{-5}$
Ephx2 Mm01313813_m1	0.16 ± 0.02	0.06 ± 0.002	0.004 ± 0.0005	0.02 ± 0.001	0.03 ± 0.002

The commercially available Taqman® Assay on Demand product ID for each gene is provided (Applied Biosystems). Data were generated by quantitative RT-PCR, and are expressed relative to *GAPDH* using the $2^{-\Delta Ct}$ method as mean ± SEM. N=18-24 for all detectable isoforms in each tissue. N.D.= not detected (N=3).

Figure Legends

Figure 2.1: Effect of LPS administration (1 mg/kg, IP) on TNF-α mRNA levels over 48 hours in liver, kidney, lung, heart, and aorta. Data are expressed as mean ± SEM-fold change in expression, relative to the saline control group, using the $2^{-\Delta\Delta Ct}$ method. N=5-6 per time point. * P<0.05 versus saline control group.

Figure 2.2: (A) The relative abundance of hepatic CYP mRNA was quantified in saline-treated mice (N=20) and normalized to *GAPDH*. The time-dependent effect of LPS administration (1 mg/kg, IP) on hepatic (B) *Cyp2c29*, *Cyp2c44*, and *Cyp2j5* and (C) *Cyp4a12a*, *Cyp4a12b*, *Cyp4f13*, and *Cyp4f16* mRNA levels were quantified by qRT-PCR and expressed relative to the saline control group [Saline (pooled): N=20; LPS 3 hours: N=6, 6 hours: N=6, 24 hours: N=15, 48 hours: N=6]. The effect of LPS administration on (D) total CYP epoxygenase (EETs+DHETs) and ω-hydroxylase (20-HETE) metabolic activity in liver microsomes was determined [Saline (pooled): N=12; LPS 3 hours: N=4, 6 hours: N=4, 24 hours: N=12, 48 hours: N=6]. * P<0.05 versus saline control group.

Figure 2.3: (A) Representative immunoblot of CYP and β-actin protein expression in liver microsomes after LPS (1 mg/kg, IP) or saline administration. (B) CYP expression was quantified by densitometry, normalized to β-actin, and expressed relative to the saline control group (Saline: N=8, LPS 3 hours: N=4, 6 hours: N=3, 24 hours: N=8, 48 hours: N=5). * P<0.05 versus saline control group.

Figure 2.4: The effect of LPS (1 mg/kg, IP) and saline administration on 14,15-, 11,12-, 8,9-, and 5,6-EET+DHET formation was determined in (A) liver, (B) kidney, (C) lung, and (D) heart microsomes [Saline (pooled): N=4-12; LPS 3 hours: N=4-6, 6 hours: N=3-6, 24 hours: N=4-12, 48 hours: N=2-6]. (E) 14,15-DHET, 11,12-DHET, 8,9-DHET, and 5,6-DHET concentrations were quantified in plasma after solid-phase extraction

[Saline (pooled): N=17; LPS 3 hours: N=6, 6 hours: N=7, 24 hours: N=15, 48 hours: N=6]. * P<0.05 compared to saline-treated mice.

Figure 2.5: (A) The relative abundance of renal CYP mRNA was quantified in saline-treated mice (N.D.: not detected; N=20 for detected isoforms; N=3 for undetectable isoforms) and normalized to *GAPDH*. The time-dependent effect of LPS administration (1 mg/kg, IP) on renal (B) *Cyp2c44* and *Cyp2j5* and (C) *Cyp4a12a*, *Cyp4a12b*, *Cyp4f13*, and *Cyp4f16* mRNA levels were quantified by qRT-PCR and expressed relative to the saline control group [Saline (pooled): N=20; LPS 3 hours: N=6, 6 hours: N=6, 24 hours: N=15, 48 hours: N=6]. The effect of LPS administration on (D) total CYP epoxygenase (EETs+DHETs) and ω-hydroxylase (20-HETE) metabolic activity in kidney microsomes was determined [Saline (pooled): N=9; LPS 3 hours: N=6, 6 hours: N=6, 24 hours: N=9, 48 hours: N=6]. * P<0.05 versus saline control group.

Figure 2.6: (A) The relative abundance of pulmonary CYP mRNA was quantified in saline-treated mice (N.D.: not detected; N=23 for detected isoforms; N=3 for undetectable isoforms) and normalized to *GAPDH*. The time-dependent effect of LPS administration (1 mg/kg, IP) on pulmonary (B) *Cyp2c44*, *Cyp2j5*, and *Cyp2j9* and (C) *Cyp4a12a*, *Cyp4a12b*, *Cyp4f13*, and *Cyp4f16* mRNA levels were quantified by qRT-PCR and expressed relative to the saline control group [Saline (pooled): N=23; LPS 3 hours: N=9, 6 hours: N=9, 24 hours: N=18, 48 hours: N=6]. The effect of LPS administration on (D) total CYP epoxygenase (EETs+DHETs) and ω-hydroxylase (20-HETE) metabolic activity in lung microsomes (N=2 mice per microsome preparation) was determined [Saline (pooled): N=6, LPS 3 hours: N=4, 6 hours: N=3, 24 hours: N=6, 48 hours: N=3]. * P<0.05 versus saline control group.

Figure 2.7: (A) The relative abundance of myocardial CYP mRNA was quantified in saline-treated mice (N.D.: not detected; N=24 for detected isoforms; N=3 for undetectable isoforms) and normalized to *GAPDH*. The time-dependent effect of LPS administration (1 mg/kg, IP) on myocardial (B) *Cyp2c44* and (C) *Cyp4f13* and *Cyp4f16* mRNA levels were quantified by qRT-PCR and expressed relative to the saline control group [Saline (pooled): N=24; LPS 3 hours: N=9, 6 hours: N=9, 24 hours: N=18, 48 hours: N=6]. The effect of LPS administration on (D) total CYP epoxygenase (EETs+DHETs) and ω-hydroxylase (20-HETE) metabolic activity in heart microsomes (N=3-4 mice per microsome preparation) was determined [Saline (pooled): N=4; LPS 24 hours: N=4, 48 hours: N=2). * $P<0.05$ versus saline control group.

Figure 2.8: The time-dependent effect of LPS administration (1 mg/kg, IP) on *Ephx2* mRNA levels in liver, kidney, lung, heart, and aorta were quantified by qRT-PCR and expressed relative to the saline control group [Saline (pooled): N=18-24; LPS 3 hours: N=6-9, 6 hours: N=6-9, 24 hours: N=15-18, 48 hours: N=6]. * $P<0.05$ versus saline control group.

Figure 2.9: The time-dependent effect of LPS administration (1 mg/kg, IP) on the ratio of 20-HETE to EET+DHET formation was determined in (A) liver, (B) kidney, (C) lung, and (D) heart microsomes. Saline: N=4-12; LPS 3 hours: N=4-6, 6 hours: N=3-6, 24 hours: N=4-12, 48 hours: N=2-6. * $P<0.05$ compared to saline-treated mice.

Figure 2.1: Effect of LPS administration on TNF-α mRNA levels over 48 hours in liver, kidney, lung, heart, and aorta

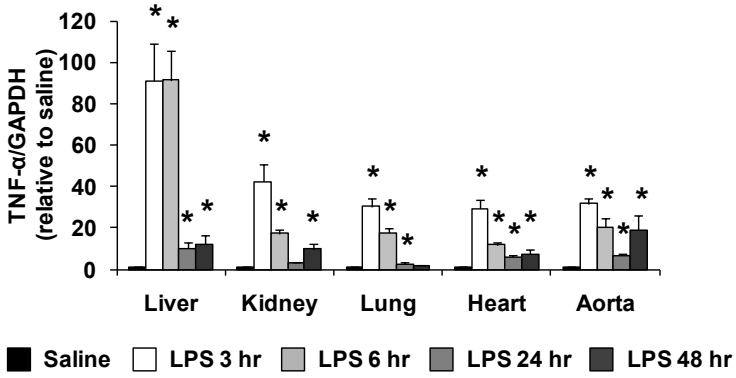

Figure 2.2: Effect of LPS administration on hepatic CYP epoxygenase and ω-hydroxylase mRNA levels and metabolic activity

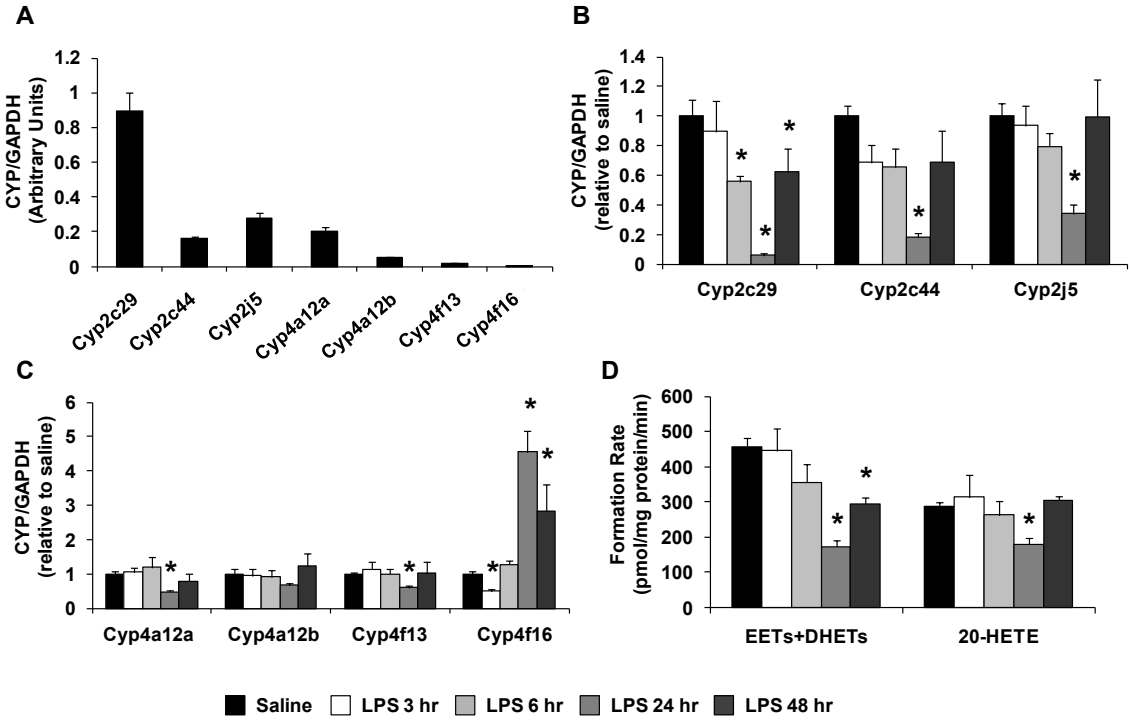

Figure 2.3: Effect of LPS administration on hepatic CYP epoxygenase and ω-hydroxylase protein expression

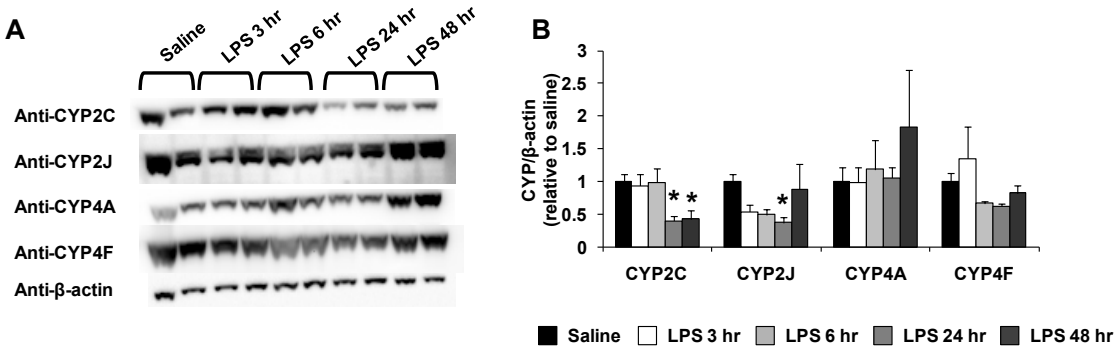

Figure 2.4: Effect of LPS administration on 14,15-, 11,12-, 8,9-, and 5,6-EET+DHET formation in liver kidney, lung, heart, and plasma

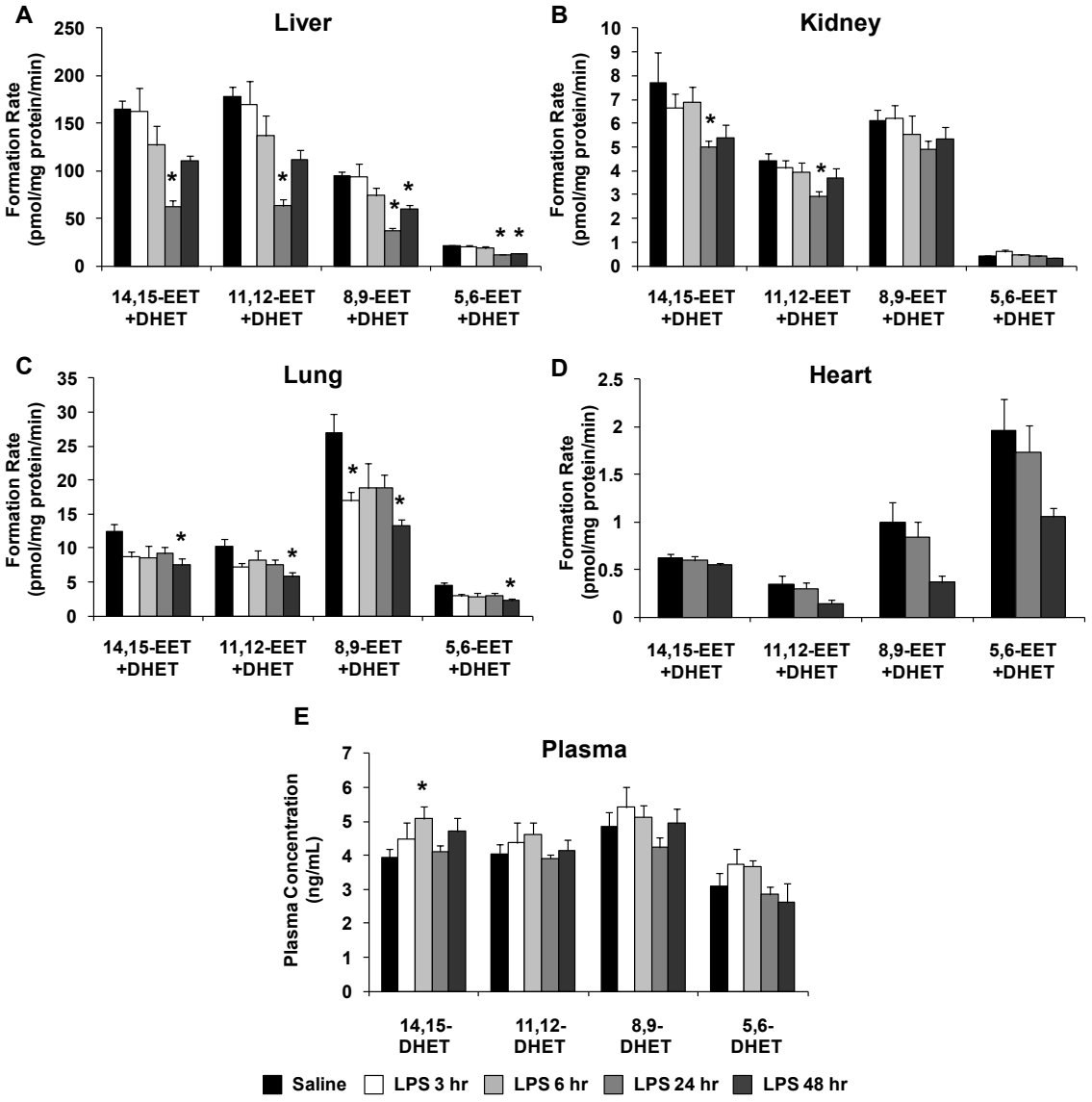

Figure 2.5: Effect of LPS administration on renal CYP epoxygenase and ω-hydroxylase mRNA levels and metabolic activity

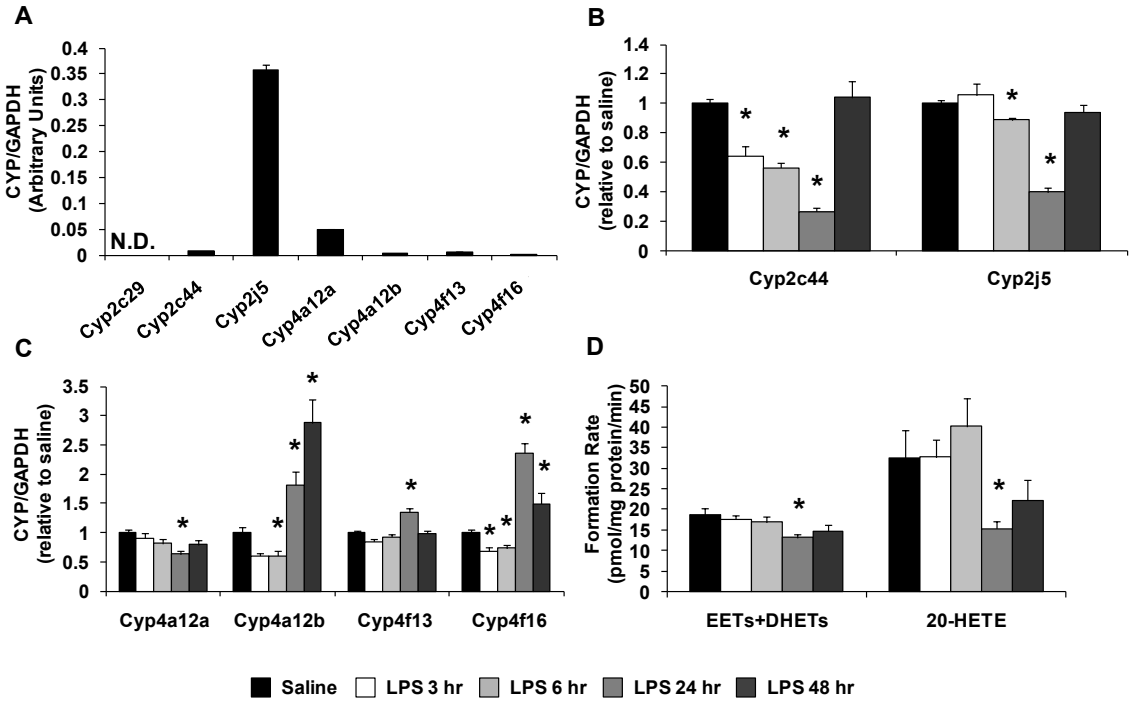

Figure 2.6: Effect of LPS administration on pulmonary CYP epoxygenase and ω-hydroxylase mRNA levels and metabolic activity

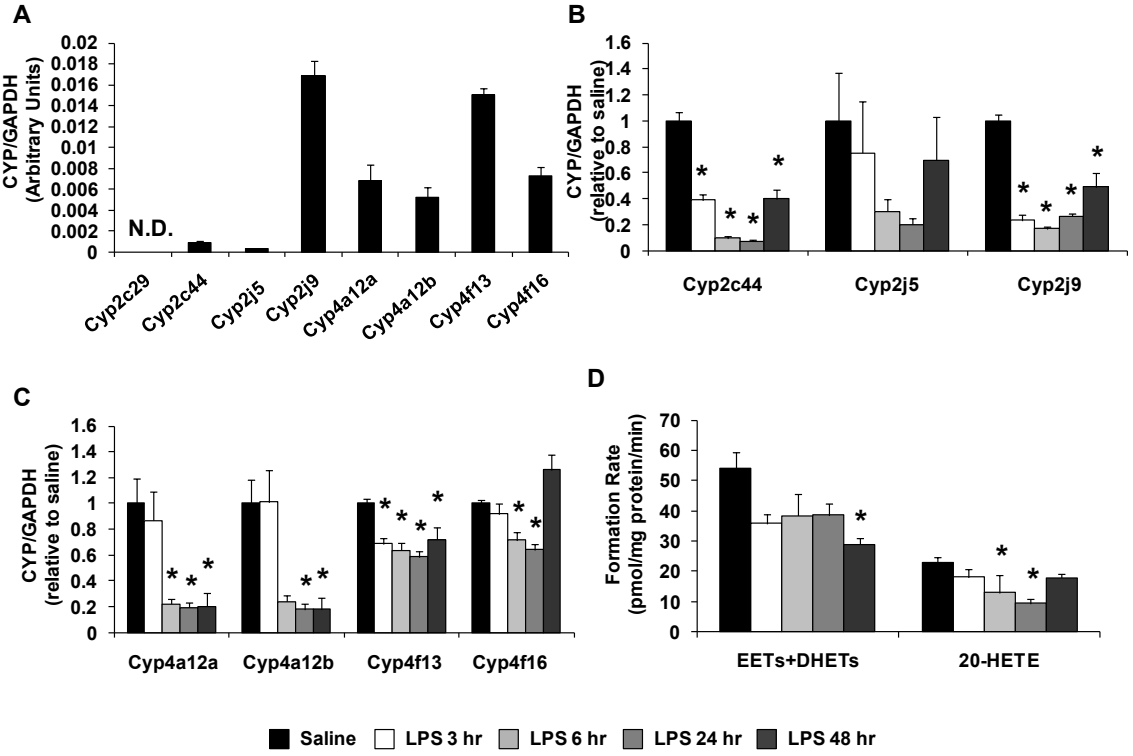

Figure 2.7: Effect of LPS administration on myocardial CYP epoxygenase and ω-hydroxylase mRNA levels and metabolic activity

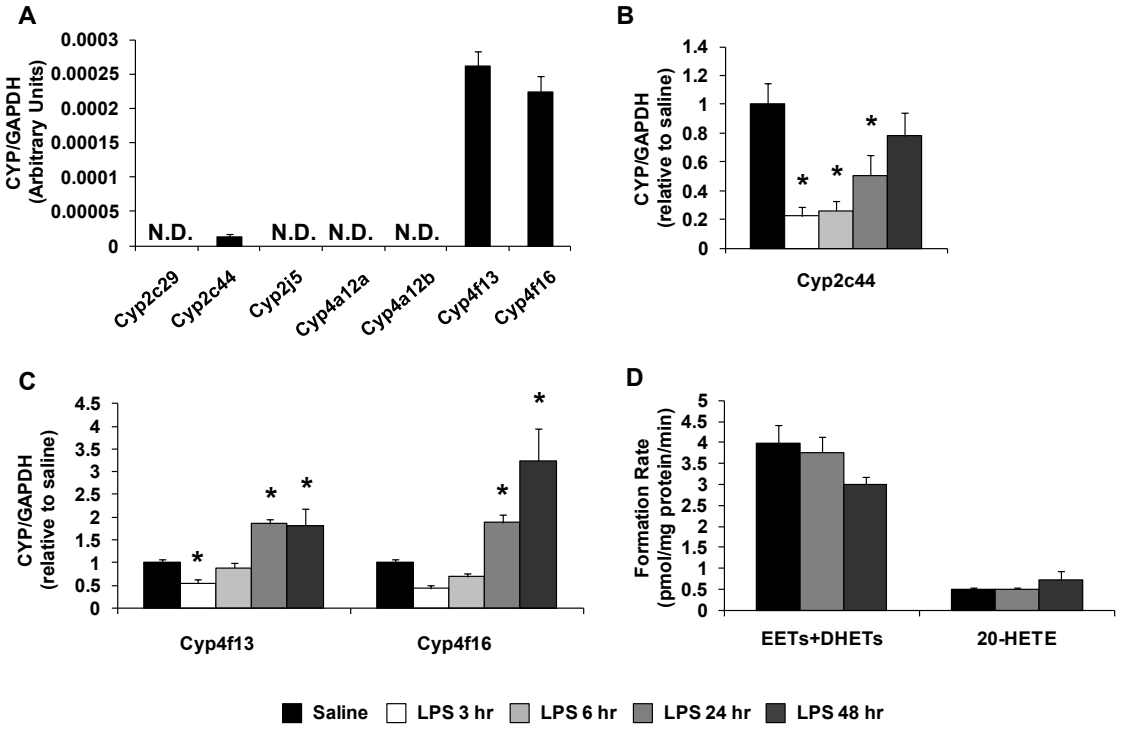

Figure 2.8: Effect of LPS administration on *Ephx2* mRNA levels over 48 hours in liver, kidney, lung, heart, and aorta

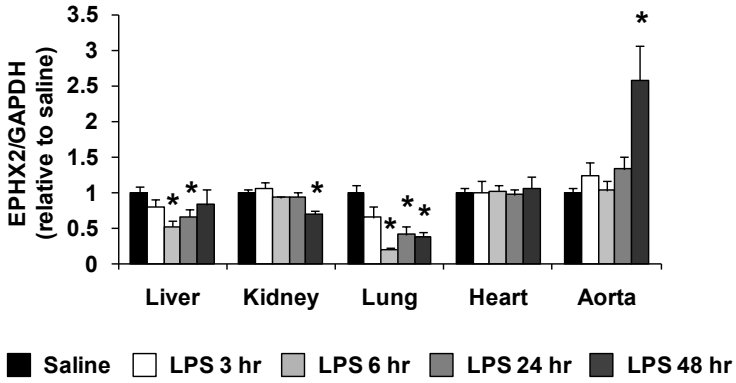

Figure 2.9: Effect of LPS administration on the functional balance between the CYP epoxygenase and ω-hydroxylase pathways in liver, kidney, lung, and heart

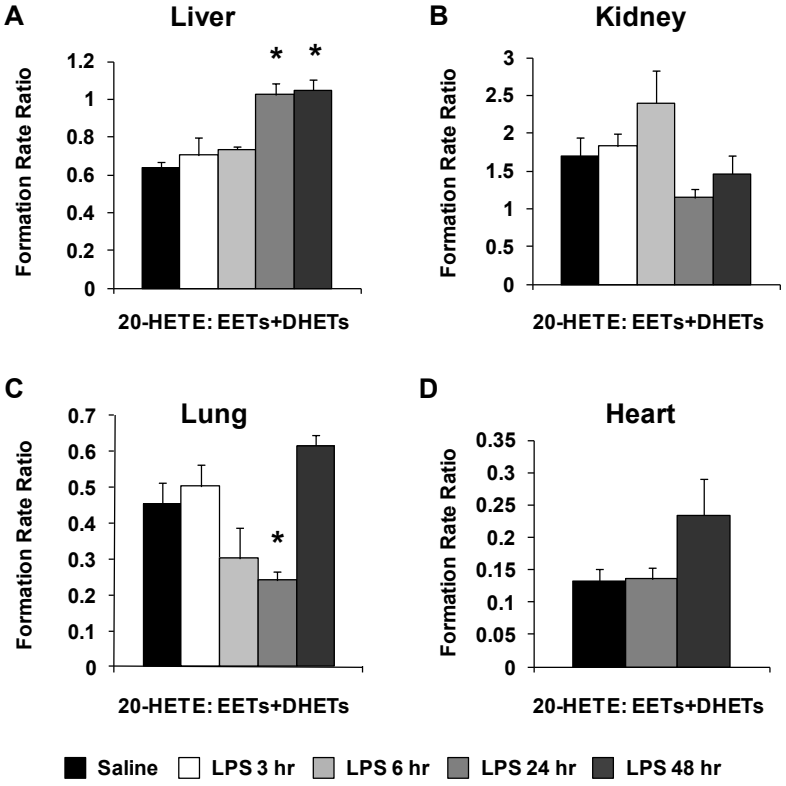

References

1. Roman RJ (2002) P-450 metabolites of arachidonic acid in the control of cardiovascular function. Physiol Rev 82: 131-185.

2. Zeldin DC (2001) Epoxygenase pathways of arachidonic acid metabolism. J Biol Chem 276: 36059-36062.

3. Deng Y, Theken KN, Lee CR (2010) Cytochrome P450 epoxygenases, soluble epoxide hydrolase, and the regulation of cardiovascular inflammation. J Mol Cell Cardiol 48: 331-341.

4. Node K, Huo Y, Ruan X, Yang B, Spiecker M, et al. (1999) Anti-inflammatory properties of cytochrome P450 epoxygenase-derived eicosanoids. Science 285: 1276-1279.

5. Ishizuka T, Cheng J, Singh H, Vitto MD, Manthati VL, et al. (2008) 20-Hydroxyeicosatetraenoic acid stimulates nuclear factor-kappaB activation and the production of inflammatory cytokines in human endothelial cells. J Pharmacol Exp Ther 324: 103-110.

6. Morgan ET (2001) Regulation of cytochrome p450 by inflammatory mediators: why and how? Drug Metab Dispos 29: 207-212.

7. Morgan ET, Goralski KB, Piquette-Miller M, Renton KW, Robertson GR, et al. (2008) Regulation of drug-metabolizing enzymes and transporters in infection, inflammation, and cancer. Drug Metab Dispos 36: 205-216.

8. Riddick DS, Lee C, Bhathena A, Timsit YE, Cheng PY, et al. (2004) Transcriptional suppression of cytochrome P450 genes by endogenous and exogenous chemicals. Drug Metab Dispos 32: 367-375.

9. Luo G, Zeldin DC, Blaisdell JA, Hodgson E, Goldstein JA (1998) Cloning and expression of murine CYP2Cs and their ability to metabolize arachidonic acid. Arch Biochem Biophys 357: 45-57.

10. Ma J, Qu W, Scarborough PE, Tomer KB, Moomaw CR, et al. (1999) Molecular cloning, enzymatic characterization, developmental expression, and cellular localization of a mouse cytochrome P450 highly expressed in kidney. J Biol Chem 274: 17777-17788.

11. DeLozier TC, Tsao CC, Coulter SJ, Foley J, Bradbury JA, et al. (2004) CYP2C44, a new murine CYP2C that metabolizes arachidonic acid to unique stereospecific products. J Pharmacol Exp Ther 310: 845-854.

12. Wang H, Zhao Y, Bradbury JA, Graves JP, Foley J, et al. (2004) Cloning, expression, and characterization of three new mouse cytochrome p450 enzymes and partial characterization of their fatty acid oxidation activities. Mol Pharmacol 65: 1148-1158.

13. Muller DN, Schmidt C, Barbosa-Sicard E, Wellner M, Gross V, et al. (2007) Mouse Cyp4a isoforms: enzymatic properties, gender- and strain-specific expression, and role in renal 20-hydroxyeicosatetraenoic acid formation. Biochem J 403: 109-118.

14. Qu W, Bradbury JA, Tsao CC, Maronpot R, Harry GJ, et al. (2001) Cytochrome P450 CYP2J9, a new mouse arachidonic acid omega-1 hydroxylase predominantly expressed in brain. J Biol Chem 276: 25467-25479.

15. Xu F, Falck JR, Ortiz de Montellano PR, Kroetz DL (2004) Catalytic activity and isoform-specific inhibition of rat cytochrome p450 4F enzymes. J Pharmacol Exp Ther 308: 887-895.

16. Christmas P, Jones JP, Patten CJ, Rock DA, Zheng Y, et al. (2001) Alternative splicing determines the function of CYP4F3 by switching substrate specificity. J Biol Chem 276: 38166-38172.

17. Powell PK, Wolf I, Jin R, Lasker JM (1998) Metabolism of arachidonic acid to 20-hydroxy-5,8,11, 14-eicosatetraenoic acid by P450 enzymes in human liver: involvement of CYP4F2 and CYP4A11. J Pharmacol Exp Ther 285: 1327-1336.

18. Pfaffl MW (2001) A new mathematical model for relative quantification in real-time RT-PCR. Nucleic Acids Res 29: e45.

19. Livak KJ, Schmittgen TD (2001) Analysis of relative gene expression data using real-time quantitative PCR and the 2(-Delta Delta C(T)) Method. Methods 25: 402-408.

20. Lee CR, Bottone FG, Jr., Krahn JM, Li L, Mohrenweiser HW, et al. (2007) Identification and functional characterization of polymorphisms in human cyclooxygenase-1 (PTGS1). Pharmacogenet Genomics 17: 145-160.

21. Poloyac SM, Tortorici MA, Przychodzin DI, Reynolds RB, Xie W, et al. (2004) The effect of isoniazid on CYP2E1- and CYP4A-mediated hydroxylation of arachidonic acid in the rat liver and kidney. Drug Metab Dispos 32: 727-733.

22. Athirakul K, Bradbury JA, Graves JP, DeGraff LM, Ma J, et al. (2008) Increased blood pressure in mice lacking cytochrome P450 2J5. Faseb J 22: 4096-4108.

23. Wu S, Moomaw CR, Tomer KB, Falck JR, Zeldin DC (1996) Molecular cloning and expression of CYP2J2, a human cytochrome P450 arachidonic acid epoxygenase highly expressed in heart. J Biol Chem 271: 3460-3468.

24. Miller TM, Donnelly MK, Crago EA, Roman DM, Sherwood PR, et al. (2009) Rapid, simultaneous quantitation of mono and dioxygenated metabolites of arachidonic acid in human CSF and rat brain. J Chromatogr B Analyt Technol Biomed Life Sci 877: 3991-4000.

25. Abdel-Razzak Z, Loyer P, Fautrel A, Gautier JC, Corcos L, et al. (1993) Cytokines down-regulate expression of major cytochrome P-450 enzymes in adult human hepatocytes in primary culture. Mol Pharmacol 44: 707-715.

26. Barclay TB, Peters JM, Sewer MB, Ferrari L, Gonzalez FJ, et al. (1999) Modulation of cytochrome P-450 gene expression in endotoxemic mice is tissue specific and peroxisome proliferator-activated receptor-alpha dependent. J Pharmacol Exp Ther 290: 1250-1257.

27. Sewer MB, Koop DR, Morgan ET (1996) Endotoxemia in rats is associated with induction of the P4504A subfamily and suppression of several other forms of cytochrome P450. Drug Metab Dispos 24: 401-407.

28. Anwar-Mohamed A, Zordoky BN, Aboutabl ME, El-Kadi AO (2010) Alteration of cardiac cytochrome P450-mediated arachidonic acid metabolism in response to lipopolysaccharide-induced acute systemic inflammation. Pharmacol Res 61: 410-418.

29. Kalsotra A, Cui X, Antonovic L, Robida AM, Morgan ET, et al. (2003) Inflammatory prompts produce isoform-specific changes in the expression of leukotriene B(4) omega-hydroxylases in rat liver and kidney. FEBS Lett 555: 236-242.

30. Cui X, Wu R, Zhou M, Simms HH, Wang P (2004) Differential expression of cytochrome P450 isoforms in the lungs of septic animals. Crit Care Med 32: 1186-1191.

31. Yaghi A, Bend JR, Webb CD, Zeldin DC, Weicker S, et al. (2004) Excess nitric oxide decreases cytochrome P-450 2J4 content and P-450-dependent arachidonic acid metabolism in lungs of rats with acute pneumonia. Am J Physiol Lung Cell Mol Physiol 286: L1260-1267.

32. Yaghi A, Bradbury JA, Zeldin DC, Mehta S, Bend JR, et al. (2003) Pulmonary cytochrome P-450 2J4 is reduced in a rat model of acute Pseudomonas pneumonia. Am J Physiol Lung Cell Mol Physiol 285: L1099-1105.

33. Kubala L, Schmelzer KR, Klinke A, Kolarova H, Baldus S, et al. (2010) Modulation of arachidonic and linoleic acid metabolites in myeloperoxidase-deficient mice during acute inflammation. Free Radic Biol Med 48: 1311-1320.

34. Schmelzer KR, Kubala L, Newman JW, Kim IH, Eiserich JP, et al. (2005) Soluble epoxide hydrolase is a therapeutic target for acute inflammation. Proc Natl Acad Sci U S A 102: 9772-9777.

35. Fife KL, Liu Y, Schmelzer KR, Tsai HJ, Kim IH, et al. (2008) Inhibition of soluble epoxide hydrolase does not protect against endotoxin-mediated hepatic inflammation. J Pharmacol Exp Ther 327: 707-715.

36. Pan J, Xiang Q, Ball S, Scatina J, Kao J, et al. (2003) Lipopolysaccharide-mediated modulation of cytochromes P450 in Stat1 null mice. Drug Metab Dispos 31: 392-397.

37. Richardson TA, Morgan ET (2005) Hepatic cytochrome P450 gene regulation during endotoxin-induced inflammation in nuclear receptor knockout mice. J Pharmacol Exp Ther 314: 703-709.

38. Szabo G, Romics L, Jr., Frendl G (2002) Liver in sepsis and systemic inflammatory response syndrome. Clin Liver Dis 6: 1045-1066.

39. Liu JY, Tsai HJ, Hwang SH, Jones PD, Morisseau C, et al. (2009) Pharmacokinetic optimization of four soluble epoxide hydrolase inhibitors for use in a murine model of inflammation. Br J Pharmacol 156: 284-296.

40. Luria A, Weldon SM, Kabcenell AK, Ingraham RH, Matera D, et al. (2007) Compensatory mechanism for homeostatic blood pressure regulation in Ephx2 gene-disrupted mice. J Biol Chem 282: 2891-2898.

Chapter III: Inhibition of the CYP ω-hydroxylase pathway does not attenuate LPS-induced acute inflammation

Accumulating evidence has demonstrated that cytochrome P450 (CYP)-derived metabolites of arachidonic acid regulate inflammation. Epoxyeicosatrienoic acids (EETs) possess potent anti-inflammatory properties by attenuating cytokine-induced leukocyte adhesion to the vascular wall via inhibition of nuclear factor-κB (NF-κB) activation [1]. Conversely, 20-hydroxyeicosatetraenoic acid (20-HETE) activates NF-κB signaling and induces expression of cellular adhesion molecules and cytokines, thereby promoting inflammation [2]. Because vascular inflammation is integral to the pathophysiology of atherosclerosis, modulation of CYP-mediated eicosanoid metabolism may represent a novel therapeutic strategy for the management of cardiovascular disease.

Although the anti-inflammatory properties of EETs have been well-established *in vitro*, the functional effects of potentiation of the CYP epoxygenase pathway, via enhancement of CYP-mediated EET formation or inhibition of sEH-mediated EET hydrolysis, on local, NF-κB-dependent inflammatory responses *in vivo* had not been rigorously investigated. Therefore, we assessed the acute vascular inflammatory response following lipopolysaccharide (LPS) administration in transgenic mice with endothelial expression of the human CYP epoxygenases (CYP2J2, CYP2C8) and mice with targeted disruption of sEH (*Ephx2*$^{-/-}$) [3]. LPS-induced NF-κB activation, cytokine, chemokine, and cellular adhesion molecule expression, and neutrophil infiltration in lung *in vivo* were significantly attenuated in CYP2J2 transgenic, CYP2C8 transgenic, and *Ephx2*$^{-/-}$ mice, compared to wild-type controls. Similar attenuation of NF-κB activation

and inflammatory mediator expression was observed in primary endothelial cells *in vitro*. Treatment with a putative EET receptor antagonist and CYP epoxygenase inhibitor abrogated this effect, demonstrating that the observed anti-inflammatory phenotype was mediated by CYP epoxygenase-derived EETs. These data demonstrate that potentiation of the CYP epoxygenase pathway attenuates acute vascular inflammation *in vivo* and may be a viable anti-inflammatory therapeutic strategy.

CYP-derived EETs and 20-HETE exhibit divergent effects on the regulation of inflammation *in vitro*, suggesting that dual modulation of the CYP epoxygenase and ω-hydroxylase pathways to increase EETs and decrease 20-HETE may have a greater anti-inflammatory effect than modulating either pathway independently. However, the role of 20-HETE in the regulation of acute inflammation *in vivo* has not been investigated. Therefore, we sought to determine whether inhibition of the CYP ω-hydroxylase pathway attenuates acute inflammation induced by LPS administration *in vivo*.

Methods

Reagents

All reagents were purchased from Fisher Scientific (Pittsburgh, PA, USA) unless otherwise noted.

Experimental protocol

All experiments were performed in 5-6 week old male C57BL/6 mice (Taconic, Hudson, NY). N-hydroxy-N'-(4-n-butyl-2-methylphenyl) formamidine (HET0016, Cayman Chemical, Ann Arbor, MI), an inhibitor of 20-HETE biosynthesis [4,5], was formulated as a hydroxypropyl-β-cyclodextrin complex, as previously described [6]. The putative 20-HETE receptor antagonist, N-[20-hydroxyeicosa-6(Z),15(Z)-dienoyl]glycine (20-HEDGE,

kindly provided by Dr. John Falck, University of Texas Southwestern Medical Center) was administered as a solution in sodium phosphate buffer [7]. In experiments 2 and 3, acute inflammation was induced by intraperitoneal (IP) injection of *E. coli* LPS (serotype O111:B4, 1,000,000 EU/mg; Sigma, St. Louis, MO).

Experiment 1: Mice were treated with HET0016 at a dose of 1 mg/kg or 2.5 mg/kg IP and were euthanized by CO_2 inhalation 30, 60, or 90 minutes following HET0016 administration (N=4/time point). Untreated mice (N=4) were used to assess basal 20-HETE levels. Liver was harvested and flash frozen in liquid nitrogen.

Experiment 2: Mice were treated with LPS 1 mg/kg (N=36) or endotoxin-free saline (N=20) by IP injection. HET0016 1 mg/kg IP, HET0016 2.5 mg/kg IP, or 20-HEDGE 30 mg/kg SC [7] was administered concurrently with LPS (N=8/group) or saline (N=4/group), and mice were euthanized by CO_2 inhalation 3 hours after treatment. Liver and heart were harvested and flash frozen in liquid nitrogen. Blood was collected in heparinized tubes, and plasma was separated by centrifugation.

Experiment 3: Mice were randomized to receive HET0016 as a single-dose (1 mg/kg IP) or multiple-dose (1 mg/kg IP x 3 days). Concurrent with the final dose of HET0016, mice were treated with LPS 1 mg/kg (N=8/group), LPS 10 mg/kg (N=8/group), or endotoxin-free saline (N=4/group) by IP injection and were euthanized by CO_2 inhalation 90 minutes later. Liver and lung were harvested and flash frozen in liquid nitrogen.

All studies were in accordance with principles outlined in the *NIH Guide for the Care and Use of Laboratory Animals* and were approved by the Institutional Animal Care and Use Committee at the University of North Carolina at Chapel Hill.

RNA isolation, reverse transcription, and qRT-PCR

Total RNA was isolated from whole tissue homogenates using the RNeasy Miniprep Kit (QIAGEN, Valencia, CA) per the manufacturer's instructions, as previously

described [8]. Total RNA was reverse transcribed to cDNA using the ABI High Capacity cDNA Reverse Transcription Kit (Applied Biosystems, Foster City, CA) with a reaction temperature of 25ºC for 10 minutes then 37ºC for 120 minutes. Expression of murine *Ccl2* (Mm00441242_m1), *Sele* (Mm00441278_m1), *Tnf* (Mm00443258_m1), and *GAPDH* (Mm99999915_m1) were quantified by quantitative RT-PCR using commercially available Taqman® Assays on Demand (Applied Biosystems). mRNA levels were normalized to *GAPDH* and expressed relative to the saline/no inhibitor controls using the $2^{-\Delta\Delta Ct}$ method [9].

Tissue Extraction

Liver tissue was homogenized in 0.12 M potassium phosphate buffer containing 0.113 mM butylated hydroxytoluene. Homogenates were centrifuged at 4ºC at 10000 x *g* for 30 minutes to remove cellular debris. The supernatant was retained, and 20-HETE-d6 was added as an internal standard. Samples were loaded onto Oasis HLB (30 mg) SPE cartridges (Waters, Milford, MA) that were conditioned and equilibrated with 1 mL of methanol and 1 mL of water, respectively. Columns were washed with three 1 mL volumes of 5% methanol and were eluted with 100% methanol. Extracts were dried under nitrogen gas at 37°C and reconstituted in 125 µL of 80:20 methanol:deionized water.

UPLC-MS/MS

Arachidonic acid metabolites (14,15-EET, 11,12-EET, 8,9-EET, 14,15-DHET, 11,12-DHET, 8,9-DHET, 5,6-DHET, and 20-HETE) in tissue extracts were quantified by UPLC-MS/MS as previously described [8,10]. Briefly, analytes were separated on a UPLC BEH C-18, 1.7 µm (2.1 mm x 100 mm) reversed-phase column (Waters, Milford, MA). Mass spectrometric analysis was performed with a TSQ Quantum Ultra (Thermo Fisher Scientific, San Jose, CA) triple quadrupole mass spectrometer coupled with

heated electrospray ionization (HESI) operated in negative selective reaction monitoring (SRM) mode. Analytical data was acquired and analyzed using Xcaliber software version 2.0.6 (ThermoFinnigan, San Jose, CA). Metabolite concentrations were calculated from a standard curve and expressed relative to tissue weight (pmol/g tissue).

Quantification of plasma leukotriene B_4 levels

Plasma leukotriene B_4 (LTB_4) concentrations were quantified using the LTB_4 Parameter™ immunoassay kit, according to the manufacturer's instructions (R&D Systems, Minneapolis, MN, USA).

NF-κB activation

Liver tissue was homogenized in ice-cold lysis buffer containing 50 mM Tris-HCl (pH 7.4), 150 mM NaCl, 1 mM EDTA, 1% Triton X, 1 mM NaF, 0.25% Na deoxycholate and protease inhibitors, and the S9 fraction was separated by centrifugation. NF-κB activity was assessed in liver lysates using the NF-κB p50/p65 EZ-TFA Transcription Factor Assay kit (Millipore, Billerica, MA), according to the manufacturer's instructions.

Statistical analysis

All data are expressed as mean ± standard error of the mean (SEM). The sum concentration of all EET and DHET regioisomers was calculated and used as an index of total CYP epoxygenase metabolic activity. Because the data were not normally distributed, mRNA levels were transformed to ranks and metabolite concentrations were log-transformed prior to statistical analysis. Data were analyzed by one-way ANOVA followed by post-hoc Tukey's test. Statistical analysis was performed using SAS software version 9.1.3 (SAS Institute, Cary, NC). $P<0.05$ was considered statistically significant.

Results

Experiment 1: Effect of HET0016 on hepatic CYP-derived eicosanoid concentrations

We quantified hepatic 20-HETE and EET+DHET concentrations following HET0016 administration to determine the time course of inhibition of 20-HETE formation and confirm that HET0016 selectively inhibited the CYP ω-hydroxylase pathway. Both doses of HET0016 (1 mg/kg and 2.5 mg/kg) significantly decreased hepatic 20-HETE levels by 75-80% 30 minutes after administration (Figure 3.1A). At 90 minutes, hepatic 20-HETE concentrations remained 55-60% lower in HET0016-treated mice, compared baseline (36.1±4.6 pmol/g tissue). Compared to untreated mice, hepatic EET+DHET concentrations were modestly lower in mice treated with HET0016 1 mg/kg at 30 minutes. However, no other significant alterations in hepatic EET+DHET concentrations were observed (Figure 3.1B), demonstrating that HET0016 selectively inhibited 20-HETE biosynthesis.

Experiment 2: Effect of HET0016 and 20-HEDGE on LPS-induced inflammatory gene expression in liver and heart

HET0016 or 20-HEDGE was administered to evaluate the effects of inhibition of 20-HETE biosynthesis or the putative 20-HETE receptor, respectively, on inflammatory gene expression 3 hours after LPS administration. In both liver and heart, LPS significantly induced *Tnf* expression, relative to saline control. In liver, treatment with HET0016 1 mg/kg, HET0016 2.5 mg/kg, or 20-HEDGE did not attenuate LPS-induced *Tnf* expression (Figure 3.2A). Myocardial *Tnf* mRNA levels were significantly higher in HET0016-treated mice, compared to LPS alone ($P<0.05$) (Figure 3.2B). No differences in myocardial *Tnf* expression were observed in 20-HEDGE-treated mice. Similar results were observed for myocardial *Ccl2* and *Sele* mRNA expression (data not shown). No

differences in *Tnf* mRNA levels in either liver or heart were observed across inhibitor groups in saline-treated mice.

CYP4F isoforms inactivate LTB_4, a pro-inflammatory eicosanoid, in addition to catalyzing 20-HETE formation [11]. Consequently, inhibition of CYP4F isoforms may result in elevated LTB_4 levels. Although no studies have reported elevations in LTB_4 levels following HET0016 administration, we measured plasma LTB_4 levels in LPS-treated mice to determine whether the lack of an anti-inflammatory effect of HET0016 treatment was due to inhibition of CYP4F-mediated LTB_4 clearance. Mice treated with HET0016 2.5 mg/kg tended to have higher plasma LTB_4 concentrations following LPS administration compared to mice that received no inhibitor, but this difference was not statistically significant (P=0.210) (Figure 3.3).

Liver 20-HETE and EET+DHET concentrations were also measured to confirm that HET0016 had selectively inhibited 20-HETE formation. No significant differences in hepatic 20-HETE or EET+DHET concentration were observed between the treatment groups (Figure 3.4), indicating that CYP ω-hydroxylase activity had returned to basal levels 3 hours after HET0016 administration.

Experiment 3: Effect of single- and multiple-dose HET0016 on LPS-induced inflammatory gene expression and NF-κB activation

Because 20-HETE formation had returned to basal levels at 3 hours, we evaluated the effect of single- or multiple-dose HET0016 on inflammatory gene expression and NF-κB activation 90 minutes after LPS administration. Both LPS 1 mg/kg (1256.8±161.4) and 10 mg/kg (877.9±108.9) significantly induced hepatic *Sele* expression at 90 minutes, compared to saline (1.1±0.4, P<0.05). Neither single- nor multiple-dose HET0016 treatment attenuated the upregulation of hepatic *Sele* expression (Figure 3.5A). Similar results were observed for hepatic *Tnf* and *Ccl2* mRNA

expression (data not shown). Consistent with these observations, no differences in hepatic NF-κB activation was observed with either single- or multiple-dose HET0016, compared to LPS alone (Figure 3.5C). Similarly, pulmonary *Sele* mRNA levels were significantly higher in LPS-treated mice (1 mg/kg: 218.3±34.5; 10 mg/kg: 246.1±58.8), compared to saline (1.1±0.3, $P<0.05$). HET0016 administered as a single- or multiple-dose regimen did not attenuate this response (Figure 3.5B).

Discussion

In vitro, 20-HETE activates NF-κB and stimulates cytokine and cellular adhesion molecule expression, but the role of the CYP ω-hydroxylase pathway in regulating the acute inflammatory response *in vivo* has not been investigated. Following LPS administration, inhibition of 20-HETE biosynthesis or the putative 20-HETE receptor did not attenuate inflammatory gene expression, regardless of the dose or treatment regimen. Collectively, our findings demonstrate the CYP ω-hydroxylase pathway does not contribute to the acute inflammatory response following LPS administration.

We have recently shown that potentiation of the CYP epoxygenase attenuates acute vascular inflammation *in vivo* [3]. Therefore, a similar study design was used in Experiment 2 to investigate the effect of inhibition of the CYP ω-hydroxylase pathway on the acute inflammatory response. In contrast to our hypothesis, inhibition of 20-HETE biosynthesis with HET0016 or inhibition of the putative 20-HETE receptor with 20-HEDGE did not attenuate hepatic or myocardial inflammatory gene expression 3 hours after LPS administration. We investigated several potential explanations for the negative results that we observed. Because CYP4F isoforms inactivate LTB_4, a pro-inflammatory eicosanoid, in addition to catalyzing 20-HETE formation [11], we measured plasma LTB_4 levels to determine whether HET0016 administration impaired LTB_4 clearance. Although not statistically significant, there was a trend toward higher plasma LTB_4 concentrations

in the mice treated with HET0016 2.5 mg/kg, which may have contributed to the trend toward modestly higher inflammatory gene expression in this treatment group. Consequently, only the HET0016 1 mg/kg dose was used in Experiment 3. We also measured hepatic 20-HETE concentrations to determine whether HET0016 administration had inhibited the CYP ω-hydroxylase pathway for the full duration of the experiment. Previous studies have shown that HET0016 has a short half-life [12], suggesting that the inhibitor may have been cleared before the 3-hour time point. We observed no significant differences in hepatic 20-HETE concentrations between mice that received no inhibitor and those treated with HET0016, indicating that CYP ω-hydroxylase activity had returned to basal levels.

Experiment 3 was designed to address these limitations, as well as investigate other potential explanations for the lack of an effect in Experiment 2. First, the time point was changed to 90 minutes, rather than 3 hours, because HET0016 inhibited 20-HETE formation through 90 minutes in Experiment 1. Studies evaluating the anti-inflammatory effect of potentiating the CYP epoxygenase pathway have typically used doses of LPS ranging from 10 to 40 mg/kg [3,13,14]. Consequently, we included a 10 mg/kg dose of LPS to determine whether an anti-inflammatory effect of inhibiting the CYP ω-hydroxylase pathway would become apparent at higher LPS doses. In addition to being formed *de novo*, 20-HETE can be stored in cell membranes and released pre-formed upon activation of phospholipase A_2 by inflammatory stimuli [15]. Therefore, we included a multiple-dose HET0016 regimen in Experiment 3 to deplete membrane stores of 20-HETE prior to LPS administration. Finally, the anti-inflammatory effect of potentiating the CYP epoxygenase pathway was most apparent in lung [3]. Therefore, we measured inflammatory gene expression in lung, as well as in liver. Regardless of the time point, LPS dose, HET0016 treatment regimen, or tissue evaluated, inhibition of the CYP ω-

hydroxylase pathway did not attenuate the acute inflammatory response to LPS administration.

LPS potently stimulates the acute innate immune response and activates multiple cell signaling cascades to promote NF-κB activation and inflammatory gene expression [16]. Our findings demonstrate that 20-HETE is not a key contributor to LPS-induced acute inflammation *in vivo*. However, accumulating evidence suggests that 20-HETE may be more relevant in the regulation of vascular inflammation in models of cardiovascular disease. In endothelial cell culture, 20-HETE stimulated the production of reactive oxygen species by NADPH oxidase [17] and endothelial nitric oxide synthase uncoupling via NF-κB activation [18,19], which are key processes in the development of endothelial dysfunction and vascular inflammation *in vivo* [20]. A recent study demonstrated that 20-HETE induced expression of angiotensin converting enzyme and the angiotensin II receptor in aorta [21], suggesting the CYP ω-hydroxylase pathway may also promote vascular inflammation by directly activating the renin-angiotensin system. In a model of androgen-induced hypertension, which is mediated by overproduction of 20-HETE in the vasculature, inhibition of the CYP ω-hydroxylase pathway lowered blood pressure, attenuated NF-κB activation, and improved endothelial function [22]. Further studies to elucidate the role of the CYP ω-hydroxylase pathway in other models of cardiovascular disease and chronic vascular inflammation are warranted.

In conclusion, our findings demonstrate that inhibition of 20-HETE biosynthesis or the putative 20-HETE receptor does not attenuate the acute inflammatory response to LPS *in vivo*. Future studies investigating the anti-inflammatory effect of inhibiting the CYP ω-hydroxylase pathway on chronic vascular inflammation are necessary.

Figure Legends

Figure 3.1: Time course of liver (A) 20-HETE and (B) EET+DHET tissue concentrations after intraperitoneal administration of HET0016 1 mg/kg (N=4/time point) or HET0016 2.5 mg/kg (N=4/time point). *P<0.05 versus baseline

Figure 3.2: The effect of HET0016 1 mg/kg, HET0016 2.5 mg/kg, or 20-HEDGE administration on *Tnf* mRNA levels in (A) liver and (B) heart, 3 hours after LPS treatment (1 mg/kg), expressed relative to the saline control group (LPS: N=12; HET0016 1 mg/kg: N=8; HET0016 2.5 mg/kg: N=8; 20-HEDGE: N=8). *P<0.05 versus LPS

Figure 3.3: The effect of HET0016 1 mg/kg or HET0016 2.5 mg/kg on plasma LTB_4 concentrations 3 hours after LPS treatment (N=5/group).

Figure 3.4: The effect of HET0016 1 mg/kg and HET0016 2.5 mg/kg on liver (A) 20-HETE and (B) EET+DHET tissue concentrations, 3 hours after the administration of LPS (N=6/group) or saline (N=4/group).

Figure 3.5: The effect of single- or multiple-dose HET0016 on (A) hepatic and (B) pulmonary *Sele* mRNA levels (N=8/group) and (C) NF-κB activity in liver lysates (N=4/group), 90 minutes after LPS treatment (1 mg/kg or 10 mg/kg), expressed relative to the saline control group.

Figure 3.1: Effect of HET0016 on hepatic 20-HETE and EET+DHET concentrations

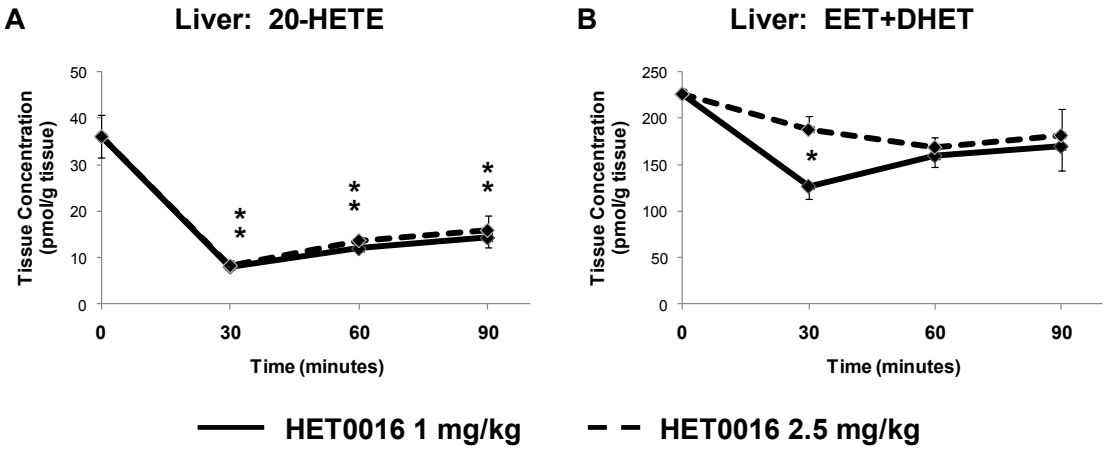

Figure 3.2: Effect of HET0016 and 20-HEDGE on LPS-induced TNF-α expression

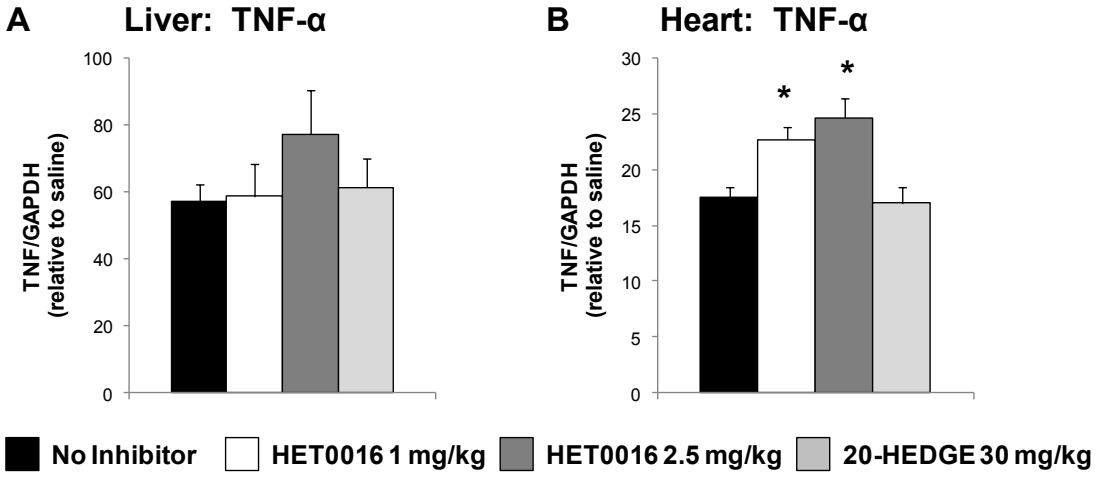

Figure 3.3: Effect of HET0016 on plasma LTB_4 levels

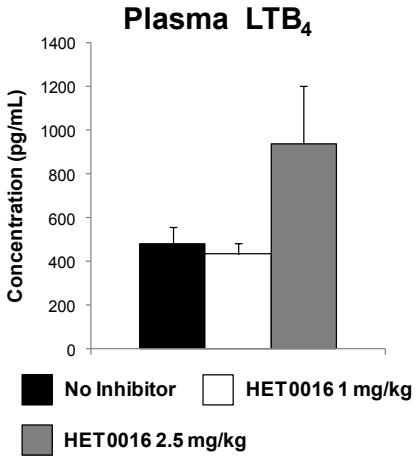

Figure 3.4: Effect of HET0016 on hepatic 20-HETE and EET+DHET concentrations 3 hours after administration

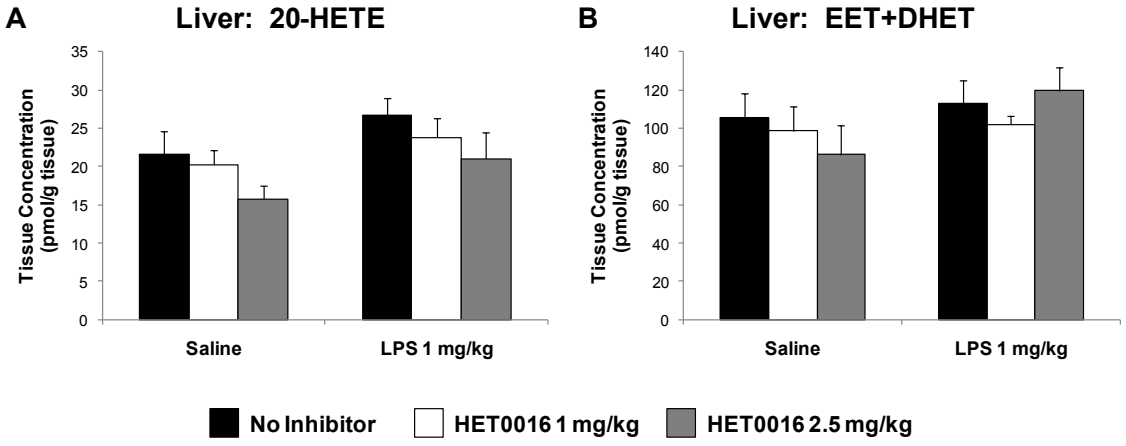

Figure 3.5: Effect of HET0016 on LPS-induced E-selection mRNA expression and NF-κB activation

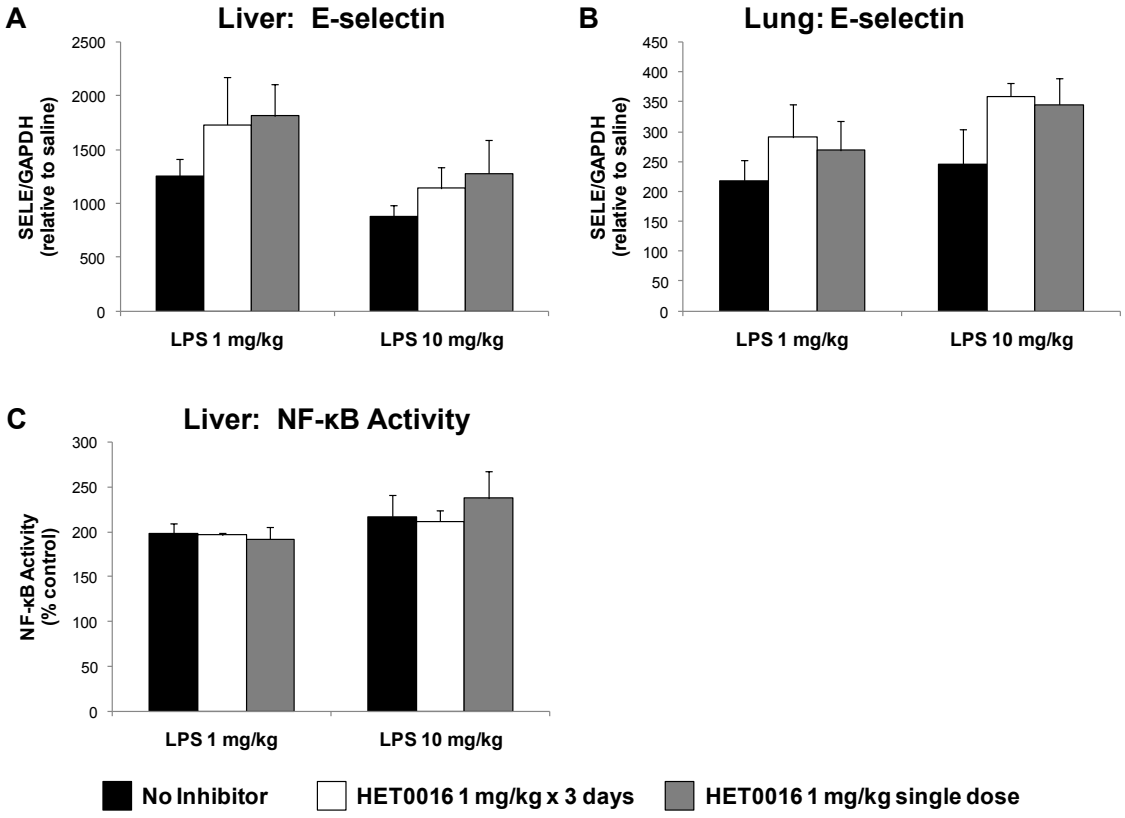

References

1. Node K, Huo Y, Ruan X, Yang B, Spiecker M, et al. (1999) Anti-inflammatory properties of cytochrome P450 epoxygenase-derived eicosanoids. Science 285: 1276-1279.

2. Ishizuka T, Cheng J, Singh H, Vitto MD, Manthati VL, et al. (2008) 20-Hydroxyeicosatetraenoic acid stimulates nuclear factor-kappaB activation and the production of inflammatory cytokines in human endothelial cells. J Pharmacol Exp Ther 324: 103-110.

3. Deng Y, Edin ML, Theken KN, Schuck RN, Flake GP, et al. (2011) Endothelial CYP epoxygenase overexpression and soluble epoxide hydrolase disruption attenuate acute vascular inflammatory responses in mice. FASEB J 25: 703-713.

4. Miyata N, Taniguchi K, Seki T, Ishimoto T, Sato-Watanabe M, et al. (2001) HET0016, a potent and selective inhibitor of 20-HETE synthesizing enzyme. Br J Pharmacol 133: 325-329.

5. Seki T, Wang MH, Miyata N, Laniado-Schwartzman M (2005) Cytochrome P450 4A isoform inhibitory profile of N-hydroxy-N'-(4-butyl-2-methylphenyl)-formamidine (HET0016), a selective inhibitor of 20-HETE synthesis. Biol Pharm Bull 28: 1651-1654.

6. Mu Y, Klamerus MM, Miller TM, Rohan LC, Graham SH, et al. (2008) Intravenous formulation of N-hydroxy-N'-(4-n-butyl-2-methylphenyl)formamidine (HET0016) for inhibition of rat brain 20-hydroxyeicosatetraenoic acid formation. Drug Metab Dispos 36: 2324-2330.

7. Tunctan B, Korkmaz B, Buharalioglu CK, Firat SS, Anjaiah S, et al. (2008) A 20-hydroxyeicosatetraenoic acid agonist, N-[20-hydroxyeicosa-5(Z),14(Z)-dienoyl]glycine, opposes the fall in blood pressure and vascular reactivity in endotoxin-treated rats. Shock 30: 329-335.

8. Theken KN, Deng Y, Kannon MA, Miller TM, Poloyac SM, et al. (2011) Activation of the acute inflammatory response alters cytochrome P450 expression and eicosanoid metabolism. Drug Metab Dispos 39: 22-29.

9. Livak KJ, Schmittgen TD (2001) Analysis of relative gene expression data using real-time quantitative PCR and the 2(-Delta Delta C(T)) Method. Methods 25: 402-408.

10. Miller TM, Donnelly MK, Crago EA, Roman DM, Sherwood PR, et al. (2009) Rapid, simultaneous quantitation of mono and dioxygenated metabolites of arachidonic acid in human CSF and rat brain. J Chromatogr B Analyt Technol Biomed Life Sci 877: 3991-4000.

11. Kalsotra A, Strobel HW (2006) Cytochrome P450 4F subfamily: at the crossroads of eicosanoid and drug metabolism. Pharmacol Ther 112: 589-611.

12. Poloyac SM, Zhang Y, Bies RR, Kochanek PM, Graham SH (2006) Protective effect of the 20-HETE inhibitor HET0016 on brain damage after temporary focal ischemia. J Cereb Blood Flow Metab 26: 1551-1561.

13. Luria A, Weldon SM, Kabcenell AK, Ingraham RH, Matera D, et al. (2007) Compensatory mechanism for homeostatic blood pressure regulation in Ephx2 gene-disrupted mice. J Biol Chem 282: 2891-2898.

14. Schmelzer KR, Kubala L, Newman JW, Kim IH, Eiserich JP, et al. (2005) Soluble epoxide hydrolase is a therapeutic target for acute inflammation. Proc Natl Acad Sci U S A 102: 9772-9777.

15. Carroll MA, Balazy M, Huang DD, Rybalova S, Falck JR, et al. (1997) Cytochrome P450-derived renal HETEs: storage and release. Kidney Int 51: 1696-1702.

16. Guha M, Mackman N (2001) LPS induction of gene expression in human monocytes. Cell Signal 13: 85-94.

17. Medhora M, Chen Y, Gruenloh S, Harland D, Bodiga S, et al. (2008) 20-HETE increases superoxide production and activates NAPDH oxidase in pulmonary artery endothelial cells. Am J Physiol Lung Cell Mol Physiol 294: L902-911.

18. Cheng J, Ou JS, Singh H, Falck JR, Narsimhaswamy D, et al. (2008) 20-hydroxyeicosatetraenoic acid causes endothelial dysfunction via eNOS uncoupling. Am J Physiol Heart Circ Physiol 294: H1018-1026.

19. Cheng J, Wu CC, Gotlinger KH, Zhang F, Falck JR, et al. (2010) 20-hydroxy-5,8,11,14-eicosatetraenoic acid mediates endothelial dysfunction via IkappaB kinase-dependent endothelial nitric-oxide synthase uncoupling. J Pharmacol Exp Ther 332: 57-65.

20. Kawashima S, Yokoyama M (2004) Dysfunction of endothelial nitric oxide synthase and atherosclerosis. Arterioscler Thromb Vasc Biol 24: 998-1005.

21. Sodhi K, Wu CC, Cheng J, Gotlinger K, Inoue K, et al. (2010) CYP4A2-induced hypertension is 20-hydroxyeicosatetraenoic acid- and angiotensin II-dependent. Hypertension 56: 871-878.

22. Wu CC, Cheng J, Zhang FF, Gotlinger KH, Kelkar M, et al. (2011) Androgen-dependent hypertension is mediated by 20-hydroxy-5,8,11,14-eicosatetraenoic acid-induced vascular dysfunction: role of inhibitor of kappaB Kinase. Hypertension 57: 788-794.

Chapter IV: Enalapril reverses high fat diet-induced alterations in cytochrome P450-mediated eicosanoid metabolism

Cytochrome P450 enzymes (CYPs) metabolize arachidonic acid to various biologically active eicosanoids. Olefin epoxidation by CYP2C and CYP2J isoforms produces four epoxyeicosatrienoic acid regioisomers (5,6-, 8,9-, 11,12-, and 14,15-EET), which possess potent vasodilatory and anti-inflammatory properties [1,2]. The EETs are rapidly hydrolyzed by soluble epoxide hydrolase (sEH) to the corresponding dihydroxyeicosatrienoic acids (DHETs), which are generally less biologically active [1,2]. In contrast, CYP4A and CYP4F isoforms catalyze the ω-hydroxylation of arachidonic acid to 20-hydroxyeicosatetraenoic acid (20-HETE), a vasoconstrictive and pro-inflammatory eicosanoid [3]. Numerous preclinical studies have demonstrated that the CYP epoxygenase and ω-hydroxylase pathways are important in the maintenance of cardiovascular homeostasis following pathologic insult [1,2,3], and modulating these pathways may be a therapeutic strategy for the treatment of cardiovascular disease.

The pathophysiology of cardiovascular disease is complex, and multiple risk factors contribute to its development and progression. One risk factor that is becoming increasing prevalent is metabolic syndrome, a pro-thrombotic, pro-inflammatory state characterized by the presence of dyslipidemia, insulin resistance, and hypertension [4]. The liver and kidney are integrally involved in the pathophysiology of metabolic syndrome via their roles in the regulation of inflammation, insulin sensitivity, and blood pressure, and CYP epoxygenases and ω-hydroxylases are most abundantly expressed in both tissues [5]. Due to the divergent effects of the CYP epoxygenase-derived EETs and CYP ω-hydroxylase-derived 20-HETE in the regulation of vascular tone and

inflammation, alterations in the functional balance between these parallel pathways in liver and kidney may contribute to the pathogenesis and progression of metabolic syndrome and cardiovascular disease.

Preclinical studies suggest that CYP expression and metabolic activity is altered in models of metabolic syndrome. Alterations in hepatic and renal CYP expression and metabolic activity have been observed in rodents genetically predisposed to obesity, including obese Zucker rats [6,7,8], *ob/ob* mice [9,10], and *db/db* mice [11,12]. Although these models exhibit many of the characteristics of human metabolic syndrome, other metabolic derangements may also be present [13]. For example, these obese rodent models appear to have lower renin-angiotensin system activity compared to lean controls [14,15,16], while the renin-angiotensin system is activated in obese humans [17]. Consequently, the alterations in CYP expression and metabolic activity observed in rodents genetically predisposed to obesity may not accurately model the pathophysiology underlying human metabolic syndrome. In contrast, the phenotype induced by high fat diet feeding in rodents more closely mimics human metabolic syndrome [18].

Importantly, the effects of high fat diet on hepatic and renal CYP epoxygenase and ω-hydroxylase expression and metabolic activity and the functional balance between the pathways have not been rigorously evaluated to date. Moreover, the mechanisms underlying the observed alterations in CYP expression and metabolic activity in response to high fat diet feeding have not been elucidated. Therefore, we sought to (1) characterize the effect of high fat diet feeding on the functional balance between the CYP epoxygenase and ω-hydroxylase pathways in liver and kidney, and (2) investigate the role of hypercholesterolemia, insulin resistance, and renin-angiotensin system activation in mediating alterations in CYP-mediated eicosanoid metabolism in high fat diet-fed mice.

Methods

Reagents

All reagents were purchased from Fisher Scientific (Pittsburgh, PA) unless otherwise noted.

Experimental Protocol

All experiments were performed in 8-10 week old male mice (Taconic, Hudson, NY). Mice randomized to high fat diet received RD Western Diet (21% fat, 0.21% cholesterol; Research Diets Inc., New Brunswick, NJ). Standard diet-fed mice received ProLab RMH 3000 rodent chow (5% fat; PMI Nutrition International LLC, Brentwood, MO). Mice had access to food and water *ad libitum*. The treatment schemes for the effect of high fat diet over time (Experiment 1) and the effects of enalapril and metformin treatment (Experiments 2 and 3) are depicted in Figure 4.1.

Experiment 1: Wild-type C57BL/6 (WT) and *ApoE*$^{-/-}$ mice were randomized to receive high fat or standard diet for two, four, or eight weeks (N=4 per group), as shown in Figure 4.1A.

Experiment 2: WT and *ApoE*$^{-/-}$ mice were randomized to high fat (N=10 per genotype) or standard diet (N=4 per genotype). After two weeks of the assigned diet, a subset of high fat diet-fed mice were treated with enalapril (30 mg/kg/day, Sigma-Aldrich, St. Louis, MO) [19] administered in the drinking water for two weeks (N=6 per genotype), as shown in Figure 4.1B.

Experiment 3: WT mice were randomized to high fat (N=18) or standard diet (N=23). After two weeks of the assigned diet, a subset of mice were treated with metformin (300 mg/kg/day, Sigma-Aldrich, N=6 per diet) [20] or enalapril (30 mg/kg/day, N=6 per diet) administered in the drinking water for two weeks, as shown in Figure 4.1B.

Mice were euthanized by CO_2 inhalation, and liver and kidney tissue was harvested and flash frozen in liquid nitrogen. Blood was collected via cardiac puncture, and plasma was separated by centrifugation. Tissue and plasma were stored at -80ºC pending analysis. Plasma insulin concentrations were measured with the Rat/Mouse Insulin ELISA kit (Millipore, Billerica, MA), per the manufacturer's instructions. Plasma glucose and total cholesterol levels were measured by the Animal Clinical Laboratory Core Facility at UNC-Chapel Hill using a Vitros 350 automated chemical analyzer (Ortho-Clinical Diagnostics, Rochester, NY).

All studies were in accordance with principles outlined in the *NIH Guide for the Care and Use of Laboratory Animals* and were approved by the Institutional Animal Care and Use Committee at the University of North Carolina at Chapel Hill.

RNA isolation, reverse transcription, and qRT-PCR

Total RNA was isolated from whole tissue homogenates using the RNeasy Miniprep Kit (QIAGEN, Valencia, CA) per the manufacturer's instructions, as previously described [5]. Total RNA was reverse transcribed to cDNA using the ABI High Capacity cDNA Reverse Transcription Kit (Applied Biosystems, Foster City, CA) with a reaction temperature of 25ºC for 10 minutes then 37ºC for 120 minutes. Expression of murine *Cyp2c29*, *Cyp2j5*, *Cyp4a12a*, and *GAPDH* were quantified by quantitative RT-PCR using commercially available Taqman® Assays on Demand (Applied Biosystems). CYP isoforms were selected because they are the most abundant CYP epoxygenase (liver: *Cyp2c29*; kidney: *Cyp2j5*) or ω-hydroxylase (liver and kidney: *Cyp4a12a*) in each tissue [5]. CYP mRNA levels were normalized to *GAPDH* and expressed relative to the WT/standard diet controls using the $2^{-\Delta\Delta Ct}$ method [21].

Microsome isolation

Hepatic and renal microsomal fractions were isolated as previously described [5]. Briefly, frozen tissue was homogenized in 0.25 M sucrose/10mM Tris-HCl buffer (pH 7.5) containing protease inhibitors. Homogenates were centrifuged at 4ºC at 2570 x *g* for 20 minutes, then at 10300 x *g* for 20 minutes to remove cellular debris. The supernatants were then centrifuged at 100000 x *g* at 4ºC for 90 minutes. The resulting microsomal pellets were resuspended in 50 mM Tris/1 mM DTT/1 mM EDTA buffer (pH 7.5) containing 20% glycerol. Protein concentrations were quantified using the Bio-Rad protein assay (Bio-Rad, Hercules, CA), per the manufacturer's instructions.

Microsomal incubations

Incubations contained 300 µg microsomal protein and 50 µM arachidonic acid in a 1 mL volume of 0.12 M potassium phosphate incubation buffer containing 5 mM magnesium chloride, as previously described [5,22]. Reactions were initiated by the addition of 1 mM NADPH and were carried out at 37ºC for 20 minutes. Incubations were carried out at saturating concentrations of substrate, and metabolite formation was linear with respect to incubation time and microsomal protein, as determined from preliminary incubations. In the presence of these saturating substrate concentrations, formation rates reflect the amount of metabolically active protein [22], and are significantly correlated with CYP mRNA and protein levels [5]. The reactions were stopped by placing the samples on ice, and 12.5 ng 20-HETE-d6 was added as an internal standard. Due to high metabolite formation, liver incubations were diluted 10-fold in incubation buffer prior to addition of internal standard. Metabolites were extracted with diethyl ether, evaporated to dryness under nitrogen gas, and reconstituted in 80% methanol in deionized water for analysis.

UPLC-MS/MS

Arachidonic acid metabolites (14,15-EET, 11,12-EET, 8,9-EET, 14,15-DHET, 11,12-DHET, 8,9-DHET, 5,6-DHET, and 20-HETE) in microsomal incubations were quantified by UPLC-MS/MS as previously described [5,23]. Briefly, analytes were separated on a UPLC BEH C-18, 1.7 μm (2.1 mm x 100 mm) reversed-phase column (Waters, Milford, MA). Mass spectrometric analysis was performed with a TSQ Quantum Ultra (Thermo Fisher Scientific, San Jose, CA) triple quadrupole mass spectrometer coupled with heated electrospray ionization (HESI) operated in negative selective reaction monitoring (SRM) mode. Analytical data was acquired and analyzed using Xcaliber software version 2.0.6 (ThermoFinnigan, San Jose, CA). Metabolite concentrations were calculated from a standard curve and expressed as formation rates (pmol/mg protein/min).

Statistical analysis

All data are expressed as mean ± standard error of the mean (SEM). The sum formation rate of all EET and DHET regioisomers was calculated and used as an index of total CYP epoxygenase metabolic activity. The functional balance between the CYP epoxygenase and ω-hydroxylase pathways was assessed by calculating the ratio of 20-HETE formation to EET+DHET formation (20-HETE:EET+DHET). Because the data were not normally distributed, mRNA levels were transformed to ranks and metabolite formation rates and clinical chemistry values were log-transformed prior to statistical analysis. To evaluate the effect of high fat diet on CYP expression and metabolic activity over time, data from WT/standard diet-fed mice at each time point were pooled to create a single control group, and data were analyzed by one-way ANOVA followed by post-hoc Dunnett's test for comparison to the pooled control group. To determine the effect of enalapril and metformin treatment, data were analyzed by one-way ANOVA

followed by post-hoc Tukey's test. The relationship between CYP mRNA levels and EET+DHET or 20-HETE formation was evaluated by Spearman rank correlation. Statistical analysis was performed using SAS software (v.9.1.3, SAS Institute, Cary, NC). $P<0.05$ was considered statistically significant.

Results

Experiment 1: Effect of high fat diet on CYP epoxygenase and ω-hydroxylase metabolic activity over time

To characterize the effect of high fat diet feeding on hepatic and renal CYP epoxygenase and ω-hydroxylase metabolic activity over time, we randomized WT and *ApoE*$^{-/-}$ mice to high fat or standard diet for 2, 4, or 8 weeks. Baseline body weight was significantly greater in *ApoE*$^{-/-}$ mice (25.5±0.5 g) compared to WT mice (21.4±0.2 g, $P<0.001$). High fat diet promoted weight gain and altered clinical chemistry values in both WT and *ApoE*$^{-/-}$ mice (Table 4.1). *ApoE*$^{-/-}$ mice had significantly higher plasma total cholesterol levels compared to WT mice fed the same diet. Within each genotype, high fat diet-fed mice had significantly higher plasma total cholesterol levels than standard diet-fed mice. In contrast, plasma insulin levels were not significantly different between WT and *ApoE*$^{-/-}$ mice fed a standard diet, but high fat diet feeding resulted in significantly higher plasma insulin levels in both genotypes. No significant differences in plasma glucose levels were observed among the diet and genotype groups.

High fat diet feeding differentially altered CYP epoxygenase and ω-hydroxylase expression and metabolic activity in liver and kidney in both WT and *ApoE*$^{-/-}$ mice (Figure 4.2). However, no significant differences were observed between WT and *ApoE*$^{-/-}$ mice fed a standard diet.

In liver, high fat diet significantly suppressed EET+DHET formation at 4 and 8 weeks in both WT and *ApoE*$^{-/-}$ mice, relative to the WT/standard diet control group

(Figure 4.2A). At 2 weeks, EET+DHET formation appeared lower in WT mice, but this difference was not statistically significant (P=0.204). Hepatic *Cyp2c29* mRNA levels were also significantly lower in high fat diet-fed mice (Figure 4.3A) and significantly correlated with total CYP epoxygenase activity (r_S=0.68, P<0.001). In contrast, no significant differences in hepatic 20-HETE formation (Figure 4.2B) or *Cyp4a12a* mRNA levels (Figure 4.3B) were observed in response to high fat diet. The 20-HETE:EET+DHET formation rate ratio was significantly greater in high fat diet-fed mice at 4 and 8 weeks, suggesting that the functional balance was shifted in favor of the CYP ω-hydroxylase pathway secondary to suppression of EET+DHET formation (Figure 4.2C).

In contrast to what was observed in liver, no significant differences in renal EET+DHET formation (Figure 4.2D) or *Cyp2j5* mRNA levels (Figure 4.3C) were observed in high fat diet-fed mice. Renal 20-HETE formation, however, was markedly induced after 2, 4, and 8 weeks of high fat diet in both WT and *ApoE*$^{-/-}$ mice, relative to the WT/standard diet group (Figure 4.2E), and was significantly correlated with *Cyp4a12a* mRNA levels (r_S=0.60, P<0.001). This induction of renal CYP ω-hydroxylase metabolic activity resulted in a significantly higher renal 20-HETE:EET+DHET formation rate ratio in high fat diet-fed mice in both genotype groups (Figure 4.2F).

Experiment 2: Effect of enalapril administration on high fat diet-induced alterations in CYP epoxygenase and ω-hydroxylase metabolic activity

Consistent with the results of Experiment 1, high fat diet significantly suppressed CYP epoxygenase metabolic activity in liver (Figure 4.4A). Hepatic *Cyp2c29* mRNA levels also tended to be lower in high fat diet-fed mice, but this difference was not statistically significant (Figure 4.4C; WT: P=0.129 vs. standard diet; *ApoE*$^{-/-}$: P=0.139 vs. standard diet). Enalapril administration reversed these effects in both WT and *ApoE*$^{-/-}$

mice. Similarly, the high fat diet-induced elevation in 20-HETE:EET+DHET formation rate ratio in liver was reversed by enalapril treatment (Figure 4.4E). No significant differences in hepatic CYP ω-hydroxylase metabolic activity (Figure 4.4B) or C*yp4a12a* mRNA levels (Figure 4.4D) were observed in high fat diet-fed mice. Enalapril significantly decreased hepatic 20-HETE formation (P=0.035 vs. standard diet) and *Cyp4a12a* mRNA levels (P<0.001 vs. standard diet; P=0.014 vs. high fat diet) in *ApoE*$^{-/-}$ mice, but no significant differences were observed in WT mice.

In kidney, 20-HETE formation (Figure 4.5B), *Cyp4a12a* mRNA levels (Figure 4.5D), and the 20-HETE:EET+DHET formation rate ratio (Figure 4.5E) were significantly higher in high fat diet fed mice, regardless of genotype, and these effects were reversed by enalapril treatment. No significant differences in renal EET+DHET formation (Figure 4.5A) or *Cyp2j5* mRNA levels (Figure 4.5C) were observed in high fat diet-fed mice. Enalapril appeared to modestly increase renal EET+DHET formation in WT (P=0.072 vs. high fat diet) and *ApoE*$^{-/-}$ (P=0.009 vs. high fat diet) mice; however, no significant differences in *Cyp2j5* mRNA levels were observed.

Consistent with prior studies demonstrating that angiotensin converting enzyme (ACE) inhibitors have insulin-sensitizing effects [24], enalapril significantly lowered plasma insulin levels in high fat diet-fed WT mice (High fat diet/no treatment: 2.95±0.82 ng/mL, High fat diet/enalapril: 0.72±0.08 ng/mL, P=0.022). A similar trend was observed in *ApoE*$^{-/-}$ mice, but this difference was not statistically significant (High fat diet/no treatment: 1.85±0.27 ng/mL, High fat diet/enalapril: 0.90±0.07 ng/mL, P=0.260).

Experiment 3: Effect of enalapril and metformin administration on high fat diet-induced alterations in CYP epoxygenase and ω-hydroxylase metabolic activity

To discern whether the effect of enalapril on high fat diet-induced alterations in CYP epoxygenase and ω-hydroxylase metabolic activity was related to its insulin-

sensitizing effects, high fat diet-fed mice were administered metformin, an insulin sensitizing agent with a mechanism of action independent of the renin-angiotensin system. Compared to untreated high fat diet-fed mice (3.14±0.60 ng/mL), both enalapril (1.53±0.30 ng/mL, P=0.036) and metformin (1.40±0.16 ng/mL, P=0.028) significantly lowered plasma insulin levels. As observed in the two previous experiments, high fat diet significantly suppressed hepatic CYP epoxygenase (Figure 4.6A) and induced renal CYP ω-hydroxylase metabolic activity (Figure 4.6D), and enalapril administration reversed these effects. In contrast, metformin treatment had no effect on high fat diet-induced changes in hepatic EET+DHET or renal 20-HETE formation. Hepatic CYP epoxygenase activity was modestly higher in standard diet-fed mice treated with metformin compared to untreated mice (Figure 4.6A). Enalapril modestly increased hepatic 20-HETE formation in high fat diet-fed mice (Figure 4.6B), but no significant differences in renal EET+DHET formation (Figure 4.6C) were observed across diet or treatment groups.

Discussion

CYP expression and metabolic activity is altered in rodent models of metabolic syndrome, but the mechanisms underlying the observed alterations remain poorly understood. To our knowledge, this is the first study to demonstrate that high fat diet feeding shifts the functional balance between the CYP epoxygenase and ω-hydroxylase pathways in liver and kidney in favor of pro-inflammatory, vasoconstrictive 20-HETE formation. Moreover, enalapril, but not metformin, reverses high fat diet-induced suppression of hepatic CYP epoxygenase metabolic activity and induction of renal CYP ω-hydroxylase metabolic activity and restores the functional balance between the pathways. Collectively, these findings implicate the renin-angiotensin system as a key

regulator of CYP-mediated eicosanoid metabolism in the presence of metabolic syndrome.

High fat diet feeding lowered hepatic CYP epoxygenase activity and *Cyp2c29* expression relative to standard diet controls, consistent with a prior study showing that hepatic Cyp2c protein was suppressed by high fat diet [25]. In kidney, we observed a marked induction of 20-HETE formation, but no differences in EET+DHET formation, in high fat diet-fed mice. In contrast, suppression of renal tubular CYP2C and CYP4A expression and metabolic activity has been observed in rats fed a high fat diet, relative to lean controls [26,27]. These conflicting results may be due to species differences in the regulation of renal CYP expression. In both liver and kidney, the 20-HETE:EET+DHET ratio was significantly greater in high fat diet-fed mice relative to controls, suggesting that the functional balance between the pathways had been shifted toward the CYP ω-hydroxylase pathway.

High fat diet feeding induces multiple metabolic derangements, including dyslipidemia, insulin resistance, and activation of the renin-angiotensin system [17,18], which may contribute to the alterations in CYP-mediated eicosanoid metabolism that we observed. In order to investigate the effect of dyslipidemia on CYP-mediated eicosanoid metabolism, we evaluated CYP epoxygenase and ω-hydroxylase expression and metabolic activity in WT and *ApoE*$^{-/-}$ mice. *ApoE*$^{-/-}$ mice have impaired cholesterol clearance and develop profound hyperlipidemia, which promotes the development of atherosclerotic lesions and vascular inflammation similar to what is observed in humans with atherosclerotic disease [28]. Although plasma total cholesterol was substantially higher in *ApoE*$^{-/-}$ mice compared to WT mice, no significant differences in CYP epoxygenase or ω-hydroxylase activity in liver or kidney were observed between WT and ApoE$^{-/-}$ mice fed a standard diet, and suppression of hepatic EET+DHET formation and induction of renal 20-HETE formation was observed in both genotypes in response

to high fat diet feeding. Thus, the observed changes in CYP epoxygenase and ω-hydroxylase metabolic activity were driven by the high fat diet, rather than by genotype, and were independent of plasma cholesterol levels.

Interestingly, enalapril treatment reversed the effects of high fat diet feeding on CYP-mediated eicosanoid metabolism in both *ApoE*$^{-/-}$ and WT mice. In addition to modulating the renin-angiotensin system to lower blood pressure, ACE inhibitors and angiotensin receptor blockers also improve insulin sensitivity in animal models [24] and prevent the development of diabetes in humans [29]. Consistent with these reports, enalapril lowered plasma insulin levels in high fat diet-fed mice. Insulin modulates CYP expression *in vitro* [30,31], and CYP expression and metabolic activity is altered in models of diabetes [11,12,32,33]. Consequently, we administered metformin, an insulin sensitizing agent, to determine whether insulin resistance was driving the changes in CYP-mediated eicosanoid metabolism observed in high fat diet-fed mice. Although metformin treatment normalized plasma insulin levels, it did not reverse the alterations in CYP expression and metabolic activity. These results support the hypothesis that enalapril reverses the high fat diet-induced suppression of hepatic CYP epoxygenase and induction of renal CYP ω-hydroxylase metabolic activity via inhibition of angiotensin II production, rather than by improving insulin sensitivity.

Accumulating evidence indicates that angiotensin II can regulate CYP-mediated eicosanoid metabolism. Studies evaluating the relationship between the CYP epoxygenase pathway and renin-angiotensin system are limited, but most suggest that angiotensin II suppresses CYP epoxygenase expression and metabolic activity. For example, renal and vascular CYP2C and EET formation are suppressed in angiotensin II-infused rats [34,35] and double transgenic rats that overexpress the human renin and angiotensinogen genes [36]. Humans with renovascular disease, a condition characterized by activation of the renin-angiotensin system, tended to have lower

plasma EET levels, compared to healthy controls [37]. Due to their similar effects on vasomotor tone, the interaction between angiotensin II and 20-HETE has been more rigorously investigated. Angiotensin II stimulates 20-HETE release in isolated perfused kidneys [38] and renal microvessels [39]. Ren-2 transgenic rats, which have elevated renal and plasma angiotensin II levels, exhibit significantly higher renal 20-HETE formation and urinary 20-HETE levels, relative to wild-type controls [40]. In humans, plasma 20-HETE levels correlated with plasma renin activity, and renovascular disease patients have significantly higher plasma 20-HETE compared to healthy controls [37]. A recent study has demonstrated that 20-HETE directly activates the renin-angiotensin system by stimulating expression of ACE and the angiotensin II receptor [41]. Although we did not directly demonstrate that angiotensin II suppresses hepatic CYP epoxygenase metabolic activity and induces renal CYP ω-hydroxylase metabolic activity in this study, our findings, taken together with prior observations, strongly implicate angiotensin II in mediating the observed high fat diet-induced alterations in CYP-mediated eicosanoid metabolism. Further investigation of the interplay between the renin-angiotensin system and CYP-mediated eicosanoid metabolism is warranted.

We did not evaluate the pathophysiologic consequences of high fat diet feeding in this study, but prolonged high fat diet feeding has been used to induced insulin resistance, steatohepatitis, hypertension, and renal injury in rodents [18,27,42,43]. CYP epoxygenase-derived EETs are vasodilatory and possess potent anti-inflammatory effects. Potentiation of the CYP epoxygenase pathway, via enhanced EET biosynthesis or inhibition of EET hydrolysis, has been shown to lower blood pressure in angiotensin II-dependent models of hypertension [44,45,46] and attenuate acute and chronic inflammation [47,48,49]. A series of studies have demonstrated that EETs also activate the phosphatidylinositol 3-kinase (PI3K)/Akt pathway [2], a key component of insulin signaling. Recent evidence suggests that potentiation of EETs enhances insulin

signaling and improves insulin sensitivity [50,51]. Thus, prolonged suppression of hepatic CYP epoxygenase metabolic activity in the presence of the metabolic syndrome would be hypothesized to promote inflammation and hepatic insulin resistance. In contrast, 20-HETE is a potent vasoconstrictor [3] and promotes inflammation via activation of nuclear factor-κB [52]; thus induction of renal CYP ω-hydroxylase metabolic activity would be hypothesized to promote hypertension and renal injury. Indeed, inhibition of 20-HETE formation has anti-hypertensive effects and attenuates renal injury [40,53]. A recent study demonstrated that elevations in plasma 20-HETE levels were associated with shortened bleeding time in mice [54], suggesting that induction of 20-HETE formation may also contribute to the pro-thrombotic state observed in metabolic syndrome patients. Collectively, our findings suggest that an angiotensin II-dependent shift in the functional balance between the CYP epoxygenase and ω-hydroxylase pathways in favor of 20-HETE formation may be a key contributor to the pathologic consequences of a high fat diet and the metabolic syndrome, and that modulating the pathways to increase EETs and/or decrease 20-HETE may have therapeutic utility to abrogate these effects. Moreover, the beneficial effects of ACE inhibitors in the metabolic syndrome may be mediated in part by restoration of the functional balance between the CYP epoxygenase and ω-hydroxylase pathways. However, further studies are necessary to test these hypotheses.

In conclusion, induction of the metabolic syndrome by high fat diet feeding suppressed hepatic CYP epoxygenase and induced renal CYP ω-hydroxylase expression and metabolic activity, thereby shifting the functional balance between the pathways in favor of 20-HETE formation. Treatment with enalapril, but not metformin, reversed this effect, implicating the renin-angiotensin system in mediating high fat diet-induced alterations in CYP-mediated eicosanoid metabolism. Further studies are necessary to elucidate the pathophysiologic significance of these alterations and

determine the therapeutic potential of modulating the CYP epoxygenase and ω-hydroxylase pathways in metabolic diseases.

Table 4.1: Weight and plasma clinical chemistry in WT and *ApoE*$^{-/-}$ mice fed a standard or high-fat diet

	2 weeks	4 weeks	8 weeks
Weight, change from baseline (g)			
WT/Standard diet	2.1 ± 0.6	3.6 ± 0.2	5.0 ± 0.5
WT/High fat diet	3.5 ± 0.9	10.3 ± 0.2 *	11.0 ± 1.5 *
ApoE$^{-/-}$/ Standard diet	3.7 ± 0.1	4.3 ± 0.2	4.2 ± 0.2
ApoE$^{-/-}$/ High fat diet	3.5 ± 0.3	4.7 ± 0.2	10.0 ± 0.9 *
Total cholesterol (mg/dL)			
WT/Standard diet	<45 #	86 ± 2	81 ± 8
WT/High fat diet	104 ± 16	248 ± 14 *	194 ± 23 *
ApoE$^{-/-}$/ Standard diet	614 ± 84 *	512 ± 49 *	918 ± 70 *
ApoE$^{-/-}$/ High fat diet	902 ± 207 *	1099 ± 130 *	1398 ± 125 *
Insulin (ng/mL)			
WT/Standard diet	0.72 ± 0.08	0.95 ± 0.14	0.68 ± 0.14
WT/High fat diet	2.23 ± 0.61 *	2.67 ± 0.54 *	4.55 ± 0.82 *
ApoE$^{-/-}$/ Standard diet	0.83 ± 0.08	0.56 ± 0.04	1.06 ± 0.17
ApoE$^{-/-}$/ High fat diet	1.90 ± 0.54 *	1.72 ± 0.31 *	4.09 ± 0.87 *
Glucose (mg/dL)			
WT/Standard diet	331 ± 19	399 ± 52	335 ± 15
WT/High fat diet	446 ± 57	386 ± 26	382 ± 32
ApoE$^{-/-}$/ Standard diet	359 ± 16	325 ± 19	306 ± 20
ApoE$^{-/-}$/ High fat diet	361 ± 34	382 ± 19	418 ± 34

* $P<0.05$ compared to WT/Standard diet

All values were below the limit of quantitation

Figure Legends

Figure 4.1: Treatment schemes to assess (A) the effect of high fat diet on CYP epoxygenase and ω-hydroxylase metabolic activity and mRNA levels over time and (B) the effect of enalapril and metformin treatment on high fat diet-induced alterations in CYP epoxygenase and ω-hydroxylase metabolic activity

Figure 4.2: Effect of high fat diet on (A) hepatic total CYP epoxygenase (EET+DHET) metabolic activity, (B) hepatic CYP ω-hydroxylase (20-HETE) metabolic activity, (C) hepatic 20-HETE:EET+DHET formation rate ratio, (D) renal total CYP epoxygenase (EET+DHET) metabolic activity, (E) renal CYP ω-hydroxylase (20-HETE) metabolic activity, and (E) renal 20-HETE:EET+DHET formation rate ratio in WT and *ApoE*$^{-/-}$ mice (N=4 per group). * P<0.05 versus WT/standard diet control group.

Figure 4.3: Effect of high fat diet on (A) hepatic *Cyp2c29*, (B) hepatic C*yp4a12a*, (C) renal *Cyp2j5* and (D) renal *Cyp4a12a* mRNA levels in WT and *ApoE*$^{-/-}$ mice (N=4 per group). * P<0.05 versus WT/standard diet control group.

Figure 4.4: Effect of high fat diet and enalapril treatment on hepatic (A) total CYP epoxygenase (EET+DHET) metabolic activity, (B) CYP ω-hydroxylase (20-HETE) metabolic activity, (C) *Cyp2c29* mRNA levels, (D) *Cyp4a12a* mRNA levels, and (E) 20-HETE:EET+DHET formation rate ratio in WT and *ApoE*$^{-/-}$ mice (Standard diet: N=4, High fat diet: N=4, High fat diet + Enalapril: N=6). * P<0.05.

Figure 4.5: Effect of high fat diet and enalapril treatment on renal (A) total CYP epoxygenase (EET+DHET) metabolic activity, (B) CYP ω-hydroxylase (20-HETE) metabolic activity, (C) *Cyp2j5* mRNA levels, (D) *Cyp4a12a* mRNA levels, and (E) 20-HETE:EET+DHET formation rate ratio in WT and *ApoE*$^{-/-}$ mice (Standard diet: N=4, High fat diet: N=4, High fat diet + Enalapril: N=6). * P<0.05.

Figure 4.6: Effect of enalapril and metformin treatment on (A) hepatic total CYP epoxygenase (EET+DHET) metabolic activity, (B) hepatic CYP ω-hydroxylase (20-HETE) metabolic activity, (C) renal total CYP epoxygenase (EET+DHET) metabolic activity, and (D) renal CYP ω-hydroxylase (20-HETE) metabolic activity (Standard diet: No treatment: N=11, Metformin: N=6, Enalapril: N=6; High fat diet: N=6 per group).

* $P<0.05$ versus no treatment/standard diet. # $P<0.05$ versus no treatment/high fat diet.

Figure 4.1: Treatment scheme for high-fat diet and enalapril and metformin administration

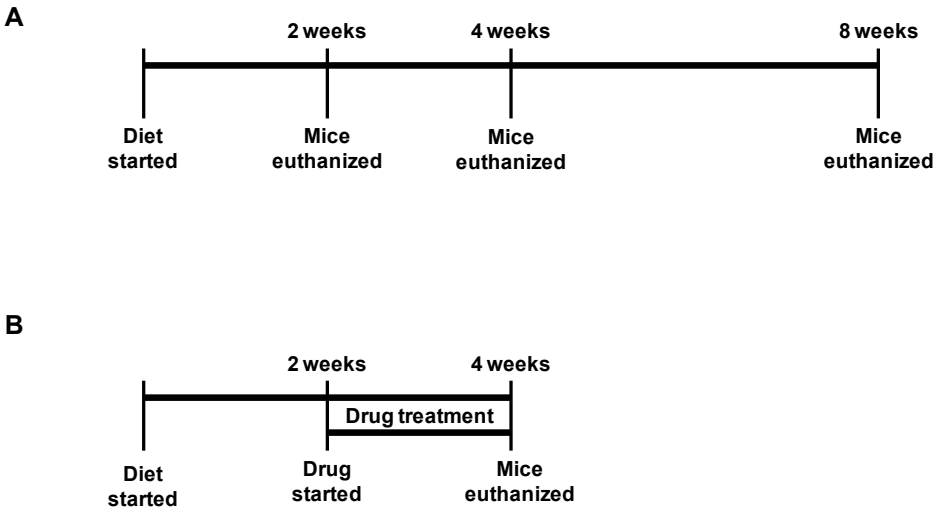

Figure 4.2: Effect of high fat diet on CYP epoxygenase and ω-hydroxylase metabolic activity in liver and kidney

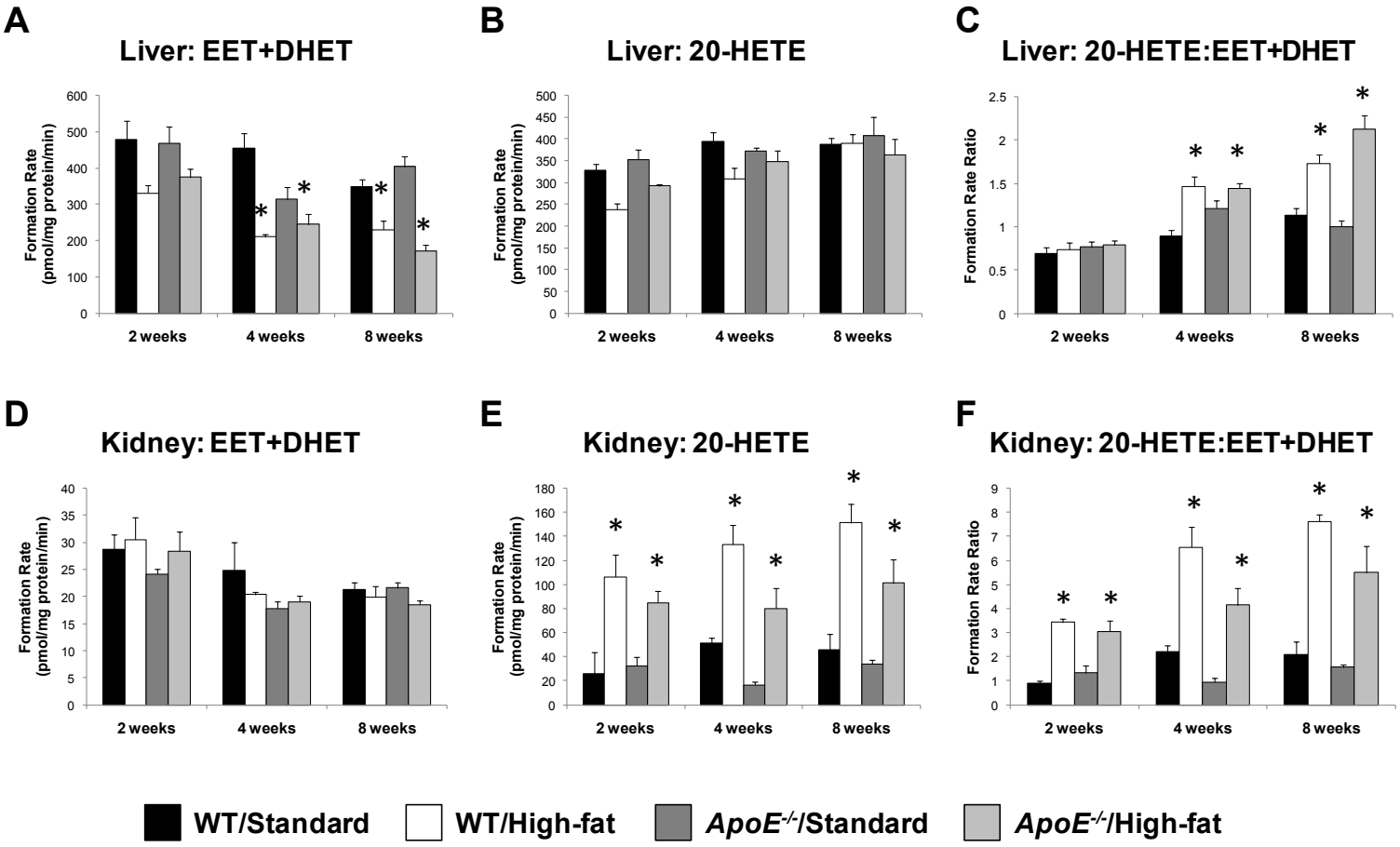

Figure 4.3: Effect of high fat diet on hepatic and renal CYP mRNA levels

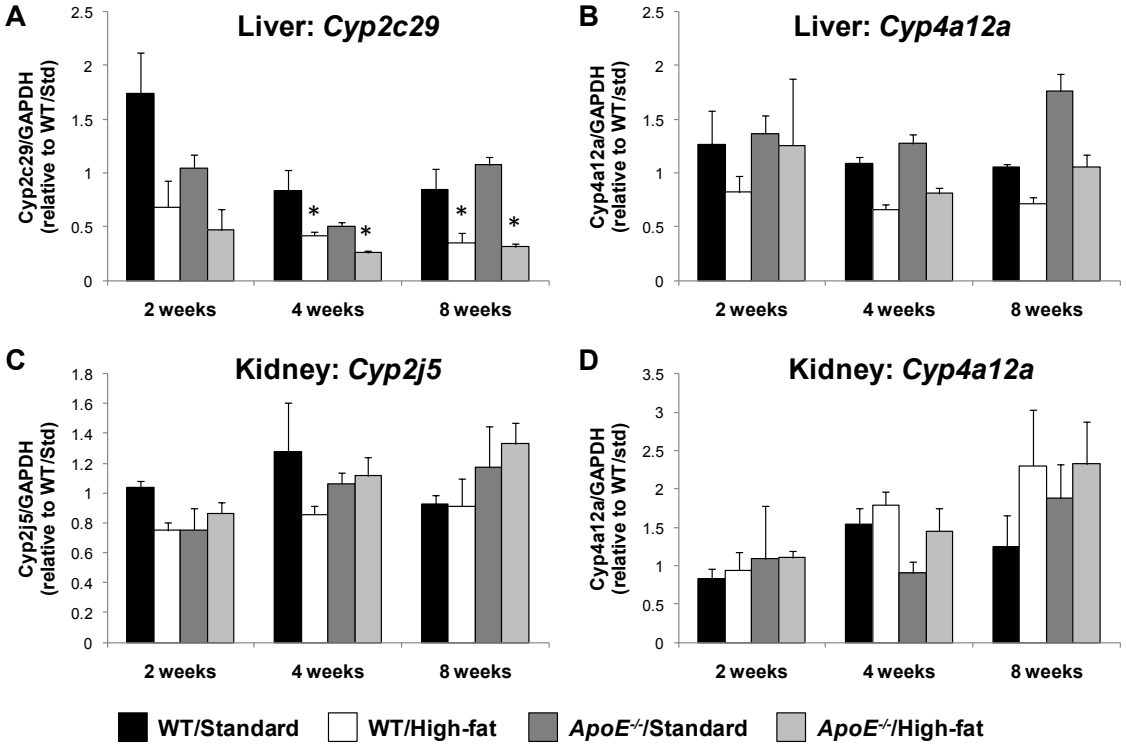

Figure 4.4: Effect of enalapril on high fat diet-induced alterations in hepatic CYP epoxygenase and ω-hydroxylase mRNA expression and metabolic activity

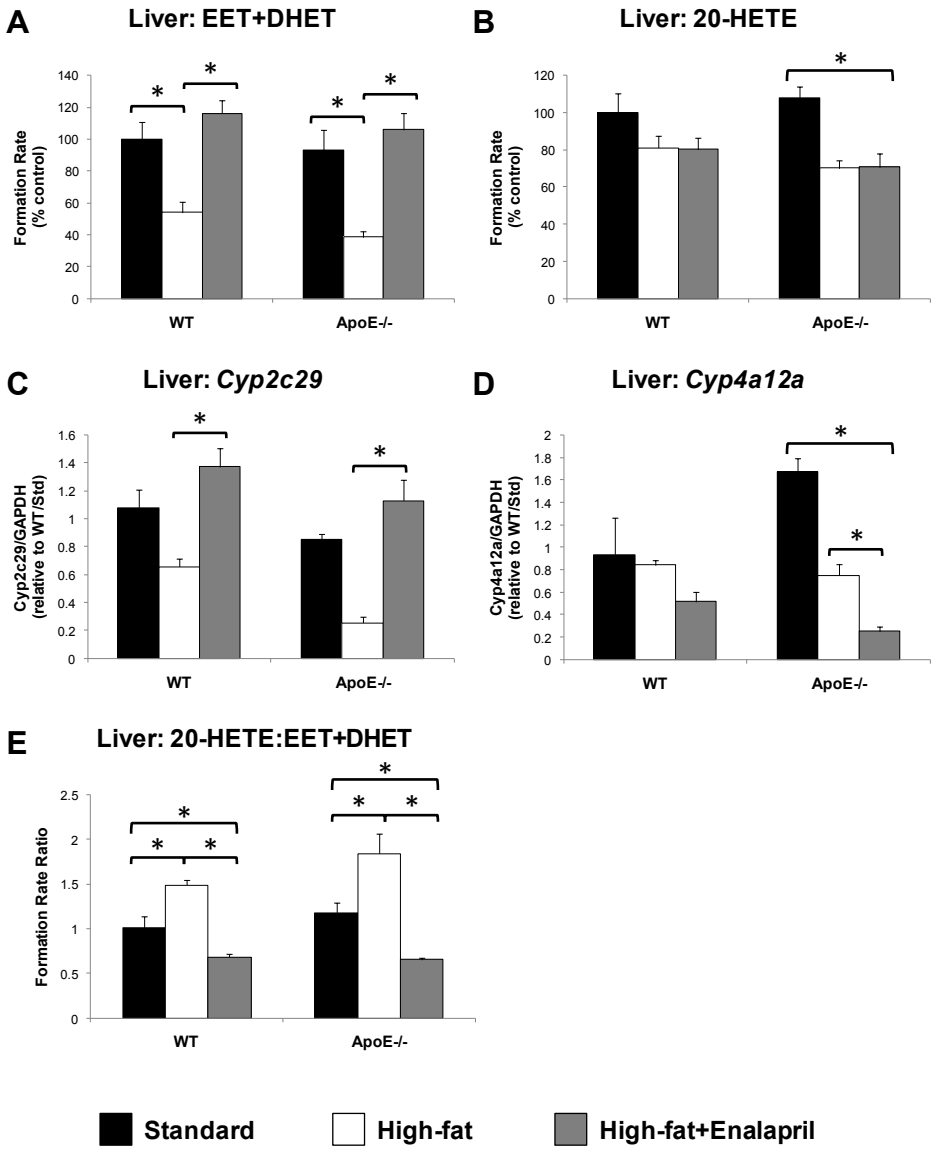

Figure 4.5: Effect of enalapril on high fat diet-induced alterations in renal CYP epoxygenase and ω-hydroxylase mRNA expression and metabolic activity

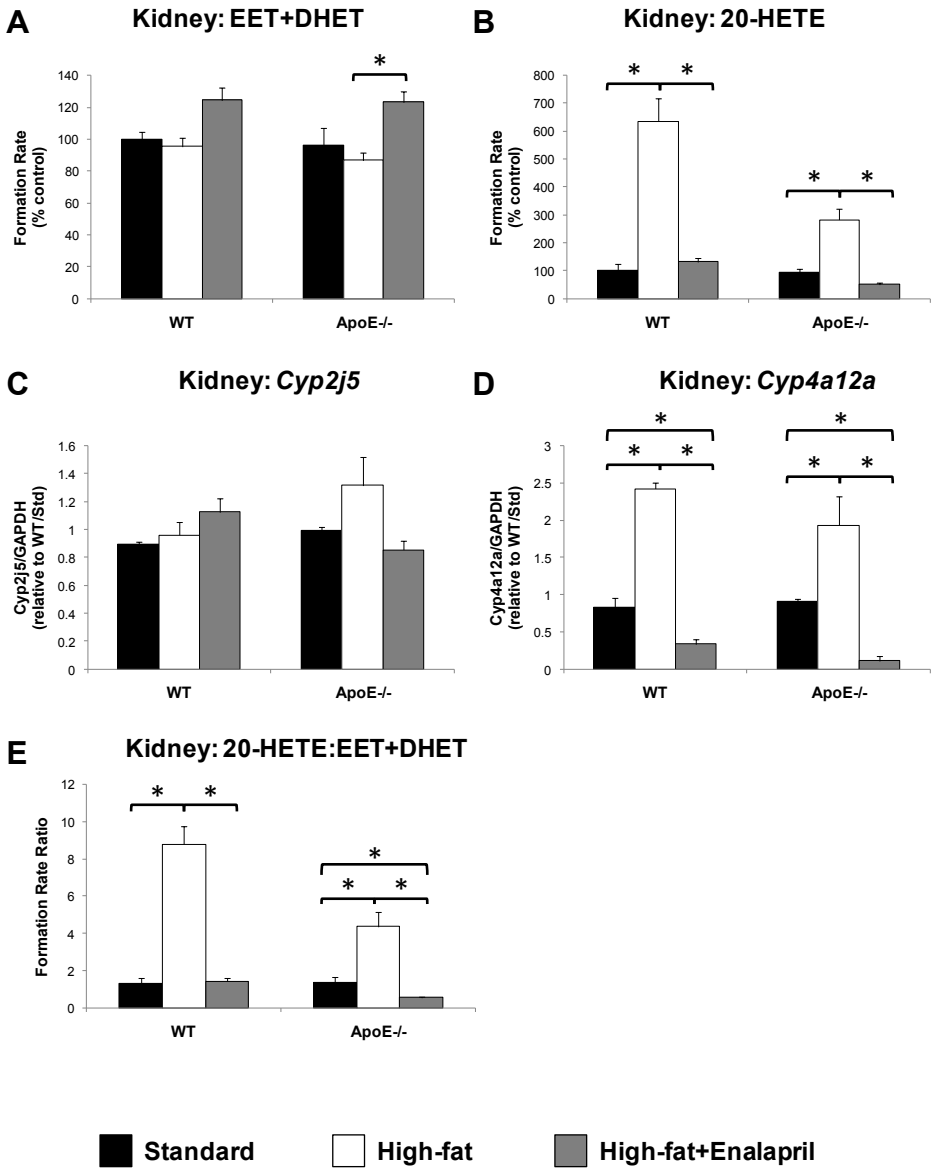

Figure 4.6: Effect of enalapril and metformin on high fat diet-induced alterations in CYP epoxygenase and ω-hydroxylase metabolic activity in liver and kidney

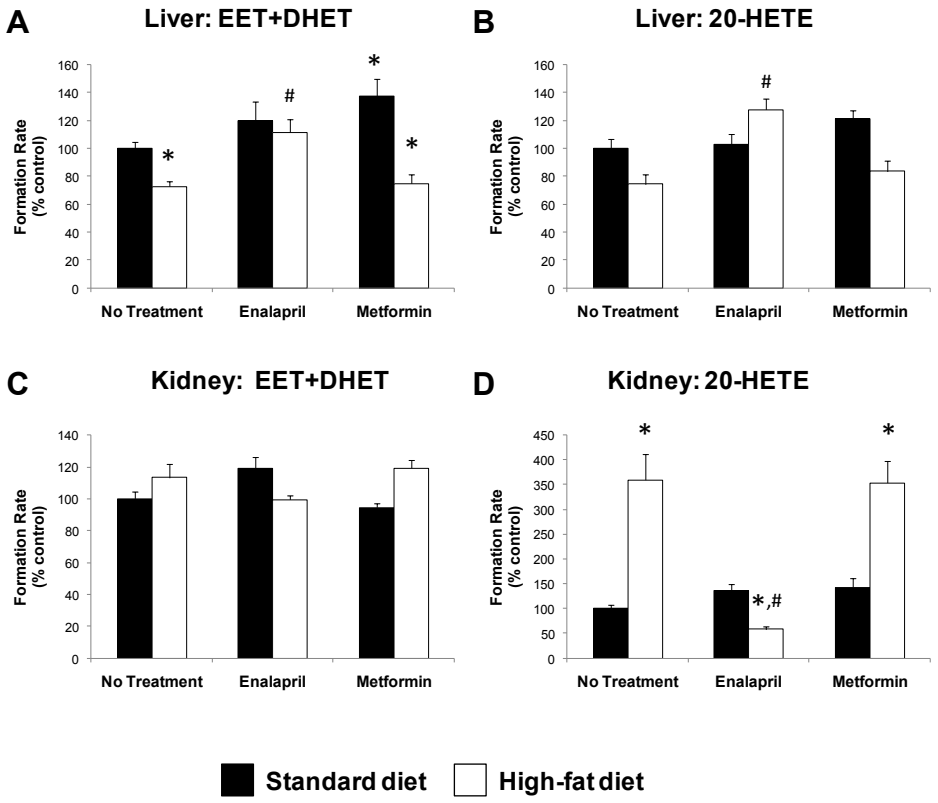

References

1. Zeldin DC (2001) Epoxygenase pathways of arachidonic acid metabolism. J Biol Chem 276: 36059-36062.

2. Deng Y, Theken KN, Lee CR (2010) Cytochrome P450 epoxygenases, soluble epoxide hydrolase, and the regulation of cardiovascular inflammation. J Mol Cell Cardiol 48: 331-341.

3. Roman RJ (2002) P-450 metabolites of arachidonic acid in the control of cardiovascular function. Physiol Rev 82: 131-185.

4. Grundy SM, Cleeman JI, Daniels SR, Donato KA, Eckel RH, et al. (2005) Diagnosis and management of the metabolic syndrome: an American Heart Association/National Heart, Lung, and Blood Institute Scientific Statement. Circulation 112: 2735-2752.

5. Theken KN, Deng Y, Kannon MA, Miller TM, Poloyac SM, et al. (2011) Activation of the acute inflammatory response alters cytochrome P450 expression and eicosanoid metabolism. Drug Metab Dispos 39: 22-29.

6. Bandyopadhyay AM, Chaudhary I, Robertson LW, Gemzik B, Parkinson A, et al. (1993) Expression of a male-specific cytochrome P450 isozyme (CYP2C11) in fa/fa Zucker rats: effect of phenobarbital treatment. Arch Biochem Biophys 307: 386-390.

7. Zhao X, Dey A, Romanko OP, Stepp DW, Wang MH, et al. (2005) Decreased epoxygenase and increased epoxide hydrolase expression in the mesenteric artery of obese Zucker rats. Am J Physiol Regul Integr Comp Physiol 288: R188-196.

8. Zhao X, Quigley JE, Yuan J, Wang MH, Zhou Y, et al. (2006) PPAR-alpha activator fenofibrate increases renal CYP-derived eicosanoid synthesis and improves endothelial dilator function in obese Zucker rats. Am J Physiol Heart Circ Physiol 290: H2187-2195.

9. Enriquez A, Leclercq I, Farrell GC, Robertson G (1999) Altered expression of hepatic CYP2E1 and CYP4A in obese, diabetic ob/ob mice, and fa/fa Zucker rats. Biochem Biophys Res Commun 255: 300-306.

10. Watson AM, Poloyac SM, Howard G, Blouin RA (1999) Effect of leptin on cytochrome P-450, conjugation, and antioxidant enzymes in the ob/ob mouse. Drug Metab Dispos 27: 695-700.

11. Lam JL, Jiang Y, Zhang T, Zhang EY, Smith BJ (2010) Expression and functional analysis of hepatic cytochromes P450, nuclear receptors, and membrane transporters in 10- and 25-week-old db/db mice. Drug Metab Dispos 38: 2252-2258.

12. Yoshinari K, Takagi S, Sugatani J, Miwa M (2006) Changes in the expression of cytochromes P450 and nuclear receptors in the liver of genetically diabetic db/db mice. Biol Pharm Bull 29: 1634-1638.

13. Argiles JM (1989) The obese Zucker rat: a choice for fat metabolism 1968-1988: twenty years of research on the insights of the Zucker mutation. Prog Lipid Res 28: 53-66.

14. Alonso-Galicia M, Brands MW, Zappe DH, Hall JE (1996) Hypertension in obese Zucker rats. Role of angiotensin II and adrenergic activity. Hypertension 28: 1047-1054.

15. Hilzendeger AM, Morais RL, Todiras M, Plehm R, da Costa Goncalves A, et al. (2010) Leptin regulates ACE activity in mice. J Mol Med 88: 899-907.

16. Harker CT, O'Donnell MP, Kasiske BL, Keane WF, Katz SA (1993) The renin-angiotensin system in the type II diabetic obese Zucker rat. J Am Soc Nephrol 4: 1354-1361.

17. de Kloet AD, Krause EG, Woods SC (2010) The renin angiotensin system and the metabolic syndrome. Physiol Behav 100: 525-534.

18. Buettner R, Scholmerich J, Bollheimer LC (2007) High-fat diets: modeling the metabolic disorders of human obesity in rodents. Obesity (Silver Spring) 15: 798-808.

19. da Cunha V, Tham DM, Martin-McNulty B, Deng G, Ho JJ, et al. (2005) Enalapril attenuates angiotensin II-induced atherosclerosis and vascular inflammation. Atherosclerosis 178: 9-17.

20. Matsui Y, Hirasawa Y, Sugiura T, Toyoshi T, Kyuki K, et al. (2010) Metformin reduces body weight gain and improves glucose intolerance in high-fat diet-fed C57BL/6J mice. Biol Pharm Bull 33: 963-970.

21. Livak KJ, Schmittgen TD (2001) Analysis of relative gene expression data using real-time quantitative PCR and the 2(-Delta Delta C(T)) Method. Methods 25: 402-408.

22. Poloyac SM, Tortorici MA, Przychodzin DI, Reynolds RB, Xie W, et al. (2004) The effect of isoniazid on CYP2E1- and CYP4A-mediated hydroxylation of arachidonic acid in the rat liver and kidney. Drug Metab Dispos 32: 727-733.

23. Miller TM, Donnelly MK, Crago EA, Roman DM, Sherwood PR, et al. (2009) Rapid, simultaneous quantitation of mono and dioxygenated metabolites of arachidonic acid in human CSF and rat brain. J Chromatogr B Analyt Technol Biomed Life Sci 877: 3991-4000.

24. Premaratna SD, Manickam E, Begg DP, Rayment DJ, Hafandi A, et al. (2011) Angiotensin-converting enzyme inhibition reverses diet-induced obesity, insulin resistance and inflammation in C57BL/6J mice. Int J Obes (Lond).

25. Yoshinari K, Takagi S, Yoshimasa T, Sugatani J, Miwa M (2006) Hepatic CYP3A expression is attenuated in obese mice fed a high-fat diet. Pharm Res 23: 1188-1200.

26. Wang MH, Smith A, Zhou Y, Chang HH, Lin S, et al. (2003) Downregulation of renal CYP-derived eicosanoid synthesis in rats with diet-induced hypertension. Hypertension 42: 594-599.

27. Zhou Y, Lin S, Chang HH, Du J, Dong Z, et al. (2005) Gender differences of renal CYP-derived eicosanoid synthesis in rats fed a high-fat diet. Am J Hypertens 18: 530-537.

28. Meir KS, Leitersdorf E (2004) Atherosclerosis in the apolipoprotein-E-deficient mouse: a decade of progress. Arterioscler Thromb Vasc Biol 24: 1006-1014.

29. Abuissa H, Jones PG, Marso SP, O'Keefe JH, Jr. (2005) Angiotensin-converting enzyme inhibitors or angiotensin receptor blockers for prevention of type 2 diabetes: a meta-analysis of randomized clinical trials. J Am Coll Cardiol 46: 821-826.

30. Woodcroft KJ, Novak RF (1999) Insulin differentially affects xenobiotic-enhanced, cytochrome P-450 (CYP)2E1, CYP2B, CYP3A, and CYP4A expression in primary cultured rat hepatocytes. J Pharmacol Exp Ther 289: 1121-1127.

31. Iber H, Li-Masters T, Chen Q, Yu S, Morgan ET (2001) Regulation of hepatic cytochrome P450 2C11 via cAMP: implications for down-regulation in diabetes, fasting, and inflammation. J Pharmacol Exp Ther 297: 174-180.

32. Kroetz DL, Yook P, Costet P, Bianchi P, Pineau T (1998) Peroxisome proliferator-activated receptor alpha controls the hepatic CYP4A induction adaptive response to starvation and diabetes. J Biol Chem 273: 31581-31589.

33. Shimojo N, Ishizaki T, Imaoka S, Funae Y, Fujii S, et al. (1993) Changes in amounts of cytochrome P450 isozymes and levels of catalytic activities in hepatic and renal microsomes of rats with streptozocin-induced diabetes. Biochem Pharmacol 46: 621-627.

34. Zhao X, Pollock DM, Inscho EW, Zeldin DC, Imig JD (2003) Decreased renal cytochrome P450 2C enzymes and impaired vasodilation are associated with angiotensin salt-sensitive hypertension. Hypertension 41: 709-714.

35. Zhao X, Pollock DM, Zeldin DC, Imig JD (2003) Salt-sensitive hypertension after exposure to angiotensin is associated with inability to upregulate renal epoxygenases. Hypertension 42: 775-780.

36. Kaergel E, Muller DN, Honeck H, Theuer J, Shagdarsuren E, et al. (2002) P450-dependent arachidonic acid metabolism and angiotensin II-induced renal damage. Hypertension 40: 273-279.

37. Minuz P, Jiang H, Fava C, Turolo L, Tacconelli S, et al. (2008) Altered release of cytochrome p450 metabolites of arachidonic acid in renovascular disease. Hypertension 51: 1379-1385.

38. Carroll MA, Balazy M, Margiotta P, Huang DD, Falck JR, et al. (1996) Cytochrome P-450-dependent HETEs: profile of biological activity and stimulation by vasoactive peptides. Am J Physiol 271: R863-869.

39. Croft KD, McGiff JC, Sanchez-Mendoza A, Carroll MA (2000) Angiotensin II releases 20-HETE from rat renal microvessels. Am J Physiol Renal Physiol 279: F544-551.

40. Chabova VC, Kramer HJ, Vaneckova I, Vernerova Z, Eis V, et al. (2007) Effects of chronic cytochrome P-450 inhibition on the course of hypertension and end-organ damage in Ren-2 transgenic rats. Vascul Pharmacol 47: 145-159.

41. Sodhi K, Wu CC, Cheng J, Gotlinger K, Inoue K, et al. (2010) CYP4A2-induced hypertension is 20-hydroxyeicosatetraenoic acid- and angiotensin II-dependent. Hypertension 56: 871-878.

42. Gomez-Lechon MJ, Jover R, Donato MT (2009) Cytochrome p450 and steatosis. Curr Drug Metab 10: 692-699.

43. Dobrian AD, Davies MJ, Prewitt RL, Lauterio TJ (2000) Development of hypertension in a rat model of diet-induced obesity. Hypertension 35: 1009-1015.

44. Imig JD, Zhao X, Capdevila JH, Morisseau C, Hammock BD (2002) Soluble epoxide hydrolase inhibition lowers arterial blood pressure in angiotensin II hypertension. Hypertension 39: 690-694.

45. Imig JD, Zhao X, Zaharis CZ, Olearczyk JJ, Pollock DM, et al. (2005) An orally active epoxide hydrolase inhibitor lowers blood pressure and provides renal protection in salt-sensitive hypertension. Hypertension 46: 975-981.

46. Lee CR, Imig JD, Edin ML, Foley J, DeGraff LM, et al. (2010) Endothelial expression of human cytochrome P450 epoxygenases lowers blood pressure and attenuates hypertension-induced renal injury in mice. FASEB J 24: 3770-3781.

47. Deng Y, Edin ML, Theken KN, Schuck RN, Flake GP, et al. (2011) Endothelial CYP epoxygenase overexpression and soluble epoxide hydrolase disruption attenuate acute vascular inflammatory responses in mice. FASEB J 25: 703-713.

48. Schmelzer KR, Kubala L, Newman JW, Kim IH, Eiserich JP, et al. (2005) Soluble epoxide hydrolase is a therapeutic target for acute inflammation. Proc Natl Acad Sci U S A 102: 9772-9777.

49. Zhang LN, Vincelette J, Cheng Y, Mehra U, Chen D, et al. (2009) Inhibition of soluble epoxide hydrolase attenuated atherosclerosis, abdominal aortic aneurysm formation, and dyslipidemia. Arterioscler Thromb Vasc Biol 29: 1265-1270.

50. Xu X, Zhao CX, Wang L, Tu L, Fang X, et al. (2010) Increased CYP2J3 expression reduces insulin resistance in fructose-treated rats and db/db mice. Diabetes 59: 997-1005.

51. Luria A, Bettaieb A, Xi Y, Shieh GJ, Liu HC, et al. (2011) Soluble epoxide hydrolase deficiency alters pancreatic islet size and improves glucose homeostasis in a model of insulin resistance. Proc Natl Acad Sci U S A.

52. Ishizuka T, Cheng J, Singh H, Vitto MD, Manthati VL, et al. (2008) 20-Hydroxyeicosatetraenoic acid stimulates nuclear factor-kappaB activation and the production of inflammatory cytokines in human endothelial cells. J Pharmacol Exp Ther 324: 103-110.

53. Certikova Chabova V, Walkowska A, Kompanowska-Jezierska E, Sadowski J, Kujal P, et al. (2010) Combined inhibition of 20-hydroxyeicosatetraenoic acid formation and of epoxyeicosatrienoic acids degradation attenuates hypertension and hypertension-induced end-organ damage in Ren-2 transgenic rats. Clin Sci (Lond) 118: 617-632.

54. Liu JY, Li N, Yang J, Qiu H, Ai D, et al. (2010) Metabolic profiling of murine plasma reveals an unexpected biomarker in rofecoxib-mediated cardiovascular events. Proc Natl Acad Sci U S A 107: 17017-17022.

Chapter V: CYP-mediated eicosanoid metabolism differs between CAD patients and healthy volunteers

Coronary artery disease (CAD) is a leading cause of morbidity and mortality in the United States [1]. Despite advances in the diagnosis and treatment of CAD, it remains a significant public health concern, and novel therapies are needed to improve outcomes. Accumulating preclinical and epidemiologic evidence suggests that modulation of cytochrome P450 (CYP)-mediated eicosanoid metabolism may be a viable therapeutic strategy for the management of CAD.

CYPs metabolize arachidonic acid to various biologically active eicosanoids. The CYP epoxygenases (CYP2J2, CYP2C8) catalyze the formation of four epoxyeicosatrienoic acid regioisomers (5,6-, 8,9-, 11,12-, 14,15-EET), which possess potent vasodilatory and anti-inflammatory effects [2,3]. EETs are rapidly hydrolyzed by soluble epoxide hydrolase (sEH) to the corresponding dihydroxyeicosatrienoic acids (DHETs), which are generally less biologically active [3,4]. Numerous preclinical studies have demonstrated that potentiation of the CYP epoxygenase pathway, via enhanced EET biosynthesis or inhibition of sEH-mediated EET hydrolysis, is protective in models of cardiovascular disease. For example, endothelial overexpression of CYP2J2 or CYP2C8 or global genetic deletion of sEH (*Ephx2*$^{-/-}$) attenuates angiotensin II/high-salt-induced hypertension [5,6] and lipopolysaccharide-induced acute inflammation [7,8] in mice. Enhanced EET biosynthesis and inhibition of EET hydrolysis are also cardioprotective [9,10,11] and neuroprotective [12] in models of ischemia/reperfusion injury, and pharmacological inhibition of sEH attenuates atherosclerotic lesion development in apolipoprotein E-deficient mice [13,14]. In contrast, ω-hydroxylation of

arachidonic acid by CYP4A11 and CYP4F2 produces 20-hydroxyeicosatetraenoic acid (20-HETE), a vasoconstrictive and pro-inflammatory eicosanoid [4]. 20-HETE promotes hypertension [15,16] and endothelial dysfunction [17,18] in rodents, and administration of a CYP ω-hydroxylase inhibitor is cardioprotective [19] and neuroprotective [20] in models of ischemia/reperfusion injury.

Although preclinical studies suggest that the CYP epoxygenase and ω-hydroxylase pathways are important in the maintenance of cardiovascular homeostasis following pathologic insult, the role of CYP-mediated eicosanoid metabolism in humans is poorly understood. Functional genetic polymorphisms in the CYP epoxygenases (*CYP2J2*, *CYP2C8*) [21], sEH (*EPHX2*) [22], and CYP ω-hydroxylases (*CYP4A11*, *CYP4F2*) [23,24,25,26] have been associated with cardiovascular disease susceptibility in several genetic epidemiologic studies, but few studies have directly measured CYP-derived eicosanoids in humans. Importantly, CYP-mediated eicosanoid metabolism has not been assessed in patients with established atherosclerotic cardiovascular disease, and the clinical factors that are associated with CYP epoxygenase, sEH, and CYP ω-hydroxylase function in this patient population have not been described. Therefore, the objectives of this study were (1) to identify clinical factors that are associated with circulating biomarkers of CYP epoxygenase, sEH, and CYP ω-hydroxylase function in a well-treated cohort of patients with established CAD and (2) to compare the plasma concentrations of EETs, DHETs, and 20-HETE between these CAD patients and healthy individuals without risk factors for cardiovascular disease.

Methods

Study population and protocol

A cohort of individuals ≤65 years of age with established CAD, defined as ≥50% stenosis in at least one major epicardial coronary artery by coronary angiography, were

identified in the UNC Cardiac Catheterization Laboratory. Exclusion criteria included pregnancy, atrial fibrillation, left-ventricular systolic dysfunction (ejection fraction ≤35%), current use of long-acting nitrates or insulin, active autoimmune disease, history of severe aortic stenosis, history of solid organ transplant or dialysis, or history of cancer within the previous 5 years.

A cohort of healthy volunteers (HV) ≤65 years of age were identified from the local Chapel Hill, NC community by advertisement. Following a detailed medical and medication history and a fasting serum chemistry and cholesterol panel, individuals with a history of cardiovascular disease, risk factors for CAD (including physician-diagnosed hypertension or diabetes, cigarette smoking within the previous 6 months, high cholesterol [defined as total cholesterol >240 mg/dL, triglycerides >200 mg/dL or LDL cholesterol >160 mg/dL], or body mass index >30 kg/m^2), or currently taking any medication for a chronic medical condition were excluded.

The study protocol was approved by the University of North Carolina at Chapel Hill Biomedical Institutional Review Board. Eligible participants provided written informed consent and returned to the UNC Clinical and Translational Research Center (CTRC) for a single morning study visit after fasting overnight and withholding their morning medications. CAD patients returned to the CTRC 62±34 days after their index catheterization and were clinically stable at the time of their study visit. Participants were also instructed to refrain from tobacco products, caffeine, and vigorous exercise the morning of the study visit, and from use of vitamin C, vitamin E, fish oil, niacin or arginine supplements, oral decongestants, non-steroidal anti-inflammatory drugs (other than low-dose aspirin), or erectile dysfunction medications for at least 7 days prior to the study visit. Individuals experiencing a respiratory tract infection within 4 weeks of the study visit were not eligible to participate. At the study visit, blood was collected by

venipuncture. Plasma was separated by centrifugation and stored at -80^{o}C pending analysis.

Quantification of plasma CYP-derived eicosanoids

Plasma eicosanoid levels were quantified as previously described [5,27]. Briefly, plasma (0.25 mL) was diluted in 0.1% acetic acid/5% methanol solution containing 0.009 mM butylated hydroxytoluene. Samples were loaded onto HyperSep Retain PEP SPE cartridges (Thermo Fisher Scientific, Waltham, MA) that had been conditioned with 0.1% acetic acid/5% methanol and spiked with 30 ng each of 10,11-epoxyheptadecanoic acid and 10,11-dihydroxynonadecanoic acid as internal standards. Columns were washed with two column volumes of 0.1% acetic acid/5% methanol, and analytes were eluted with 1 mL acetonitrile. Extracts were dried under nitrogen gas at 37°C and reconstituted in 40% ethanol.

CYP-derived metabolites of arachidonic acid (14,15-EET, 11,12-EET, 8,9-EET, 14,15-DHET, 11,12-DHET, 8,9-DHET, 5,6-DHET, and 20-HETE) and linoleic acid (9,10- and 12,13-epoxyoctadecenoic acid (9,10-EpOME and 12,13-EpOME) and 9,10- and 12,13-dihydroxyoctadecenoic acid (9,10-DHOME and 12,13-DHOME)) were separated by reverse phase HPLC on a 1x150 mm, 5µm Luna C18(2) column (Phenomenex, Torrance, CA) and quantified using a MDS Sciex API 3000 triple quadrupole mass spectrometer (Applied Biosystems, Foster City, CA) with negative mode electrospray ionization and multiple reaction monitoring, as previously described [28].

Data were acquired and analyzed with Analyst software, version 1.5 (Applied Biosystems), and the relative response ratios of each analyte to the appropriate internal standard were used to calculate concentrations. Extraction efficiency for each sample was calculated based on the recovery of the internal standards. Samples for which the extraction efficiency was greater than two standard deviations below the mean were

considered to be analytical failures and excluded from the statistical analysis. A concentration equal to half that of the lowest standard was imputed for samples in which the calculated concentration fell below that value. Analytes for which more than 20% of the values were imputed were dropped from the statistical analysis [29]. Consequently, 11,12-EET was excluded from the analysis.

Statistical analysis

Data are presented as mean ± standard deviation or median (interquartile range) unless otherwise indicated. In addition to analyzing each separately, EET regioisomers (14,15-EET and 8,9-EET) and DHET regioisomers (14,15-DHET, 11,12-DHET, 8,9-DHET, and 5,6-DHET) were summed to evaluate total plasma concentrations of EETs and DHETs, respectively. The sum of all EET and DHET regioisomers (EETs+DHETs) was calculated as an index of total epoxygenase activity. Epoxide:diol ratios (14,15-EET:14,15-DHET, 9,10-EpOME:9,10-DHOME, and 12,13-EpOME:12,13-DHOME) were calculated as indices of sEH activity. Previous studies in *Ephx2*$^{-/-}$ mice and in humans demonstrate that these ratios in plasma are sensitive and specific biomarkers of sEH activity *in vivo*, with lower ratios indicative of higher sEH activity [10,22]. Parameters that were not normally distributed, including serum chemistry, plasma CYP-derived eicosanoid levels, and epoxide:diol ratios, were log-transformed prior to statistical analysis.

Study population characteristics were compared across the CAD and HV cohorts using a one-way ANOVA or chi-squared test, as appropriate. Inter-metabolite correlations were assessed by Spearman rank correlation. To identify clinical factors that influence sum EETs, sum DHETs, 20-HETE, and 14,15-EET:14,15-DHET ratios in CAD patients, stepwise multiple regression analysis was performed. Potential covariates included demographic factors (age, gender, race), indices of CAD severity (presence of

multivessel disease, presence of acute coronary syndrome at index catheterization), comorbidities (hypertension, diabetes, cigarette smoking), body mass index, and ACE inhibitor/angiotensin receptor blocker use. These comorbidities were considered because alterations in CYP epoxygenase and ω-hydroxylase pathway expression and metabolic activity have been observed in rodent models of hypertension [30], obesity [31,32,33], and chronic tobacco smoke exposure [34]. ACE inhibitor/angiotensin II receptor blocker use was included because angiotensin II regulates CYP-mediated eicosanoid metabolism in preclinical models [35,36] and in humans [37]. Due to the high prevalence of beta-blocker, aspirin, and statin use in CAD patients, use of these medications was not considered as a covariate. Covariates with $p<0.15$ were included in the final model.

Sum EETs, sum DHETs, 20-HETE, and epoxide:diol ratios in the CAD and HV cohorts were compared by regression in an unadjusted model; a model adjusted for age, gender, and race; and a model adjusted for continuous covariates identified in the multiple regression analysis in CAD patients. Analyses stratified by the categorical covariates identified in the multiple regression analysis were also performed. Stratified analyses were also completed to assess the potential contribution of confounding factors to the observed differences in each biomarker between the CAD and HV cohorts. The primary analysis was the case-control comparison of the sum EETs, sum DHETs, 20-HETE, and epoxide:diol ratios. Therefore, the significance level was set at P=0.0125 (0.05/4) to account for the impact of multiple statistical tests. At an α=0.0125 level, we had >80% power to detect a 35% difference in each biomarker between the CAD and HV cohorts, assuming a coefficient of variation of 50% [22]. In a secondary analysis, plasma levels of individual EET and DHET regioisomers were compared between the CAD and HV cohorts by one-way ANOVA. All analyses were performed using SAS 9.1.3 (SAS Institute, Cary, NC).

Results

Study population

The characteristics of the study population are shown in Table 5.1. Compared to the healthy volunteers, CAD patients were significantly older, and had higher body mass index, blood pressure, serum triglycerides and C-reactive protein. CAD patients had lower HDL, LDL, and total cholesterol levels than individuals in the HV cohort. This observation is likely due to treatment with lipid-lowering therapies, as no differences in the total:HDL cholesterol ratio were observed. Among the CAD patients, the majority had advanced disease, with 25 (30.5%) presenting with an acute coronary syndrome at their index catheterization and 52 (63.4%) diagnosed with multivessel disease.

The plasma levels of EETs, DHETs, 20-HETE, EpOMEs, and DHOMEs in CAD patients are shown in Figure 5.1A. EETs circulated at the lowest concentrations, followed by the DHETs and 20-HETE. The linoleic acid metabolites (9,10-EpOME, 9,10-DHOME, 12,13-EpOME, 12,13-DHOME) were present at much higher concentrations than the arachidonic acid metabolites. All epoxide metabolites were highly positively correlated, as were the diols (Figure 5.1B). In addition, 20-HETE was positively correlated with the diols, but not the epoxides. Both 14,15-EET and 12,13-EpOME were negatively correlated with 14,15-DHET and 11,12-DHET, while 9,10-EpOME was negatively correlated with all DHET regioisomers. The 14,15-EET:14,15-DHET ratio was significantly positively correlated with the 9,10-EpOME:9,10-DHOME (r_S=0.81; P<0.001) and 12,13-EpOME:12,13-DHOME (r_S=0.86, P<0.001) ratios, which were also significantly correlated (r_S=0.88; P<0.001). Similar inter-metabolite correlations were observed in healthy volunteers (Figure 5.2).

Identification of clinical factors associated with plasma CYP-derived eicosanoid levels in CAD patients

Several clinical covariates were associated with CYP epoxygenase pathway function in subjects with CAD (Table 5.2). Plasma sum EETs were negatively associated with body mass index and age. Similarly, plasma sum EETs were significantly lower in patients with a body mass index ≥30 kg/m^2 (Median (IQR): 0.25 (0.17)), compared to patients with a body mass index <30 kg/m^2 (0.34 (0.32); P<0.001). Plasma sum DHETs were significantly higher in smokers, and significantly lower in patients with diabetes. Consistent with these relationships, the 14,15-EET:14,15-DHET ratio tended to be lower in smokers and negatively correlated with body mass index. Moreover, the 14,15-EET:14,15-DHET ratio was significantly lower in patients with a body mass index ≥30 kg/m^2 (0.23 (0.49)), compared to patients with a body mass index <30 kg/m^2 (0.52 (0.59); P=0.011). Plasma 20-HETE levels were significantly lower in patients treated with an ACE inhibitor/ARB (Table 5.2); however, no significant association with age, body mass index, diabetes or smoking was observed. Moreover, no significant differences in plasma 20-HETE levels were observed in patients with a body mass index ≥30 kg/m^2 (1.41 (0.66)), compared to patients with a body mass index <30 kg/m^2 (1.60 (0.97); P=0.249). No significant relationships were observed between sum EETs, sum DHETs, the 14,15-EET:14,15-DHET ratio, or 20-HETE and gender, race, presence of multivessel disease, or presence of acute coronary syndrome at the index catheterization.

Comparison of plasma eicosanoid levels between healthy volunteers and CAD patients

CAD patients had significantly higher plasma sum EETs compared to healthy volunteers (P<0.001; Figure 5.3A). This relationship remained significant after adjusting for age, gender, and race (P<0.001), and age and body mass index (P<0.001), and stratifying the study population by body mass index (P<0.001; Figure 5.4A). CAD patients tended to have lower plasma sum DHETs compared to healthy volunteers

(P=0.030), but this difference was not statistically significant at the α=0.0125 level (Figure 5.3B). A similar relationship was observed after adjusting for demographic factors (P=0.033). Non-smoking CAD patients exhibited significantly lower plasma sum DHETs compared to healthy volunteers (P=0.003; Figure 5.4B), but no significant differences in plasma sum DHETs were observed when the CAD cohort was limited to patients without diabetes (P=0.152; Figure 5.4C). No differences in total CYP epoxygenase activity (EETs+DHETs) were observed between CAD patients and healthy volunteers (Figure 5.3C).

The epoxide:diol ratios were markedly different between the cohorts. The 14,15-EET:14,15-DHET, 9,10-EpOME:9,10-DHOME, and 12,13-EpOME:12,13-DHOME ratios were each significantly higher in CAD patients, compared to healthy volunteers (Figure 5.5). These relationships remained statistically significant when adjusted for age, gender, and race (P<0.001 versus HV for all), and age and body mass index (P<0.001 versus HV for all). Similar results were also observed when the study population was stratified by gender (Figure 5.6), body mass index (Figure 5.7A), smoking status (Figure 5.7B), and diabetes status (Figure 5.7C) (P<0.001 versus HV for all).

Consistent with the results observed for the sum EETs, CAD patients had significantly higher 14,15-EET, 8,9-EET, 9,10-EpOME, and 12,13-EpOME plasma concentration compared to healthy volunteers. CAD patients also tended to have lower plasma levels of the individual diol regioisomers, although only 5,6-DHET reached statistical significance (Table 5.3).

No differences in plasma 20-HETE levels were observed between CAD patients and healthy volunteers in either the unadjusted regression model (P=0.988) or after adjustment for age, gender, and race (P=0.852). However when CAD patients were stratified by ACE inhibitor/ARB use, plasma 20-HETE levels in CAD patients not treated

with an ACE inhibitor or ARB tended to be higher than in healthy volunteers, though this difference was not statistically significant (P=0.086; Figure 5.4D).

Discussion

Genetic variation in the CYP epoxygenases, sEH, and the CYP ω-hydroxylases has been associated with cardiovascular disease risk, supporting the hypothesis that modulating CYP-mediated eicosanoid metabolism may have therapeutic utility in the management of CAD. However, few studies have measured CYP-derived eicosanoids in humans. To our knowledge, this is the first study to evaluate CYP epoxygenase, sEH, and CYP ω-hydroxylase function in patients with established atherosclerosis. Collectively, our findings identify clinical factors that influence CYP epoxygenase, sEH, and CYP ω-hydroxylase metabolic function in CAD patients and demonstrate that CYP-mediated eicosanoid metabolism is altered in the presence of atherosclerotic cardiovascular disease.

Most notably, we observed that the epoxide:diol ratios were markedly higher in CAD patients compared to healthy volunteers in all subsets of the population, indicating significantly lower apparent sEH metabolic activity in the presence of advanced cardiovascular disease. Consistent with these findings, CAD patients also had higher plasma EETs and lower plasma DHETs compared to healthy volunteers, but no differences in total CYP epoxygenase activity were observed between the groups. Preclinical models have demonstrated that genetic disruption or pharmacological inhibition of sEH lowers blood pressure [6,38], attenuates acute inflammation [7,8], is cardioprotective following ischemia/reperfusion injury [10,11], and attenuates atherosclerotic lesion development [13,14]. In humans, carriers of a genetic polymorphism associated with higher sEH activity *in vivo* (*EPHX2* K55R) had a greater risk of incident CAD [22]. Thus, the apparent suppression of sEH metabolic activity that

we observed in CAD patients may be a compensatory response to the presence of cardiovascular disease. However, few studies have investigated the factors that regulate sEH metabolic activity *in vivo*. Reactive oxygen species inhibit sEH metabolic activity *in vitro* [39,40], suggesting that oxidative stress contributes to the suppression of sEH metabolic activity in CAD patients. A recent study demonstrated that 15-deoxy prostaglandin J_2, an electrophilic cyclopentenone prostaglandin, inhibits sEH *in vitro* via covalent adduct formation [41], but levels of 15-deoxy prostaglandin J_2 have not been measured in CAD patients. Future studies are necessary to elucidate the mechanisms by which sEH metabolic activity is regulated in the presence of cardiovascular disease. Importantly, sEH inhibitors are currently in clinical development for the treatment of cardiovascular and metabolic disease [42]. Understanding the clinical factors that influence CYP epoxygenase pathway function in humans may help identify patients who would most benefit from treatment with sEH inhibitors.

Within the CAD cohort, we identified several clinical factors that were associated with CYP epoxygenase and sEH metabolic function. Body mass index was the strongest predictor of plasma EET levels in CAD patients. The observed inverse relationship suggests that CYP epoxygenase activity is suppressed in obese individuals, consistent with lower CYP epoxygenase expression and metabolic activity reported in rat models of obesity [31,32,33]. We also observed an inverse correlation between body mass index and the 14,15-EET:14,15-DHET ratio. This relationship may indicate higher sEH activity in obese individuals, but may reflect the observed correlation between plasma EET levels and body mass index. Preclinical studies assessing the effects of obesity on sEH expression and activity have yielded conflicting results. For example, elevated sEH expression has been observed in mesenteric arteries of obese Zucker rats [33], while sEH activity appeared to be suppressed in a model of diet-induced obesity in

mice [43]. Thus, further study is necessary to directly assess the impact of obesity on sEH activity.

Several of the comorbidities present in the CAD cohort were associated with CYP epoxygenase pathway function. CAD patients with diabetes tended to have lower plasma DHETs compared to non-diabetic patients, suggesting suppression of CYP epoxygenase and/or sEH activity. Preclinical studies suggest that hyperglycemia and/or hyperinsulinemia may influence CYP epoxygenase pathway function. CYP2C expression and metabolic activity is suppressed in rodents treated with streptozotocin, a model of Type 1 diabetes [44,45]. In contrast, higher *Cyp2c29* expression relative to controls was observed in *db/db* mice, which display a phenotype similar to Type 2 diabetes [46,47]. High glucose suppressed sEH expression *in vitro,* and hepatic and renal sEH protein levels were significantly lower in streptozotocin-treated mice relative to control [40]. Of note, our study population included only non-insulin-dependent diabetes patients. Accumulating preclinical evidence has suggested that potentiation of EETs or inhibition of sEH enhances insulin signaling and improves insulin sensitivity [48,49]; thus future studies investigating the effect of modulating the CYP epoxygenase pathway in patients with diabetes are warranted. We also observed that cigarette smoking was associated with higher sum DHETs and lower epoxide:diol ratios in CAD patients. This suggests that cigarette smoking increases sEH expression or metabolic activity, which is consistent with higher vascular sEH expression observed in mice chronically exposed to tobacco smoke [34]. Interestingly, cigarette smoking modifies the risk of CAD in individuals who carry function genetic variants in *EPHX2* [22], *CYP2C8* [21], and *CYP2J2* [50], such that variant allele carriers who smoke have the highest risk. Our findings suggest that these interactions may be mediated in part by upregulation of sEH activity by cigarette smoking. However, studies evaluating the direct effect of cigarette smoke exposure on sEH function in humans are needed to confirm this hypothesis.

Of the clinical factors that we evaluated, only ACE inhibitor/ARB use was associated with plasma 20-HETE concentrations in CAD patients. Our observation that plasma 20-HETE levels were lower in patients treated with an ACE inhibitor/ARB are consistent with previous findings that plasma 20-HETE levels are significantly higher in patients with renovascular disease, a condition characterized by activation of the renin-angiotensin system. Minuz and colleagues also observed a positive correlation between plasma 20-HETE levels and plasma renin activity in all study subjects [37]. In preclinical models, angiotensin II stimulates 20-HETE release in isolated perfused kidneys [51] and renal microvessels [52]. Further study is warranted to investigate the interplay between the renin-angiotensin system and the CYP ω-hydroxylase pathway in humans.

In contrast to prior studies showing a correlation between urinary 20-HETE levels and body mass index [53,54], we observed no relationship between plasma 20-HETE and obesity in CAD patients. Several factors may account for these differences. First, our study population was composed of CAD patients with multiple comorbidities, while previous studies have enrolled individuals with hypertension or metabolic syndrome. Also, the patients in prior studies were untreated. In contrast, we withheld medications only the morning of the study visit. Consequently, effects of drug therapy, such as the relationship that we observed with ACE inhibitor/ARB use, may have masked other factors that influence plasma 20-HETE levels in CAD patients. Finally, urinary 20-HETE levels may reflect local production in the kidney rather than systemic levels. As a result, the clinical factors that influence urinary 20-HETE excretion may differ from those associated with plasma 20-HETE concentrations.

There are several limitations to our analysis. Due to the cross-sectional and observational design of the study, we are unable to establish a cause-effect relationship between presence of CAD and the apparent suppression of sEH activity. In addition, our analysis compared well-treated CAD patients with established atherosclerosis and

multiple comorbidities to healthy individuals with no risk factors for cardiovascular disease. Thus there are many potential confounding factors which may have influenced the relationships we observed. For example, we cannot determine whether our observations are due to the presence of atherosclerotic disease, the presence of comorbidities/cardiovascular risk factors, or a consequence of drug therapy. Also, nearly all the CAD patients were treated with aspirin, statins, and beta-blockers, so we were unable to evaluate the effects of these treatments on CYP-mediated eicosanoid metabolism. Moreover, many of the clinical characteristics in the CAD patients, such as serum lipid levels and blood pressure values, were influenced by drug therapy, and our analysis was underpowered to evaluate such drug-disease interactions. Consequently, our analysis was not comprehensive, and other clinical factors may influence CYP-derived eicosanoid levels in humans. Finally, although we adjusted the significance level to account for the impact of multiple statistical tests, replication in an independent cohort is necessary to validate our results. Despite these limitations, our analysis is the first to measure plasma levels of CYP-derived eicosanoids in CAD patients and lays a foundation for future interventional studies seeking to evaluate the therapeutic effect of modulating the CYP epoxygenase and ω-hydroxylase pathways in humans.

In conclusion, we observed that CAD patients had significantly higher plasma epoxide:diol ratios compared to healthy volunteers, suggesting that sEH activity is suppressed in the presence of cardiovascular disease. Future studies are necessary to elucidate the mechanism by which sEH activity is suppressed in CAD patients, as well as to investigate the therapeutic potential of modulation of CYP-mediated eicosanoid metabolism as a strategy for the treatment of CAD.

Table 5.1: Study population characteristics

Characteristic	CAD	HV
N	82	36
Age (years)	54.8 ± 7.2	50.0 ± 7.3 *
Female gender (%)	31 (37.8%)	20 (55.6%)
African-American race (%)	14 (17.1%)	6 (16.7%)
Body mass index (kg/m^2)	30.6 ± 5.9	25.7 ± 2.4 *
<25 kg/m^2	16 (19.5%)	12 (33.3%)
25-29.9 kg/m^2	20 (24.4%)	24 (66.7%)
≥30 kg/m^2	46 (56.1%)	0 (0%) †
Current smoker (%)	22 (26.8%)	0 (0%) †
Diabetes (%)	22 (26.8%)	0 (0%) †
Hypertension (%)	63 (76.8%)	0 (0%) †
Systolic blood pressure (mmHg)	135 ± 17	122 ± 13 *
Diastolic blood pressure (mmHg)	80 ± 10	75 ± 8 *
Total cholesterol (mg/dL)	156 (47)	191 (29) *
LDL cholesterol (mg/dL)	85 (41)	117 (29) *
HDL cholesterol (mg/dL)	45 (15)	65 (21) *
Triglycerides (mg/dL)	104 (81)	69 (36) *
Total:HDL cholesterol (ratio)	3.4 (1.7)	3.1 (1.1)
High sensitivity C-reactive protein (mg/L)	1.9 (3.5)	0.7 (1.6) *
ACE inhibitor or ARB use (%)	50 (61.0%)	0 (0%) †
Beta-blocker use (%)	69 (84.2%)	0 (0%) †
Statin use (%)	76 (92.7%)	0 (0%) †
Aspirin use (%)	79 (96.3%)	0 (0%) †
Clopidogrel use (%)	65 (79.3%)	0 (0%) †

ACE = angiotensin converting enzyme, ARB=angiotensin receptor blocker, CAD=coronary artery disease, HDL=high density lipoprotein, HV=healthy volunteer, LDL=low density lipoprotein

Data presented as mean ± standard deviation, median (interquartile range) or count (proportion).

*P<0.05 versus CAD. † Exclusion criterion in HV cohort.

Table 5.2: Clinical factors that are significantly associated with plasma CYP-derived eicosanoid levels in CAD patients

	Parameter Estimate	SE	Partial R^2	p
Sum EETs				
Body mass index	-0.036	0.009	0.122	0.001
Age	-0.014	0.007	0.048	0.037
Sum DHETs				
Smoking	0.273	0.121	0.051	0.041
Diabetes	-0.255	0.121	0.051	0.038
20-HETE				
ACEI/ARB use	-0.320	0.109	0.098	0.004
14,15-EET:14,15-DHET				
Smoking	-0.531	0.213	0.043	0.061
Body mass index	-0.038	0.016	0.041	0.064

ACEI = angiotensin converting enzyme inhibitor; ARB = angiotensin receptor blocker

Sum EETs, sum DHETs, 20-HETE, and 14,15-EET:14,15-DHET ratio were log-transformed prior to analysis.

Table 5.3: Comparison of plasma CYP-derived eicosanoid levels between CAD patients and healthy volunteers

Analyte (ng/mL)	CAD	HV	P
14,15-EET	0.18 (0.19)	0.10 (0.06)	<0.001
8,9-EET	0.11 (0.08)	0.09 (0.02)	0.003
14,15-DHET	0.53 (0.35)	0.64 (0.34)	0.137
11,12-DHET	0.48 (0.32)	0.59 (0.30)	0.064
8,9-DHET	0.14 (0.10)	0.19 (0.09)	0.064
5,6-DHET	0.15 (0.13)	0.25 (0.12)	<0.001
20-HETE	1.46 (0.90)	1.48 (0.70)	0.988
9,10-EpOME	3.62 (2.87)	2.33 (1.52)	<0.001
9,10-DHOME	4.63 (3.40)	6.14 (3.32)	0.014
12,13-EpOME	6.23 (4.87)	4.68 (3.15)	0.018
12,13-DHOME	3.36 (2.40)	5.61 (4.26)	<0.001

Data presented as median (interquartile range). Following log-transformation, plasma levels of each analyte were compared by one-way ANOVA.

Figure Legends

Figure 5.1: (A) Distribution of plasma concentrations of CYP-derived eicosanoid metabolites in CAD patients (n=82) plotted on a log_{10}-scale. The line within the box defines the median, the ends of the boxes define the 25^{th} and 75^{th} percentiles, the error bars define the 10^{th} and 90^{th} percentiles, and the individual points identify values outside the 10^{th} and 90^{th} percentiles. (B) Heat map depicting strength of Spearman rank correlations between analytes. Gray boxes indicate no significant correlation. Colored boxes indicate a significant correlation, with the strength of the correlation indicated by the intensity of the color.

Figure 5.2: (A) Distribution of plasma concentrations of CYP-derived eicosanoid metabolites in healthy volunteers (n=36) plotted on a log_{10}-scale. (B) Heat map depicting strength of Spearman rank correlations between analytes. Gray boxes indicate no significant correlation. Colored boxes indicate a significant correlation, with the strength of the correlation indicated by the intensity of the color.

Figure 5.3: Distribution of plasma (A) sum EETs, (B) sum DHETs, (C) and total epoxygenase activity (EETs+DHETs) in healthy volunteers (HV, n=36) and CAD patients (n=82) plotted on a log_{10}-scale. *Unadjusted $P<0.0125$ versus HV. $^{\dagger}P<0.0125$ versus HV after adjusting for age, gender, and race. ‡ $P<0.0125$ versus HV after adjusting for age and body mass index.

Figure 5.4: Distribution of (A) plasma sum EETs in healthy volunteers (HV, n=36) and CAD patients with body mass index <30 kg/m^2 (CAD: n=36), plasma sum DHETs in healthy volunteers (HV, n=36) and (B) non-smoker CAD patients (CAD: n=60) and (C) non-diabetic CAD patients (CAD: n=60) and (D) plasma 20-HETE in healthy volunteers (HV, n=36) and CAD patients not treated with an ACE inhibitor or ARB (n=32) plotted on

a $\log_{10}$-scale. *Unadjusted P<0.0125 versus HV. †P<0.0125 versus HV after adjusting for age, gender, and race.

Figure 5.5: Distribution of plasma (A) 14,15-EET:14,15-DHET, (B) 9,10-EpOME:9,10-DHOME, (C) 12,13-EpOME:12,13-DHOME in healthy volunteers (HV, n=36) and CAD patients (n=82) plotted on a $\log_{10}$-scale. *Unadjusted P<0.0125 versus HV. †P<0.0125 versus HV after adjusting for age, gender, and race. ‡P<0.0125 versus HV after adjusting for body mass index.

Figure 5.6: Distribution of plasma 14,15-EET:14,15-DHET, 9,10-EpOME:9,10-DHOME, 12,13-EpOME:12,13-DHOME in (A) men (HV: n=16; CAD: n=51) and (B) women (HV: n=20; CAD: n=31) plotted on a $\log_{10}$-scale. *Unadjusted P<0.0125 versus HV. †P<0.0125 versus HV after adjusting for age and race. ‡P<0.0125 versus HV after adjusting for body mass index.

Figure 5.7: Distribution of plasma 14,15-EET:14,15-DHET, 9,10-EpOME:9,10-DHOME, 12,13-EpOME:12,13-DHOME in healthy volunteers (HV, n=36) and (A) CAD patients with BMI≤30 kg/m^2 (n=36), (B) non-smoking CAD patients (n=60), and (C) non-diabetic CAD patients (n=60) plotted on a $\log_{10}$-scale. *Unadjusted P<0.0125 versus HV. †P<0.0125 versus HV after adjusting for age, gender, and race. ‡P<0.0125 versus HV after adjusting for body mass index.

Figure 5.1: Plasma CYP-derived eicosanoid levels and inter-metabolite correlations in CAD patients

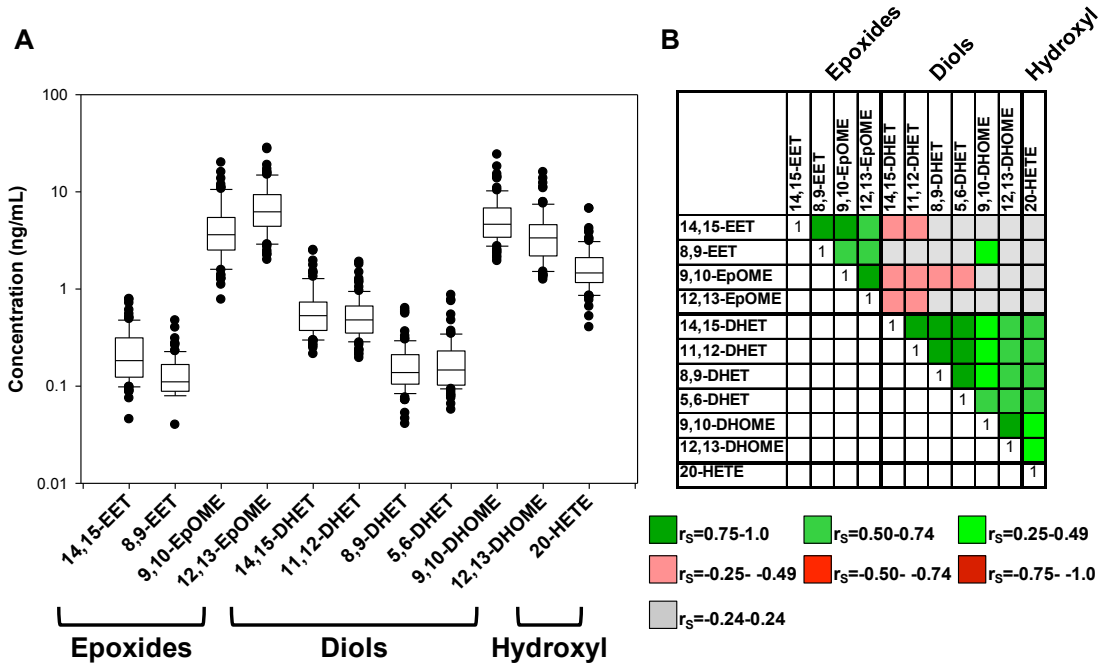

Figure 5.2: Plasma CYP-derived eicosanoid levels and inter-metabolite correlations in healthy volunteers

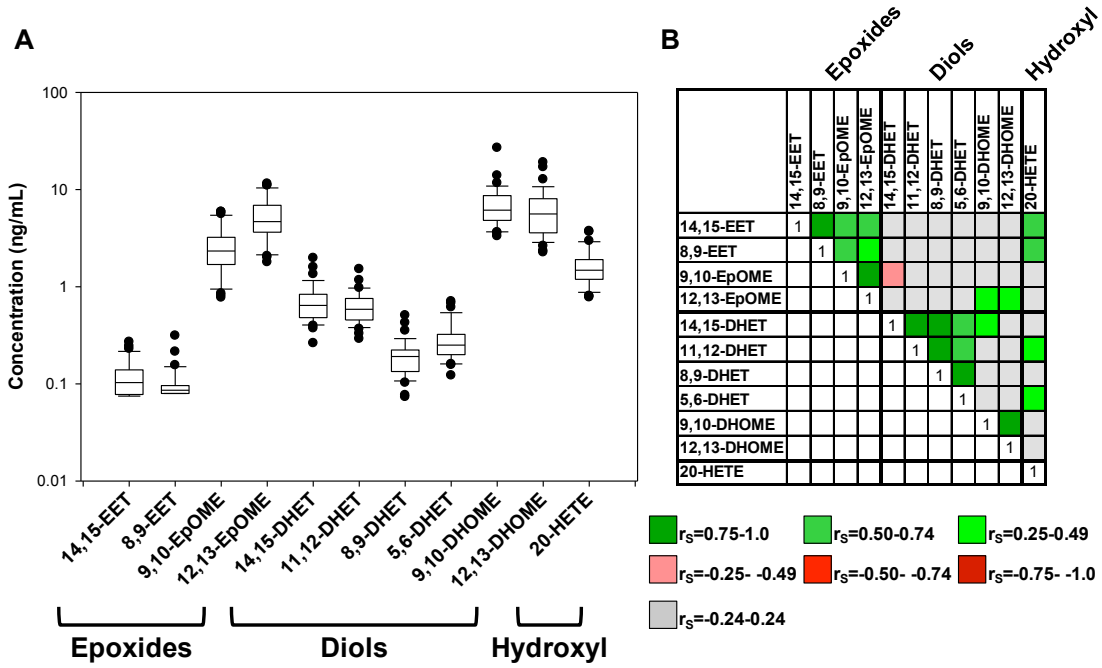

Figure 5.3: Comparison of plasma EETs, DHETs, and total epoxygenase activity in CAD patients and healthy volunteers

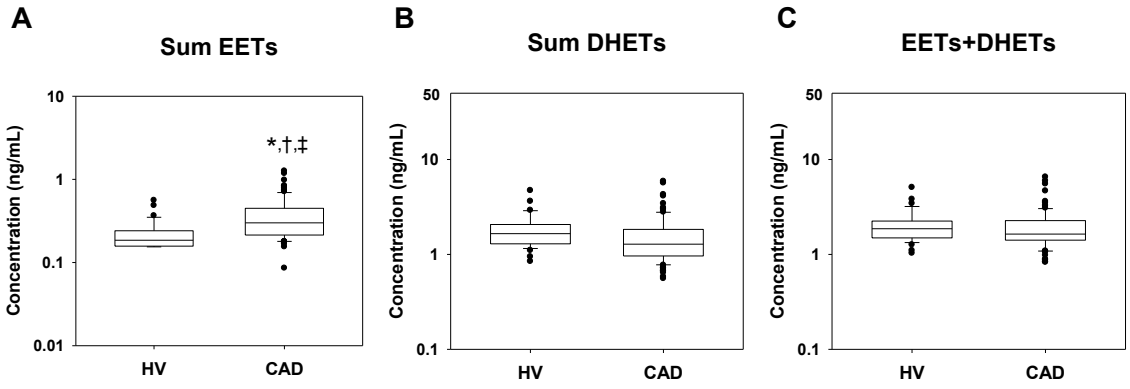

Figure 5.4: Case-control comparison of plasma EETs, plasma DHETs, and 20-HETE stratified by body mass index, smoking status, diabetes status, and ACE inhibitor/ARB use

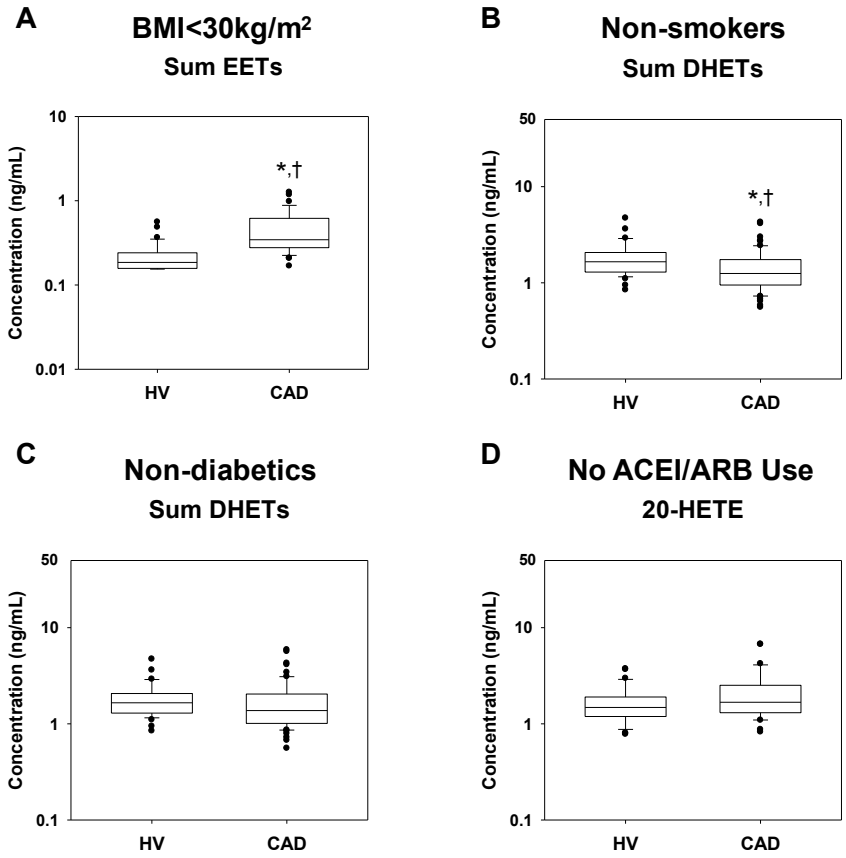

Figure 5.5: Comparison of epoxide:diol ratios in CAD patients and healthy volunteers

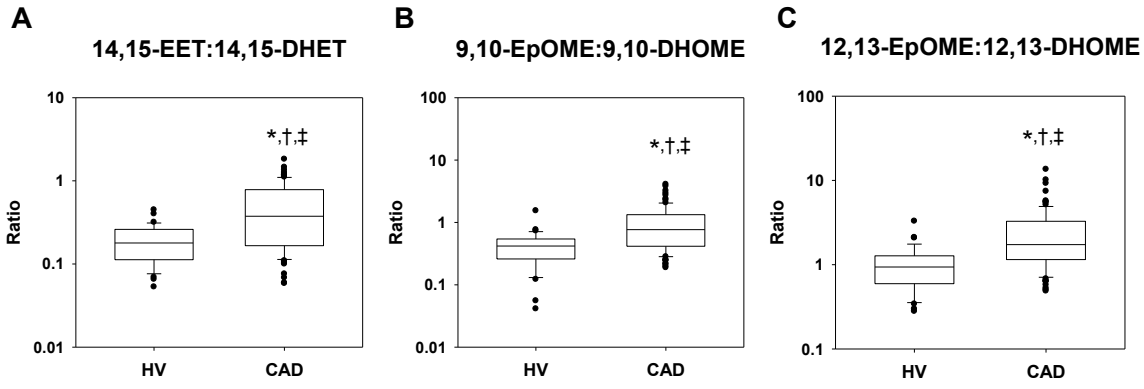

Figure 5.6: Case-control comparison of plasma epoxide:diol ratios stratified by gender

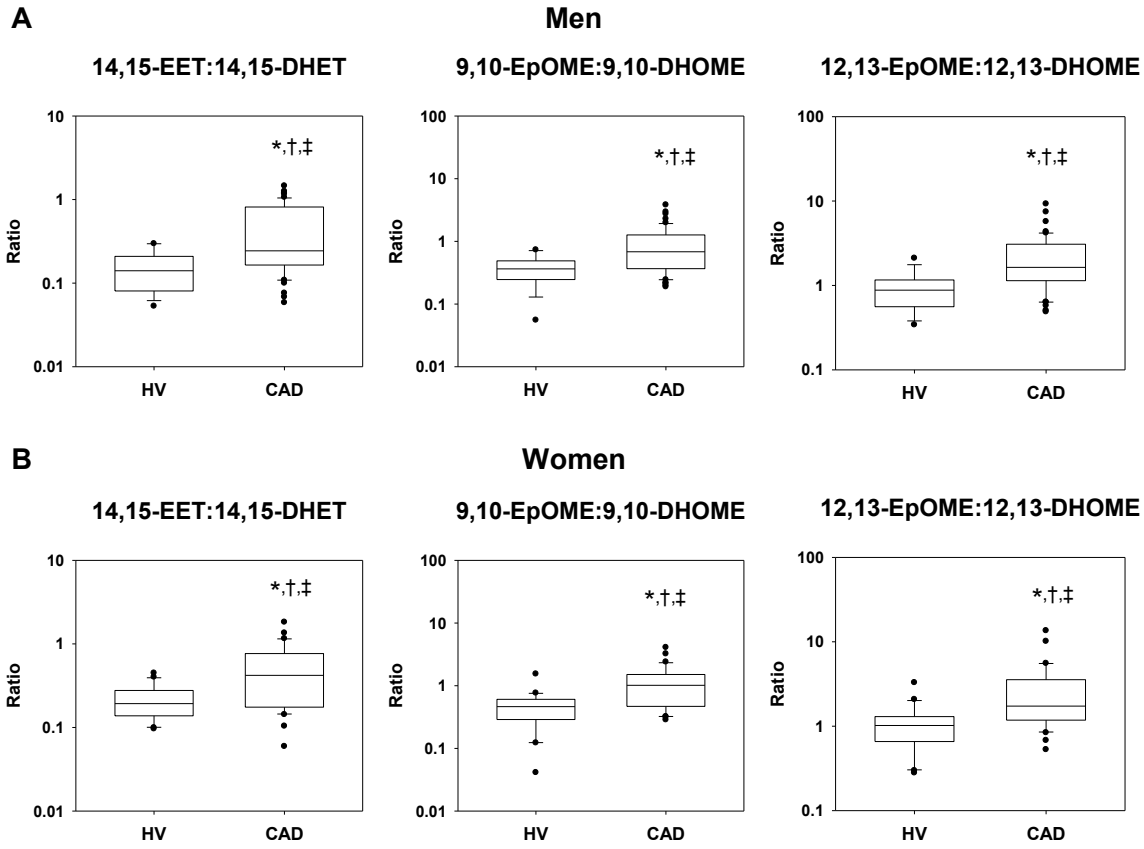

Figure 5.7: Case-control comparison of plasma epoxide:diol ratios stratified by body mass index, smoking status, and diabetes status

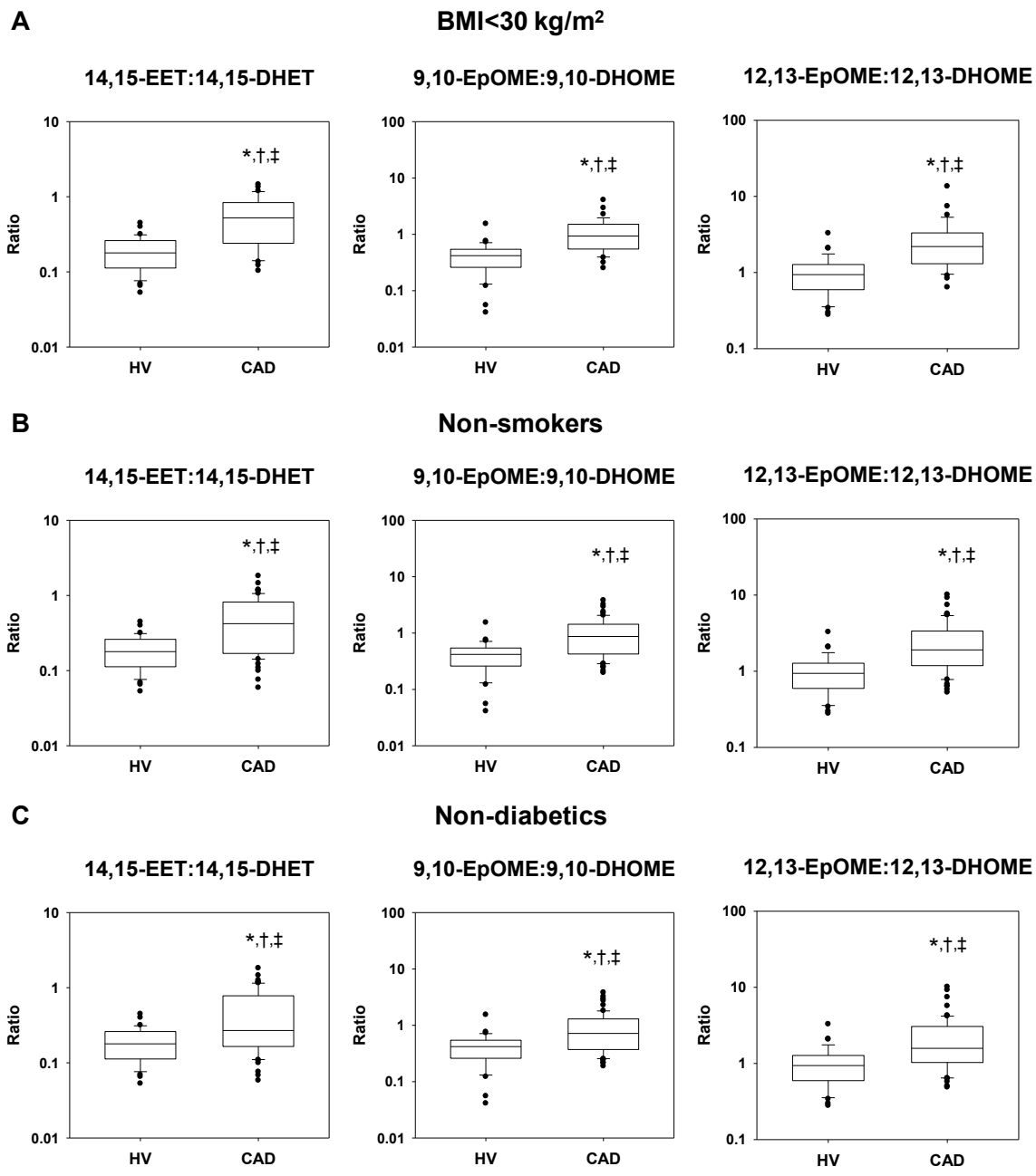

References

1. Roger VL, Go AS, Lloyd-Jones DM, Adams RJ, Berry JD, et al. (2011) Heart disease and stroke statistics--2011 update: a report from the American Heart Association. Circulation 123: e18-e209.

2. Deng Y, Theken KN, Lee CR (2010) Cytochrome P450 epoxygenases, soluble epoxide hydrolase, and the regulation of cardiovascular inflammation. J Mol Cell Cardiol 48: 331-341.

3. Zeldin DC (2001) Epoxygenase pathways of arachidonic acid metabolism. J Biol Chem 276: 36059-36062.

4. Roman RJ (2002) P-450 metabolites of arachidonic acid in the control of cardiovascular function. Physiol Rev 82: 131-185.

5. Lee CR, Imig JD, Edin ML, Foley J, DeGraff LM, et al. (2010) Endothelial expression of human cytochrome P450 epoxygenases lowers blood pressure and attenuates hypertension-induced renal injury in mice. FASEB J 24: 3770-3781.

6. Imig JD, Zhao X, Capdevila JH, Morisseau C, Hammock BD (2002) Soluble epoxide hydrolase inhibition lowers arterial blood pressure in angiotensin II hypertension. Hypertension 39: 690-694.

7. Schmelzer KR, Kubala L, Newman JW, Kim IH, Eiserich JP, et al. (2005) Soluble epoxide hydrolase is a therapeutic target for acute inflammation. Proc Natl Acad Sci U S A 102: 9772-9777.

8. Deng Y, Edin ML, Theken KN, Schuck RN, Flake GP, et al. (2011) Endothelial CYP epoxygenase overexpression and soluble epoxide hydrolase disruption attenuate acute vascular inflammatory responses in mice. FASEB J 25: 703-713.

9. Seubert J, Yang B, Bradbury JA, Graves J, Degraff LM, et al. (2004) Enhanced postischemic functional recovery in CYP2J2 transgenic hearts involves mitochondrial ATP-sensitive K+ channels and p42/p44 MAPK pathway. Circ Res 95: 506-514.

10. Seubert JM, Sinal CJ, Graves J, DeGraff LM, Bradbury JA, et al. (2006) Role of soluble epoxide hydrolase in postischemic recovery of heart contractile function. Circ Res 99: 442-450.

11. Motoki A, Merkel MJ, Packwood WH, Cao Z, Liu L, et al. (2008) Soluble epoxide hydrolase inhibition and gene deletion are protective against myocardial ischemia-reperfusion injury in vivo. Am J Physiol Heart Circ Physiol 295: H2128-2134.

12. Zhang W, Otsuka T, Sugo N, Ardeshiri A, Alhadid YK, et al. (2008) Soluble epoxide hydrolase gene deletion is protective against experimental cerebral ischemia. Stroke 39: 2073-2078.

13. Ulu A, Davis BB, Tsai HJ, Kim IH, Morisseau C, et al. (2008) Soluble epoxide hydrolase inhibitors reduce the development of atherosclerosis in apolipoprotein e-knockout mouse model. J Cardiovasc Pharmacol 52: 314-323.

14. Zhang LN, Vincelette J, Cheng Y, Mehra U, Chen D, et al. (2009) Inhibition of soluble epoxide hydrolase attenuated atherosclerosis, abdominal aortic aneurysm formation, and dyslipidemia. Arterioscler Thromb Vasc Biol 29: 1265-1270.

15. Sodhi K, Wu CC, Cheng J, Gotlinger K, Inoue K, et al. (2010) CYP4A2-induced hypertension is 20-hydroxyeicosatetraenoic acid- and angiotensin II-dependent. Hypertension 56: 871-878.

16. Wu CC, Cheng J, Zhang FF, Gotlinger KH, Kelkar M, et al. (2011) Androgen-dependent hypertension is mediated by 20-hydroxy-5,8,11,14-eicosatetraenoic acid-induced vascular dysfunction: role of inhibitor of kappaB Kinase. Hypertension 57: 788-794.

17. Cheng J, Ou JS, Singh H, Falck JR, Narsimhaswamy D, et al. (2008) 20-hydroxyeicosatetraenoic acid causes endothelial dysfunction via eNOS uncoupling. Am J Physiol Heart Circ Physiol 294: H1018-1026.

18. Yousif MH, Benter IF (2010) Role of 20-hydroxyeicosatetraenoic and epoxyeicosatrienoic acids in the regulation of vascular function in a model of hypertension and endothelial dysfunction. Pharmacology 86: 149-156.

19. Nithipatikom K, Gross ER, Endsley MP, Moore JM, Isbell MA, et al. (2004) Inhibition of cytochrome P450omega-hydroxylase: a novel endogenous cardioprotective pathway. Circ Res 95: e65-71.

20. Poloyac SM, Zhang Y, Bies RR, Kochanek PM, Graham SH (2006) Protective effect of the 20-HETE inhibitor HET0016 on brain damage after temporary focal ischemia. J Cereb Blood Flow Metab 26: 1551-1561.

21. Lee CR, North KE, Bray MS, Couper DJ, Heiss G, et al. (2007) CYP2J2 and CYP2C8 polymorphisms and coronary heart disease risk: the Atherosclerosis Risk in Communities (ARIC) study. Pharmacogenet Genomics 17: 349-358.

22. Lee CR, North KE, Bray MS, Fornage M, Seubert JM, et al. (2006) Genetic variation in soluble epoxide hydrolase (EPHX2) and risk of coronary heart disease: The Atherosclerosis Risk in Communities (ARIC) study. Hum Mol Genet 15: 1640-1649.

23. Liu H, Zhao Y, Nie D, Shi J, Fu L, et al. (2008) Association of a functional cytochrome P450 4F2 haplotype with urinary 20-HETE and hypertension. J Am Soc Nephrol 19: 714-721.

24. Fava C, Montagnana M, Almgren P, Rosberg L, Lippi G, et al. (2008) The V433M variant of the CYP4F2 is associated with ischemic stroke in male Swedes beyond its effect on blood pressure. Hypertension 52: 373-380.

25. Ward NC, Tsai IJ, Barden A, van Bockxmeer FM, Puddey IB, et al. (2008) A single nucleotide polymorphism in the CYP4F2 but not CYP4A11 gene is associated with increased 20-HETE excretion and blood pressure. Hypertension 51: 1393-1398.

26. Gainer JV, Bellamine A, Dawson EP, Womble KE, Grant SW, et al. (2005) Functional variant of CYP4A11 20-hydroxyeicosatetraenoic acid synthase is associated with essential hypertension. Circulation 111: 63-69.

27. Newman JW, Watanabe T, Hammock BD (2002) The simultaneous quantification of cytochrome P450 dependent linoleate and arachidonate metabolites in urine by HPLC-MS/MS. J Lipid Res 43: 1563-1578.

28. Edin ML, Wang Z, Bradbury JA, Graves JP, Lih FB, et al. (2011) Endothelial expression of human cytochrome P450 epoxygenase CYP2C8 increases susceptibility to ischemia-reperfusion injury in isolated mouse heart. FASEB J.

29. Bijlsma S, Bobeldijk I, Verheij ER, Ramaker R, Kochhar S, et al. (2006) Large-scale human metabolomics studies: a strategy for data (pre-) processing and validation. Anal Chem 78: 567-574.

30. Zhao X, Pollock DM, Inscho EW, Zeldin DC, Imig JD (2003) Decreased renal cytochrome P450 2C enzymes and impaired vasodilation are associated with angiotensin salt-sensitive hypertension. Hypertension 41: 709-714.

31. Wang MH, Smith A, Zhou Y, Chang HH, Lin S, et al. (2003) Downregulation of renal CYP-derived eicosanoid synthesis in rats with diet-induced hypertension. Hypertension 42: 594-599.

32. Zhou Y, Lin S, Chang HH, Du J, Dong Z, et al. (2005) Gender differences of renal CYP-derived eicosanoid synthesis in rats fed a high-fat diet. Am J Hypertens 18: 530-537.

33. Zhao X, Dey A, Romanko OP, Stepp DW, Wang MH, et al. (2005) Decreased epoxygenase and increased epoxide hydrolase expression in the mesenteric artery of obese Zucker rats. Am J Physiol Regul Integr Comp Physiol 288: R188-196.

34. Maresh JG, Xu H, Jiang N, Gairola CG, Shohet RV (2005) Tobacco smoke dysregulates endothelial vasoregulatory transcripts in vivo. Physiol Genomics 21: 308-313.

35. Chabova VC, Kramer HJ, Vaneckova I, Vernerova Z, Eis V, et al. (2007) Effects of chronic cytochrome P-450 inhibition on the course of hypertension and end-organ damage in Ren-2 transgenic rats. Vascul Pharmacol 47: 145-159.

36. Kaergel E, Muller DN, Honeck H, Theuer J, Shagdarsuren E, et al. (2002) P450-dependent arachidonic acid metabolism and angiotensin II-induced renal damage. Hypertension 40: 273-279.

37. Minuz P, Jiang H, Fava C, Turolo L, Tacconelli S, et al. (2008) Altered release of cytochrome p450 metabolites of arachidonic acid in renovascular disease. Hypertension 51: 1379-1385.

38. Imig JD, Zhao X, Zaharis CZ, Olearczyk JJ, Pollock DM, et al. (2005) An orally active epoxide hydrolase inhibitor lowers blood pressure and provides renal protection in salt-sensitive hypertension. Hypertension 46: 975-981.

39. Barbosa-Sicard E, Fromel T, Keseru B, Brandes RP, Morisseau C, et al. (2009) Inhibition of the soluble epoxide hydrolase by tyrosine nitration. J Biol Chem 284: 28156-28163.

40. Oguro A, Fujita N, Imaoka S (2009) Regulation of soluble epoxide hydrolase (sEH) in mice with diabetes: high glucose suppresses sEH expression. Drug Metab Pharmacokinet 24: 438-445.

41. Charles RL, Burgoyne JR, Mayr M, Weldon SM, Hubner N, et al. (2011) Redox regulation of soluble epoxide hydrolase by 15-deoxy-delta-prostaglandin J2 controls coronary hypoxic vasodilation. Circ Res 108: 324-334.

42. Chen D, Whitcomb R, Macintyre E, Tran V, Do ZN, et al. (2011) Pharmacokinetics and Pharmacodynamics of AR9281, an Inhibitor of Soluble Epoxide Hydrolase, in Single- and Multiple-Dose Studies in Healthy Human Subjects. J Clin Pharmacol.

43. Zhang LN, Vincelette J, Chen D, Gless RD, Anandan SK, et al. (2011) Inhibition of soluble epoxide hydrolase attenuates endothelial dysfunction in animal models of diabetes, obesity and hypertension. Eur J Pharmacol 654: 68-74.

44. Donahue BS, Skottner-Lundin A, Morgan ET (1991) Growth hormone-dependent and -independent regulation of cytochrome P-450 isozyme expression in streptozotocin-diabetic rats. Endocrinology 128: 2065-2076.

45. Shimojo N, Ishizaki T, Imaoka S, Funae Y, Fujii S, et al. (1993) Changes in amounts of cytochrome P450 isozymes and levels of catalytic activities in hepatic and renal microsomes of rats with streptozocin-induced diabetes. Biochem Pharmacol 46: 621-627.

46. Lam JL, Jiang Y, Zhang T, Zhang EY, Smith BJ (2010) Expression and functional analysis of hepatic cytochromes P450, nuclear receptors, and membrane transporters in 10- and 25-week-old db/db mice. Drug Metab Dispos 38: 2252-2258.

47. Yoshinari K, Takagi S, Sugatani J, Miwa M (2006) Changes in the expression of cytochromes P450 and nuclear receptors in the liver of genetically diabetic db/db mice. Biol Pharm Bull 29: 1634-1638.

48. Luria A, Bettaieb A, Xi Y, Shieh GJ, Liu HC, et al. (2011) Soluble epoxide hydrolase deficiency alters pancreatic islet size and improves glucose homeostasis in a model of insulin resistance. Proc Natl Acad Sci U S A 108: 9038-9043.

49. Xu X, Zhao CX, Wang L, Tu L, Fang X, et al. (2010) Increased CYP2J3 expression reduces insulin resistance in fructose-treated rats and db/db mice. Diabetes 59: 997-1005.

50. Liu PY, Li YH, Chao TH, Wu HL, Lin LJ, et al. (2006) Synergistic effect of cytochrome P450 epoxygenase CYP2J2*7 polymorphism with smoking on the onset of premature myocardial infarction. Atherosclerosis.

51. Carroll MA, Balazy M, Margiotta P, Huang DD, Falck JR, et al. (1996) Cytochrome P-450-dependent HETEs: profile of biological activity and stimulation by vasoactive peptides. Am J Physiol 271: R863-869.

52. Croft KD, McGiff JC, Sanchez-Mendoza A, Carroll MA (2000) Angiotensin II releases 20-HETE from rat renal microvessels. Am J Physiol Renal Physiol 279: F544-551.

53. Laffer CL, Laniado-Schwartzman M, Nasjletti A, Elijovich F (2004) 20-HETE and circulating insulin in essential hypertension with obesity. Hypertension 43: 388-392.

54. Ward NC, Rivera J, Hodgson J, Puddey IB, Beilin LJ, et al. (2004) Urinary 20-hydroxyeicosatetraenoic acid is associated with endothelial dysfunction in humans. Circulation 110: 438-443.

Chapter VI: Genetic variation in the CYP epoxygenase and ω-hydroxylase pathways is associated with survival in ACS patients

Acute coronary syndromes (ACS), the clinical consequence of unstable coronary artery disease (CAD), are a major cause of morbidity and mortality worldwide [1]. Vascular inflammation is integral to the development and progression of atherosclerotic lesions, and ultimately promotes plaque instability and rupture, leading to ACS [2]. Moreover, elevations in plasma inflammatory biomarkers have been associated with poor outcomes following an ACS event [3,4,5,6,7], suggesting that pharmacologic agents that attenuate vascular inflammation may have therapeutic potential.

Modulation of cytochrome P450 (CYP)-mediated arachidonic acid metabolism may represent a novel anti-inflammatory treatment strategy for ACS. Epoxyeicosatrienoic acids (EETs), the products of olefin epoxidation of arachidonic acid by CYP2J and CYP2C isoforms, possess potent vasodilatory and anti-inflammatory properties, but are rapidly hydrolyzed by soluble epoxide hydrolase (sEH) to the less biologically active dihydroxyeicosatrienoic acids (DHETs) [8]. In contrast, ω-hydroxylation of arachidonic acid by CYP4A and CYP4F isoforms produces 20-hydroxyeicosatetraenoic acid (20-HETE), a vasoconstrictive and pro-inflammatory eicosanoid [9]. In addition to regulating inflammation, CYP-derived eicosanoids also influence the recovery from ischemia/reperfusion injury in preclinical models. Potentiation of the CYP epoxygenase pathway, via enhancement of CYP-mediated EET biosynthesis or inhibition of sEH-mediated EET hydrolysis, improves functional recovery following myocardial ischemia/reperfusion injury [10,11,12]. Conversely, inhibition of the

CYP ω-hydroxylase pathway is cardioprotective following ischemia/reperfusion injury [13,14,15,16].

Although these studies suggest that potentiation of CYP epoxygenase-derived EETs and inhibition of CYP ω-hydroxylase-derived 20-HETE may improve outcomes following an ACS event, pharmacologic agents that specifically modulate CYP-mediated eicosanoid metabolism are not approved for use in humans. Thus, the therapeutic utility of directly manipulating the CYP epoxygenase and ω-hydroxylase pathways in ACS patients has not been investigated. Importantly, functional genetic polymorphisms in the CYP epoxygenases (*CYP2J2*, *CYP2C8*), sEH (*EPHX2*), and the CYP ω-hydroxylases (*CYP4A11*, *CYP4F2*) (Table 6.1) have been associated with cardiovascular disease risk [17,18,19,20,21,22,23,24], suggesting that CYP-derived eicosanoids play an important role in the cardiovascular system in humans. However, the relationship between these variants and prognosis in patients with ACS has not been characterized to date. Therefore, we sought to investigate the association between functional genetic variants in *CYP2J2*, *CYP2C8*, *EPHX2*, *CYP4A11*, and *CYP4F2* and 5-year survival in a well-phenotyped cohort of ACS patients.

Methods

Study population

The analysis was performed in a cohort of patients with confirmed ACS (INvestigation oF Outcomes from acute coronary syndRoMes study (INFORM); N=721), prospectively recruited from the Mid America Heart Institute and Truman Medical Center in Kansas City, MO. The methods of recruitment and characteristics of the population have been reported previously [25,26,27]. Briefly, all patients admitted between March 1, 2001 and October 31, 2002, who had a troponin blood test were screened for possible ACS. Myocardial infarction (MI) was defined by elevated troponin level in combination

with chest pain symptoms or electrocardiographic findings (ST-segment elevation or non-ST-segment elevation) consistent with MI. Unstable angina was defined by a negative troponin level and any one of the following: new-onset angina (<2 months), prolonged angina (>20 minutes) at rest, recent worsening angina, or angina that occurred within 2 weeks of MI [28].

Demographic, economic, and health status information was obtained by patient interview; medical history, laboratory results, and disease severity were ascertained from medical records. Patient vital status was assessed by searching the Social Security Administration Death Master File (http://www.ntis.gov/products/ssa-dmf.aspx).

Genotyping

Genotyping was completed in the laboratory of Dr. Sharon Cresci (Washington University, St. Louis, MO), as previously described [29]. Patients were genotyped for the variants listed in Table 6.1, which were chosen due to their known functional effect on enzyme expression or activity and previous association with cardiovascular disease susceptibility. Genotyping was performed by pyrosequencing (rs10509681, rs41507953, rs751141, rs1126742, rs3093098, rs2108622) or using a Taqman allelic discrimination assay (rs890293) (Applied Biosystems, Foster City, CA).

Statistical Analysis

Data are presented as mean ± standard deviation or count (proportion) unless otherwise indicated. Baseline characteristics by genotype were compared by Student's t-test, one-way ANOVA, or chi-squared test, as appropriate. Deviations from Hardy-Weinberg equilibrium were evaluated by chi-squared test.

For each variant, 5-year survival was compared between genotype groups by a log-rank test, assuming a dominant mode of inheritance. If a relationship between genotype and survival was observed, Cox proportional hazards modeling adjusted for

pre-specified covariates (Model 1: age, sex, and race; Model 2: age, sex, race, ACS type (ST elevation MI/left bundle branch block, non ST elevation MI, unstable angina), treatment strategy (medical management, percutaneous coronary intervention/coronary artery bypass graft surgery), and diabetes) was performed. The *CYP4F2 -91T>C* and Val433Met variants have opposite effects on 20-HETE formation *in vivo* [17,19]. Therefore, we also constructed a "co-dominant" model for *CYP4F2* genotype in which patients who were wild-type at both loci were compared to patients who carried only the Met433 variant and patients who carried the *-91C* variant regardless of Val433Met genotype.

Survival analysis was performed in the entire cohort and in Caucasians only to account for potential confounding due to population stratification. The small number of events in African-Americans precluded separate statistical analysis in this subgroup. Analyses were performed using SAS 9.2 (SAS Institute, Cary, NC), and $P<0.05$ was considered statistically significant.

To minimize the impact of multiple statistical tests conducted in our analysis, we estimated the false discovery rate (FDR) q-value of our findings, which is defined as the expected proportion of statistical tests deemed significant that are actually false positives (QVALUE) [30]. Due to the significant overlap between the full cohort and the Caucasians only cohort, q-values were estimated for just the Caucasians only analyses. We considered statistical tests from the unadjusted and adjusted association analyses as independent, even though each model assessed the same independent variable. Only q-values for significant findings are presented.

Results

The study population was 79% Caucasian and 36% women, and the overall 5-year all-cause mortality rate was 17%. The genotype distributions within each racial

group were consistent with Hardy-Weinberg equilibrium (P>0.05), except for the *CYP4A11* Phe434Ser variant (Table 6.2). Consequently, the *CYP4A11* polymorphism was excluded from further statistical analysis. The *CYP2J2 -50G>T*, *EPHX2* Lys55Arg, *EPHX2* Arg287Gln, and *CYP4F2* Val433Met polymorphisms were more frequent in African-Americans; the *CYP2C8* Lys399Arg and *CYP4F2 -91T>C* polymorphisms were more frequent in Caucasians.

EPHX2 Lys55Arg, *CYP2J2 -50G>T*, and *CYP4F2* genotype were significantly associated with survival following an ACS event (Table 6.3). Patient characteristics by *EPHX2* Lys55Arg, *CYP2J2 -50G>T*, and *CYP4F2* genotype in all subjects and in Caucasians only are shown in Tables 6.4-6.9. No significant differences in baseline characteristics were observed between the *EPHX2* Lys55Arg (Tables 6.4 and 6.5) and *CYP4F2* (Tables 6.8 and 6.9) genotype groups. In *CYP2J2 -50T* carriers, discharge HDL cholesterol was significantly higher compared to wild-type individuals (Tables 6.6 and 6.7).

Compared to wild-type individuals, *EPHX2* Arg55 variant allele carriers had a significantly higher risk of death following an ACS event (Figure 6.1). This relationship was most pronounced in Caucasians and persisted after adjustment for demographic and clinical covariates (Model 2: hazard ratio (HR) 1.61 95% confidence interval (CI) 1.01-2.55, P=0.045, q=0.064).

In contrast, the 5-year mortality rate in *CYP2J2 -50T* carriers was lower than in wild-type individuals in the full cohort (9.6% vs. 18.1%) and in Caucasians only (5.6% vs. 17.3%) (Figure 6.2). In Caucasians, this association remained significant after adjustment for demographic and clinical covariates (Model 2: HR 0.31 95% CI 0.11-0.84, P=0.021, q=0.064).

CYP4F2 genotype also influenced survival in ACS patients. In the single variant analysis, *CYP4F2* Met433 carriers tended to have a higher risk of death compared to

wild-type individuals in the full cohort (19.5% vs. 14.6%; HR 1.35 95% CI 0.93-1.96, P=0.118) and in Caucasians only (17.8% vs. 13.3%; HR 1.32 95% CI 0.86-2.05, P=0.207). No association was observed between survival and *CYP4F2 -91T>C* in the full cohort (HR 0.92 95% CI 0.63-1.35, P=0.677), but 5-year mortality tended to be lower in *CYP4F2 -91C* carriers compared to wild-type individuals in the Caucasians only analysis (17.8% vs. 14.4%; HR 0.78 95% CI 0.49-1.23, P=0.275). In the co-dominant analysis, carriers of the *CYP4F2* Met433 variant allele alone had a significantly higher risk of death compared to individuals who were wild-type at both loci, but this relationship was abolished in those also carrying the *-91C* variant allele (Figure 6.3). In Caucasians, the association between the Met433 variant and mortality remained significant after adjusting for age and gender (Model 1: HR 1.69 95% CI 1.01-2.85, P=0.048, q=0.064), but the relationship was attenuated and not statistically significant after adjusting for clinical covariates (Model 2: HR 1.62 95% CI 0.96-2.75, P=0.072).

No association was observed between survival and *EPHX2* Arg287Gln (All Subjects: HR 0.88 95% CI 0.55-1.41, P=0.598; Caucasians: HR 0.91 95% CI 0.52-1.59, P=0.745; Figure 6.4) or *CYP2C8* Lys399Arg genotype (All Subjects: HR 0.87 95% CI 0.54-1.40, P=0.574; Caucasians: HR 0.87 95% CI 0.53-1.45, P=0.600; Figure 6.5).

Discussion

Although preclinical studies suggest that potentiation of CYP epoxygenase-derived EETs and inhibition of CYP ω-hydroxylase-derived 20-HETE may improve outcomes following an ACS event, investigation of this therapeutic strategy in humans has been limited by the lack of approved pharmacologic agents that specifically modulate CYP-mediated eicosanoid metabolism. Consequently, genetic epidemiologic studies investigating the association between functional genetic variation in the CYP epoxygenase and ω-hydroxylase pathways and cardiovascular disease susceptibility

have been performed to initially characterize the biologic relevance of the pathways in humans at the population level. To our knowledge, this is the first study to demonstrate that genetic variation in the CYP epoxygenases, sEH, and the CYP ω-hydroxylases is associated with survival in ACS patients. Our findings suggest that alterations in CYP-mediated eicosanoid metabolism influence prognosis in patients with established CAD Moreover, our observations support the development of drugs that target these pathways as treatments for CAD and may help to identify subsets of the population that would most benefit from such therapies.

EETs possess potent vasodilatory and anti-inflammatory effects [8,31], and are cardioprotective following ischemia/reperfusion injury [10,11,12]. Therefore, we hypothesized that genetic variants which result in lower EET biosynthesis or greater EET hydrolysis *in vivo* would have deleterious effects on survival. Consistent with this hypothesis, presence of the *EPHX2* Arg55 variant, which has higher apparent sEH activity *in vivo* [22], was associated with a greater risk of death following an ACS event. This association was most apparent in Caucasians and persisted after adjustment for demographic and clinical covariates. Our observations are consistent with a prior study in the ARIC cohort demonstrating that presence of the *EPHX2* Arg55 variant allele was associated with significantly higher risk of incident CAD in Caucasians [22]. Of note, sEH inhibitors are currently in clinical development for the treatment of cardiovascular and metabolic diseases [32]. Our results suggest that sEH inhibitors may have the greatest therapeutic utility in the subset of patients who are *EPHX2* Arg55 variant allele carriers. Future studies to evaluate the therapeutic efficacy of sEH inhibition specifically in Arg55 carriers are warranted.

The *CYP2J2 -50T* polymorphism disrupts a Sp1 transcription factor binding site, leading to decreased *CYP2J2* transcription *in vivo* [33]. The *-50T* polymorphism has been associated with higher risk of prevalent CAD in a German population [24], and

higher risk of prevalent MI in a Han Chinese population [23]. In contrast to our hypothesis, we observed that presence of the *CYP2J2 -50T* variant allele was associated with the lower risk of death in ACS patients. Interestingly, the *-50T* allele has also been associated with a lower risk of incident CAD in African-Americans in the ARIC cohort [21] and a lower risk of prevalent hypertension in Caucasians [34]. Although lower *CYP2J2* transcription would be hypothesized to result in lower EET levels *in vivo*, we did not measure EET levels in this study, and so cannot establish a mechanistic link between the *CYP2J2 -50T* polymorphism, CYP epoxygenase activity, and survival in ACS patients. Thus, additional studies are necessary to elucidate the mechanism underlying the observed association between *CYP2J2 -50G>T* and mortality.

In contrast to the EETs, 20-HETE is vasoconstrictive and pro-inflammatory [9], and inhibition of 20-HETE formation is protective in preclinical models of myocardial ischemia/reperfusion injury [13,14,15,16]. *CYP4F2* Val433Met has been associated with higher urinary 20-HETE excretion [19], and higher risk of hypertension [19] and stroke [18]. In contrast, the *CYP4F2 -91T>C* variant disrupts a nuclear factor-κB (NF-κB) binding site, resulting in less *CYP4F2* transcription, lower urinary 20-HETE excretion, and lower risk of hypertension [17]. Consistent with the opposite effects of the *CYP4F2 -91C>T* and Val433Met variants on 20-HETE formation *in vivo*, we observed that patients who carried only the Met433 polymorphism had a significantly greater risk of death, but that this relationship was abolished in individuals who also carried the *-91C* allele. Of note, very few patients in INFORM carried the *-91C* allele without the Met433 variant. Thus future studies in larger cohorts are necessary to determine the relationship between the *CYP4F2 -91T>C* polymorphism and survival.

There are several limitations to this study. First, systemic levels of CYP-derived eicosanoids or inflammatory biomarkers were not measured in the INFORM cohort. Thus, we were unable to evaluate whether the association between *EPHX2* Lys55Arg,

CYP2J2 -50G>T, and *CYP4F2* genotype and mortality was specifically related to differences in eicosanoid levels or vascular inflammation, and future studies are necessary to elucidate the mechanism underlying the observed associations. Also, the INFORM cohort was recruited exclusively from one city and was composed predominantly of Caucasian patients. Consequently, our results may not be generalizable to other patient populations or racial groups. In addition, although all-cause mortality is a clinically relevant and robust endpoint, other outcomes, including hospitalizations, cardiovascular mortality, or development of heart failure, are also important endpoints to consider when evaluating prognosis following an ACS event. Finally, although we assessed the false discovery rate to minimize the impact of the multiple statistical tests, there is the potential for false positive associations. The q-values in the Caucasians only cohort were estimated to be ≤0.064. Thus we have a high level of confidence in our results, but replication in an independent cohort is needed to validate our findings. Despite these limitations, this is the first study to demonstrate that genetic variation in the CYP epoxygenases, sEH, and the CYP ω-hydroxylases is associated with prognosis in ACS patients and lays an important foundation for future studies seeking to elucidate the role of these pathways in patients with established CAD.

In conclusion, we observed that *EPHX2* Lys55Arg, *CYP2J2 -50G>T*, and *CYP4F2* genotype were associated with survival in ACS patients. Future studies are necessary to validate these findings and explore the therapeutic potential of modulating the CYP epoxygenase and ω-hydroxylase pathways in humans with established CAD.

Table 6.1: Functional genetic variants in the CYP epoxygenases (*CYP2J2*, *CYP2C8*), sEH (*EPHX2*), and CYP ω-hydroxylases (*CYP4A11*, *CYP4F2*) genotyped in the INFORM cohort

Variant	Nucleotide *	Amino Acid	Functional Effect		References
			In vitro	*In vivo*	
CYP2J2					
rs890293	-50G>T	N/A	↓ *CYP2J2* transcription	↓ *CYP2J2* expression	[24,33]
CYP2C8					
rs10509681	30411A>G	Lys399Arg	↓ EET formation	Unknown	[35,36]
EPHX2					
rs41507953	9846A>G	Lys55Arg	↑ EET hydrolysis	↓ plasma epoxide:diol	[22,37,38,39]
rs751141	25206G>A	Arg387Gln	↓ EET hydrolysis	Unknown	[37,38,39]
CYP4A11					
rs1126742	8610T>C	Phe434Ser	↓ 20-HETE formation	↓ urinary 20-HETE	[19,20]
CYP4F2					
rs3093098	-91T>C	N/A	↓ *CYP4F2* transcription	↓ urinary 20-HETE	[17]
rs2108622	18000G>A	Val433Met	↓ 20-HETE formation	↑ urinary 20-HETE	[19,40]

* Relative to transcriptional start site, GenBank accession numbers: AF272142 (*CYP2J2*), AL359672 (*CYP2C8*), NT_022666 (*EPHX2*), AY369778.1 (*CYP4A11*), and AF467894 (*CYP4F2*).

Table 6.2: Genotype frequencies in INFORM by race

Variant	Caucasians Count (Proportion)	HW P-value	African-Americans Count (Proportion)	HW P-value
CYP2J2				
-50G>T				
G/G	486 (87.3%)	0.109	101 (81.5%)	0.868
G/T	66 (11.8%)		22 (17.7%)	
T/T	5 (0.9%)		1 (0.8%)	
CYP2C8				
Lys399Arg				
A/A	416 (76.1%)	0.509	116 (95.1%)	0.781
A/G	124 (22.7%)		6 (4.9%)	
G/G	7 (1.3%)		0 (0%)	
EPHX2				
Lys55Arg				
A/A	426 (78.2%)	0.540	76 (62.3%)	0.508
A/G	110 (20.2%)		39 (32.0%)	
G/G	9 (1.7%)		7 (5.7%)	
Arg287Gln				
G/G	439 (80.9%)	0.535	89 (72.4%)	0.647
G/A	97 (17.9%)		32 (26.0%)	
A/A	7 (1.3%)		2 (1.6%)	
CYP4A11				
Phe434Ser				
T/T	0 (0%)	<0.001	0 (0%)	<0.001
T/C	522 (97.4%)		115 (93.5%)	
C/C	14 (2.6%)		8 (6.5%)	
CYP4F2				
-91T>C				
T/T	354 (66.3%)	0.566	59 (50.4%)	0.789
T/C	164 (30.7%)		49 (41.9%)	
C/C	16 (3.0%)		9 (7.7%)	
Val433Met				
G/G	256 (48.1%)	0.678	95 (81.9%)	0.371
G/A	229 (43.1%)		19 (16.4%)	
A/A	47 (8.8%)		2 (1.7%)	
Co-dominant				
WT	232 (46.0%)	N/A	45 (41.3%)	N/A
-91C only *	1 (0.2%)		44 (40.4%)	
Met433 only	103 (20.4%)		10 (9.2%)	
Both variants	168 (33.3%)		10 (9.2%)	

Genotypes are presented as count (proportion).

* Because very few individuals carried only the *-91C* variant, the "*-91C* only" and "Both variants" groups were combined for the survival analysis (*-91C*±Val433Met).

HW=Hardy-Weinberg, WT=wild-type

Table 6.3: Hazard ratios between *CYP2J2 -50G>T*, *EPHX2* Lys55Arg, and *CYP4F2* genotype and 5-year mortality

	All Subjects			Caucasians only		
Variant	**HR**	**95% CI**	**P-value**	**HR**	**95% CI**	**P-value**
***EPHX2* Lys55Arg**						
G/A+G/G vs. *AA*						
Unadjusted	1.50	1.02-2.22	0.042	1.64	1.04-2.58	0.032
Model 1	1.40	0.94-2.08	0.099	1.58	1.01-2.49	0.047
Model 2	1.40	0.93-2.09	0.103	1.61	1.01-2.55	0.045
CYP2J2 -50G>T						
G/T+T/T vs. *G/G*						
Unadjusted	0.51	0.26-0.99	0.049	0.30	0.11-0.83	0.020
Model 1	0.52	0.26-1.02	0.060	0.33	0.12-0.91	0.031
Model 2	0.51	0.26-1.01	0.052	0.31	0.11-0.84	0.021
***CYP4F2 -91T>C* ± Val433Met**						
Met433 only vs. WT						
Unadjusted	1.72	1.07-2.79	0.026	1.75	1.04-2.94	0.035
Model 1	1.81	1.11-2.94	0.017	1.69	1.01-2.85	0.048
Model 2	1.75	1.08-2.85	0.024	1.62	0.96-2.75	0.072
-91C ± Met433 vs. WT						
Unadjusted	1.16	0.75-1.80	0.501	0.96	0.57-1.63	0.883
Model 1	1.05	0.68-1.63	0.828	0.88	0.52-1.50	0.637
Model 2	1.08	0.69-1.69	0.736	0.99	0.58-1.70	0.977

Model 1: adjusted for age, gender, and race

Model 2: adjusted for age, gender, race, ACS type (STEMI/LBBB, NSTEMI, unstable angina), diabetes, treatment strategy (medical management, PCI/CABG)

CI=confidence interval, HR=hazard ratio, WT=wild-type

Table 6.4: Study population characteristics by *EPHX2* Lys55Arg genotype in all subjects

Characteristic	Lys/Lys N=502	Lys/Arg+Arg/Arg N=165	P-Value
Age (years)	60.4 ± 12.4	60.8 ± 12.8	0.693
Female gender (%)	177 (35.3%)	64 (38.8%)	0.413
African-American race (%)	76 (15.1%)	46 (27.9%)	<0.001
ACS Classification Type			0.064
ST elevation MI/LBBB	154 (30.7%)	36 (21.8%)	
Non ST elevation MI	152 (30.3%)	52 (31.5%)	
Unstable angina	196 (39.0%)	77 (46.7%)	
History/Risk Factors			
MI (%)	159 (31.7%)	58 (35.2%)	0.408
Hypertension (%)	324 (64.5%)	113 (68.5%)	0.355
Diabetes (%)	136 (27.1%)	51 (30.9%)	0.344
Hyperlipidemia (%)	295 (58.8%)	109 (66.1%)	0.096
Heart Failure (%)	38 (7.6%)	14 (8.5%)	0.704
Smoking Status			0.869
Current	183 (36.5%)	57 (34.5%)	
Former	178 (35.5%)	62 (37.6%)	
Never	140 (27.9%)	46 (27.9%)	
BMI (kg/m^2) *	29.6 ± 6.3	30.2 ± 6.7	0.282
SBP (mmHg) *	136.6 ± 26.6	138.8 ± 25.5	0.339
DBP (mmHg) *	73.9 ± 15.6	76.2 ± 18.7	0.118
Total cholesterol (mg/dL) #	178.4 ± 39.6	181.6 ± 49.1	0.436
LDL (mg/dL) #	103.5 ± 34.5	102.3 ± 44.2	0.757
HDL (mg/dL) #	41.6 ± 14.7	43.6 ± 17.9	0.183
Triglycerides (mg/dL) #	176.4 ± 117.8	181.2 ± 144.9	0.698
Treatment Strategy			0.252
Medical Management	182 (36.3%)	68 (41.2%)	
PCI	299 (59.6%)	87 (52.7%)	
CABG	21 (4.2%)	10 (6.1%)	
Discharge Medications			
Beta-blocker (%)	412 (82.2%)	124 (75.6%)	0.063
Statin (%)	382 (76.1%)	121 (73.3%)	0.475
Aspirin (%)	463 (92.4%)	157 (95.7%)	0.142

ACS=acute coronary syndrome, BMI=body mass index, CABG=coronary artery bypass graft, DBP=diastolic blood pressure, HDL=high density lipoprotein, LBBB=left bundle branch block, LDL=low density lipoprotein, MI=myocardial infarction, PCI=percutaneous coronary intervention, SBP=systolic blood pressure

Data presented as mean ± standard deviation or count (proportion). Continuous variables were compared between groups by Student's t-test. Categorical variables were compared between groups by chi-squared test or Fisher's exact test.

* Measured at admission # Measured at discharge

Table 6.5: Study population characteristics by *EPHX2* Lys55Arg genotype in Caucasians

Characteristic	Lys/Lys N=426	Lys/Arg+Arg/Arg N=119	P-Value
Age (years)	61.6 ± 12.5	63.3 ± 12.3	0.186
Female gender (%)	143 (33.6%)	46 (38.7%)	0.303
ACS Classification Type			0.600
ST elevation MI/LBBB	134 (31.5%)	35 (29.4%)	
Non ST elevation MI	135 (31.7%)	41 (34.5%)	
Unstable angina	157 (36.9%)	43 (36.1%)	
History/Risk Factors			
MI (%)	135 (31.7%)	38 (31.9%)	0.960
Hypertension (%)	265 (62.2%)	76 (63.9%)	0.741
Diabetes (%)	101 (23.7%)	33 (27.7%)	0.368
Hyperlipidemia (%)	263 (61.7%)	84 (70.6%)	0.076
Heart Failure (%)	22 (5.2%)	8 (6.7%)	0.510
Smoking Status			0.543
Current	144 (33.9%)	34 (28.6%)	
Former	159 (37.4%)	49 (41.2%)	
Never	122 (28.7%)	36 (30.3%)	
BMI (kg/m^2) *	29.4 ± 5.9	29.8 ± 5.8	0.521
SBP (mmHg) *	134.6 ± 24.6	135.6 ± 24.5	0.713
DBP (mmHg) *	72.5 ± 14.3	72.4 ± 16.4	0.949
Total cholesterol (mg/dL) #	177.1 ± 38.8	180.4 ± 48.1	0.469
LDL (mg/dL) #	102.4 ± 33.2	100.0 ± 41.1	0.550
HDL (mg/dL) #	40.3 ± 14.0	41.7 ± 17.5	0.419
Triglycerides (mg/dL) #	182.5 ± 123.2	196.6 ± 157.7	0.340
Treatment Strategy			0.154
Medical Management	131 (30.8%)	27 (22.7%)	
PCI	277 (65.0%)	84 (70.6%)	
CABG	18 (4.2%)	8 (6.7%)	
Discharge Medications			
Beta-blocker (%)	352 (82.8%)	93 (78.2%)	0.243
Statin (%)	334 (78.4%)	98 (82.4%)	0.347
Aspirin (%)	396 (93.2%)	116 (97.5%)	0.078

ACS=acute coronary syndrome, BMI=body mass index, CABG=coronary artery bypass graft, DBP=diastolic blood pressure, HDL=high density lipoprotein, LBBB=left bundle branch block, LDL=low density lipoprotein, MI=myocardial infarction, PCI=percutaneous coronary intervention, SBP=systolic blood pressure

Data presented as mean ± standard deviation or count (proportion). Continuous variables were compared between groups by Student's t-test. Categorical variables were compared between groups by chi-squared test or Fisher's exact test.

* Measured at admission # Measured at discharge

Table 6.6: Study population characteristics by *CYP2J2 -50G>T* genotype in all subjects

Characteristic	G/G N=587	G/T+T/T N=94	P-Value
Age (years)	60.8 ± 12.6	58.7 ± 11.5	0.123
Female gender (%)	210 (35.8%)	40 (42.6%)	0.206
African-American race (%)	101 (17.2%)	23 (24.5%)	0.090
ACS Classification Type			0.585
ST elevation MI/LBBB	168 (28.6%)	25 (26.6%)	
Non ST elevation MI	185 (31.5%)	25 (26.6%)	
Unstable angina	234 (39.9%)	44 (46.8%)	
History/Risk Factors			
MI (%)	192 (32.7%)	31 (33.0%)	0.959
Hypertension (%)	387 (65.9%)	57 (60.6%)	0.317
Diabetes (%)	166 (28.3%)	22 (23.4%)	0.326
Hyperlipidemia (%)	358 (61.0%)	52 (55.3%)	0.297
Heart Failure (%)	48 (8.2%)	5 (5.3%)	0.337
Smoking Status			0.455
Current	211 (36.0%)	33 (35.1%)	
Former	208 (35.5%)	39 (41.5%)	
Never	167 (28.5%)	22 (23.4%)	
BMI (kg/m^2) *	29.7 ± 6.3	29.8 ± 6.9	0.960
SBP (mmHg) *	137.0 ± 26.9	136.4 ± 24.0	0.844
DBP (mmHg) *	74.2 ± 16.7	75.7 ± 14.9	0.393
Total cholesterol (mg/dL) #	178.2 ± 41.5	182.8 ± 45.4	0.360
LDL (mg/dL) #	102.2 ± 37.0	107.1 ± 37.5	0.288
HDL (mg/dL) #	41.5 ± 14.5	45.4 ± 20.5	0.037
Triglycerides (mg/dL) #	179.0 ± 126.9	171.5 ± 110.8	0.619
Treatment Strategy			0.853
Medical Management	216 (36.8%)	37 (39.4%)	
PCI	344 (58.6%)	54 (57.4%)	
CABG	27 (4.6%)	3 (3.2%)	
Discharge Medications			
Beta-blocker (%)	475 (81.1%)	73 (77.7%)	0.439
Statin (%)	436 (74.3%)	77 (81.9%)	0.111
Aspirin (%)	546 (93.2%)	89 (94.7%)	0.585

ACS=acute coronary syndrome, BMI=body mass index, CABG=coronary artery bypass graft, DBP=diastolic blood pressure, HDL=high density lipoprotein, LBBB=left bundle branch block, LDL=low density lipoprotein, MI=myocardial infarction, PCI=percutaneous coronary intervention, SBP=systolic blood pressure

Data presented as mean ± standard deviation or count (proportion). Continuous variables were compared between groups by Student's t-test. Categorical variables were compared between groups by chi-squared test or Fisher's exact test.

* Measured at admission # Measured at discharge

Table 6.7: Study population characteristics by *CYP2J2 -50G>T* genotype in Caucasians

Characteristic	G/G N=486	G/T+T/T N=71	P-Value
Age (years)	62.2 ± 12.6	60.3 ± 11.6	0.222
Female gender (%)	171 (35.2%)	25 (35.2%)	0.997
ACS Classification Type			0.209
ST elevation MI/LBBB	154 (31.7%)	19 (26.8%)	
Non ST elevation MI	161 (33.1%)	18 (25.4%)	
Unstable angina	171 (35.2%)	34 (47.9%)	
History/Risk Factors			
MI (%)	155 (31.9%)	24 (33.8%)	0.748
Hypertension (%)	308 (63.4%)	40 (56.3%)	0.253
Diabetes (%)	123 (25.3%)	12 (16.9%)	0.123
Hyperlipidemia (%)	309 (63.6%)	41 (57.7%)	0.342
Heart Failure (%)	28 (5.8%)	3 (4.2%)	0.785
Smoking Status			0.517
Current	159 (32.8%)	23 (32.4%)	
Former	182 (37.5%)	31 (43.7%)	
Never	144 (29.7%)	17 (23.9%)	
BMI (kg/m^2) *	29.6 ± 5.9	28.6 ± 5.9	0.167
SBP (mmHg) *	134.3 ± 25.0	136.2 ± 21.5	0.554
DBP (mmHg) *	72.1 ± 15.0	74.7 ± 14.3	0.170
Total cholesterol (mg/dL) #	176.8 ± 40.3	182.1 ± 45.3	0.338
LDL (mg/dL) #	101.0 ± 35.1	105.3 ± 35.2	0.388
HDL (mg/dL) #	40.0 ± 13.5	44.9 ± 21.7	0.017
Triglycerides (mg/dL) #	186.4 ± 132.9	182.6 ± 121.0	0.834
Treatment Strategy			0.765
Medical Management	138 (28.4%)	22 (31.0%)	
PCI	324 (66.7%)	47 (66.2%)	
CABG	24 (4.9%)	2 (2.8%)	
Discharge Medications			
Beta-blocker (%)	402 (82.7%)	54 (76.1%)	0.174
Statin (%)	381 (78.4%)	59 (83.1%)	0.363
Aspirin (%)	455 (93.6%)	70 (98.6%)	0.105

ACS=acute coronary syndrome, BMI=body mass index, CABG=coronary artery bypass graft, DBP=diastolic blood pressure, HDL=high density lipoprotein, LBBB=left bundle branch block, LDL=low density lipoprotein, MI=myocardial infarction, PCI=percutaneous coronary intervention, SBP=systolic blood pressure

Data presented as mean ± standard deviation or count (proportion). Continuous variables were compared between groups by Student's t-test. Categorical variables were compared between groups by chi-squared test or Fisher's exact test.

* Measured at admission # Measured at discharge

Table 6.8: Study population characteristics by *CYP4F2* genotype in all subjects

Characteristic	No Variants N=277	Met433 Only N=113	*-91C*±Met433 N=223	P-Value
Age (years)	60.2 ± 12.3	61.4 ± 12.7	61.1 ± 12.8	0.576
Female gender (%)	102 (36.8%)	50 (44.2%)	74 (33.2%)	0.139
African-American race (%)	45 (16.2%)	10 (8.8%)	54 (24.2%)	0.002
ACS Classification Type				0.820
ST elevation MI/LBBB	78 (28.2%)	32 (28.3%)	64 (28.7%)	
Non ST elevation MI	93 (33.6%)	35 (31.0%)	64 (28.7%)	
Unstable angina	106 (38.3%)	46 (40.7%)	95 (42.6%)	
History/Risk Factors				
MI (%)	98 (35.4%)	39 (34.5%)	65 (29.1%)	0.313
Hypertension (%)	179 (64.6%)	75 (66.4%)	145 (65.0%)	0.947
Diabetes (%)	83 (30.0%)	32 (28.3%)	52 (23.3%)	0.243
Hyperlipidemia (%)	170 (61.4%)	64 (56.6%)	132 (59.2%)	0.675
Heart Failure (%)	22 (7.9%)	8 (7.1%)	21 (9.4%)	0.729
Smoking Status				0.647
Current	103 (37.2%)	44 (38.9%)	73 (32.7%)	
Former	96 (34.7%)	41 (36.3%)	90 (40.4%)	
Never	78 (28.2%)	28 (24.8%)	60 (26.9%)	
BMI (kg/m^2) *	29.3 ± 6.0	30.4 ± 6.7	30.0 ± 6.9	0.252
SBP (mmHg) *	136.0 ± 24.6	138.1 ± 27.9	137.1 ± 26.5	0.748
DBP (mmHg) *	73.4 ± 16.0	73.1 ± 17.2	75.3 ± 15.5	0.340
Total cholesterol (mg/dL) #	178.8 ± 44.5	184.2 ± 44.1	176.7 ± 40.0	0.357
LDL (mg/dL) #	103.9 ± 40.2	104.8 ± 36.9	102.0 ± 35.4	0.814
HDL (mg/dL) #	41.2 ± 12.3	41.8 ± 18.1	43.3 ± 17.8	0.413
Triglycerides (mg/dL) #	174.7 ± 131.1	196.2 ± 117.1	166.5 ± 113.6	0.146
Treatment Strategy				0.908
Medical Management	100 (36.1%)	43 (38.1%)	84 (37.7%)	
PCI	162 (58.5%)	65 (57.5%)	132 (59.2%)	
CABG	15 (5.4%)	5 (4.4%)	7 (3.1%)	
Discharge Medications				
Beta-blocker (%)	226 (81.6%)	88 (77.9%)	181 (81.5%)	0.667
Statin (%)	220 (79.4%)	86 (76.1%)	159 (71.3%)	0.108
Aspirin (%)	267 (96.4%)	104 (92.0%)	203 (91.4%)	0.052

ACS=acute coronary syndrome, BMI=body mass index, CABG=coronary artery bypass graft, DBP=diastolic blood pressure, HDL=high density lipoprotein, LBBB=left bundle branch block, LDL=low density lipoprotein, MI=myocardial infarction, PCI=percutaneous coronary intervention, SBP=systolic blood pressure

Data presented as mean ± standard deviation or count (proportion). Continuous variables were compared between groups by Student's t-test. Categorical variables were compared between groups by chi-squared test or Fisher's exact test.

* Measured at admission # Measured at discharge

Table 6.9: Study population characteristics by *CYP4F2* genotype in Caucasians

Characteristic	No Variants N=232	Met433 Only N=103	*-91C*±Met433 N=169	P-Value
Age (years)	61.3 ± 12.4	62.5 ± 12.6	62.9 ± 12.9	0.397
Female gender (%)	82 (35.3%)	45 (43.7%)	50 (29.6%)	0.061
ACS Classification Type				0.484
ST elevation MI/LBBB	70 (30.2%)	29 (28.2%)	57 (33.7%)	
Non ST elevation MI	84 (36.2%)	32 (31.1%)	49 (29.0%)	
Unstable angina	78 (33.6%)	42 (40.8%)	63 (37.3%)	
History/Risk Factors				
MI (%)	83 (35.8%)	34 (33.0%)	46 (27.2%)	0.192
Hypertension (%)	146 (62.9%)	66 (64.1%)	103 (60.9%)	0.860
Diabetes (%)	62 (26.7%)	29 (28.2%)	30 (17.8%)	0.063
Hyperlipidemia (%)	142 (61.2%)	61 (59.2%)	110 (65.1%)	0.582
Heart Failure (%)	14 (6.0%)	8 (7.8%)	8 (4.7%)	0.589
Smoking Status				0.884
Current	78 (33.6%)	36 (35.0%)	51 (30.2%)	
Former	85 (36.6%)	39 (37.9%)	69 (40.8%)	
Never	69 (29.7%)	28 (27.2%)	49 (29.0%)	
BMI (kg/m^2) *	29.1 ± 5.8	30.1 ± 6.1	29.4 ± 6.2	0.400
SBP (mmHg) *	133.2 ± 23.2	136.5 ± 26.0	136.3 ± 25.4	0.342
DBP (mmHg) *	71.4 ± 14.6	71.9 ± 16.1	73.9 ± 14.3	0.237
Total cholesterol (mg/dL) #	176.4 ± 41.0	183.9 ± 45.3	176.0 ± 39.7	0.286
LDL (mg/dL) #	101.7 ± 35.5	103.7 ± 37.3	102.0 ± 35.0	0.916
HDL (mg/dL) #	40.1 ± 12.0	41.2 ± 18.3	41.4 ± 16.3	0.693
Triglycerides (mg/dL) #	182.0 ± 138.1	202.9 ± 118.3	172.3 ± 121.0	0.202
Treatment Strategy				0.202
Medical Management	68 (29.3%)	36 (35.0%)	42 (24.9%)	
PCI	151 (65.1%)	63 (61.2%)	121 (71.6%)	
CABG	13 (5.6%)	4 (3.9%)	6 (3.6%)	
Discharge Medications				
Beta-blocker (%)	193 (83.2%)	79 (76.7%)	140 (82.8%)	0.330
Statin (%)	188 (81.0%)	80 (77.7%)	133 (78.7%)	0.736
Aspirin (%)	225 (97.0%)	94 (91.3%)	159 (94.1%)	0.079

ACS=acute coronary syndrome, BMI=body mass index, CABG=coronary artery bypass graft, DBP=diastolic blood pressure, HDL=high density lipoprotein, LBBB=left bundle branch block, LDL=low density lipoprotein, MI=myocardial infarction, PCI=percutaneous coronary intervention, SBP=systolic blood pressure

Data presented as mean ± standard deviation or count (proportion). Continuous variables were compared between groups by Student's t-test. Categorical variables were compared between groups by chi-squared test or Fisher's exact test.

* Measured at admission # Measured at discharge

Figure Legends

Figure 6.1: Kaplan-Meier curves and mortality rates by *EPHX2* Lys55Arg genotype in (A) all subjects and (B) Caucasians only.

Figure 6.2: Kaplan-Meier curves and mortality rates by *CYP2J2 -50G>T* genotype in (A) all subjects and (B) Caucasians only.

Figure 6.3: Kaplan-Meier curves and mortality rates by *CYP4F2* genotype in (A) all subjects and (B) Caucasians only.

Figure 6.4: Kaplan-Meier curves and mortality rates by *EPHX2* Arg287Gln genotype in (A) all subjects and (B) Caucasians only.

Figure 6.5: Kaplan-Meier curves and mortality rates by *CYP2C8* Lys399Arg genotype in (A) all subjects and (B) Caucasians only.

Figure 6.1: Prognosis in ACS patients by *EPHX2* Lys55Arg genotype

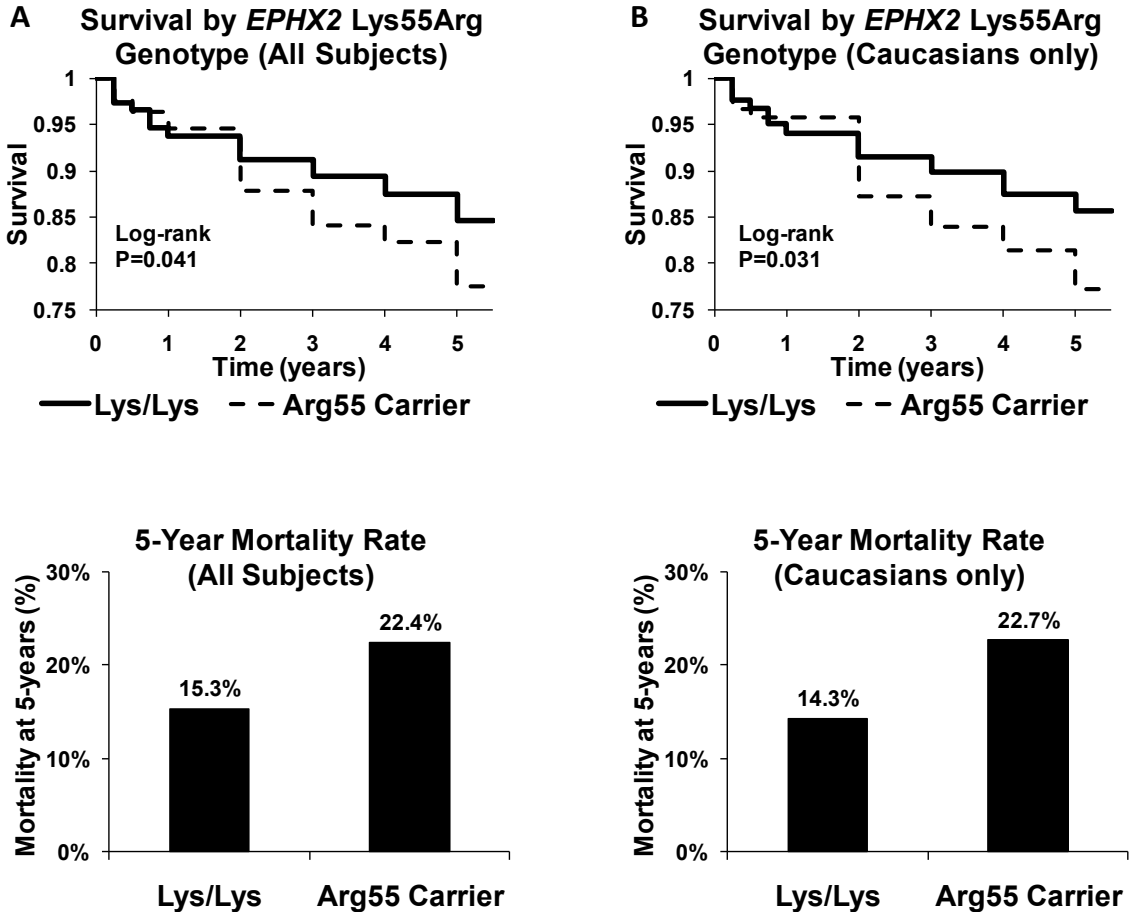

Figure 6.2: Prognosis in ACS patients by *CYP2J2 -50G>T* genotype

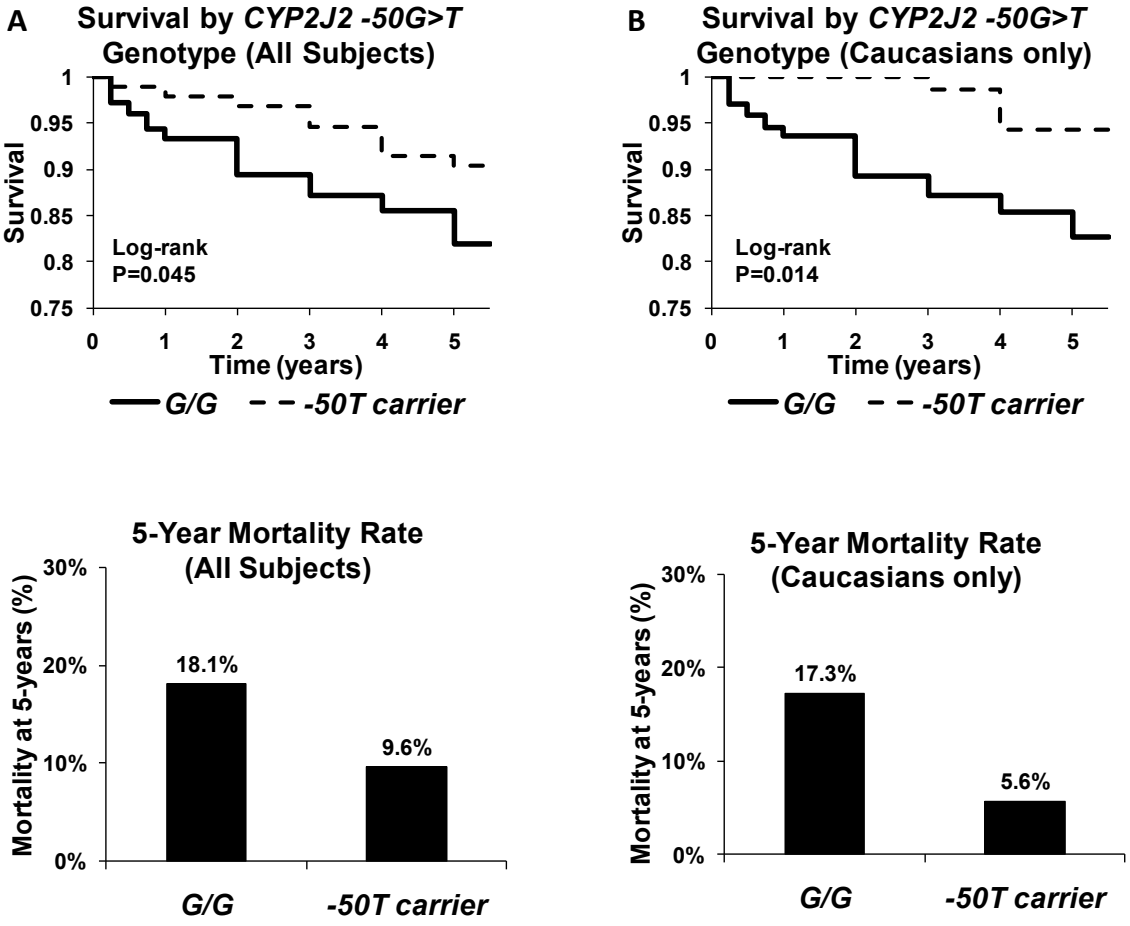

Figure 6.3: Prognosis in ACS patients by *CYP4F2* genotype

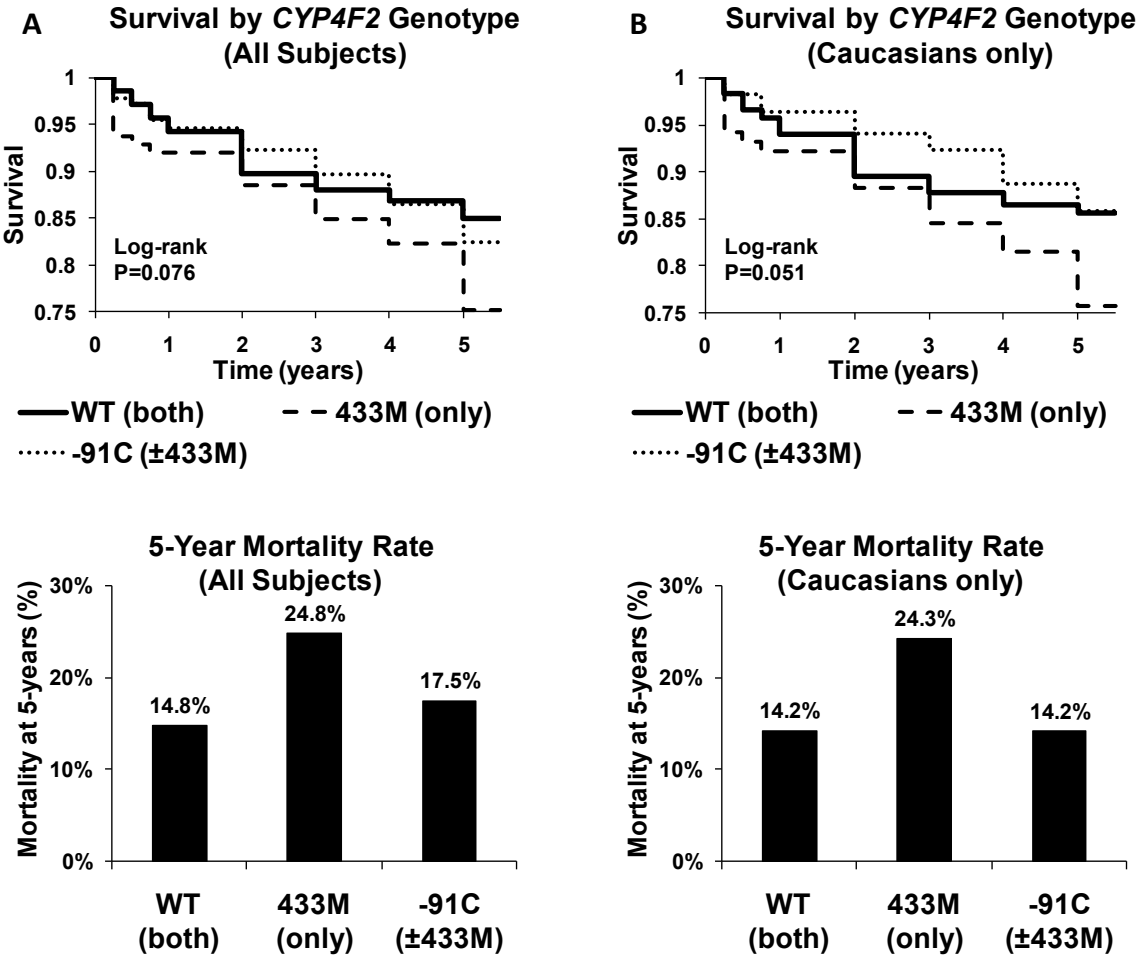

Figure 6.4: Prognosis in ACS patients by *EPHX2* Arg287Gln genotype

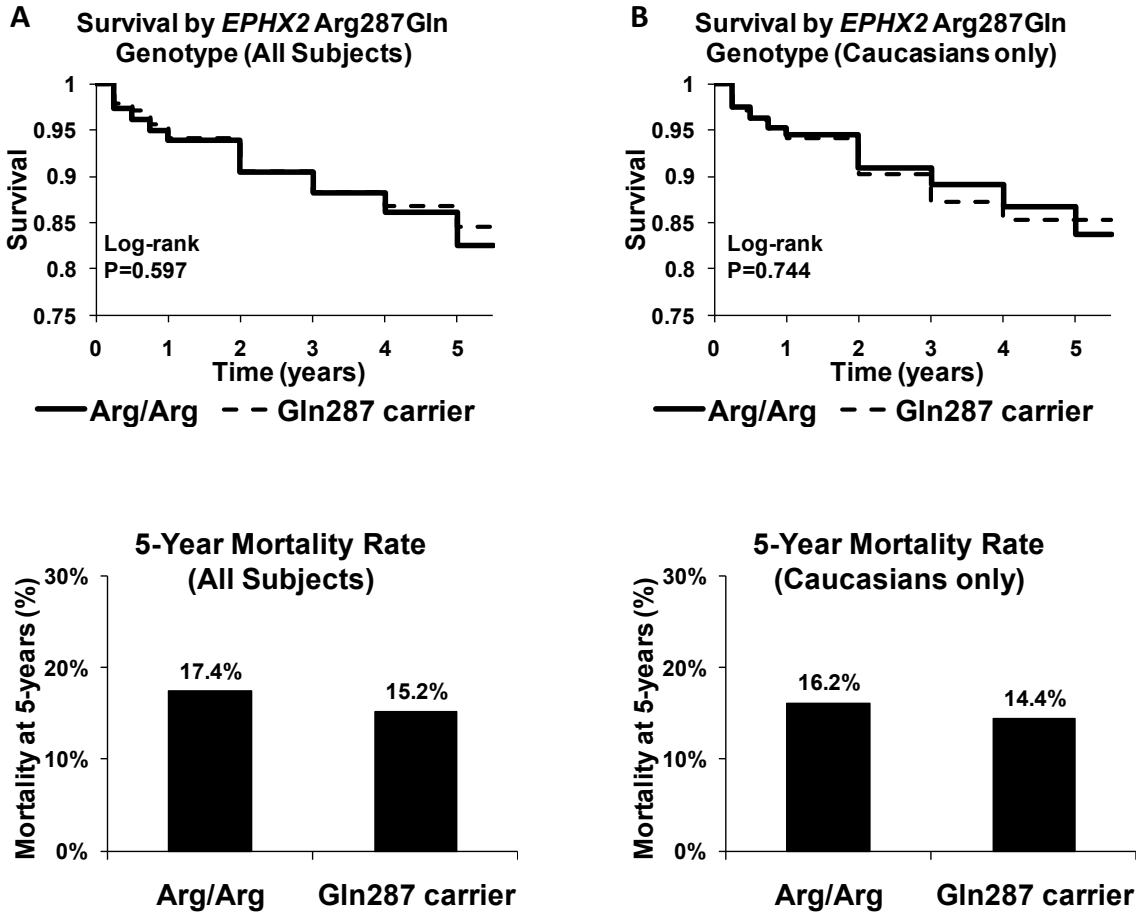

Figure 6.5: Prognosis in ACS patients by *CYP2C8* Lys399Arg genotype

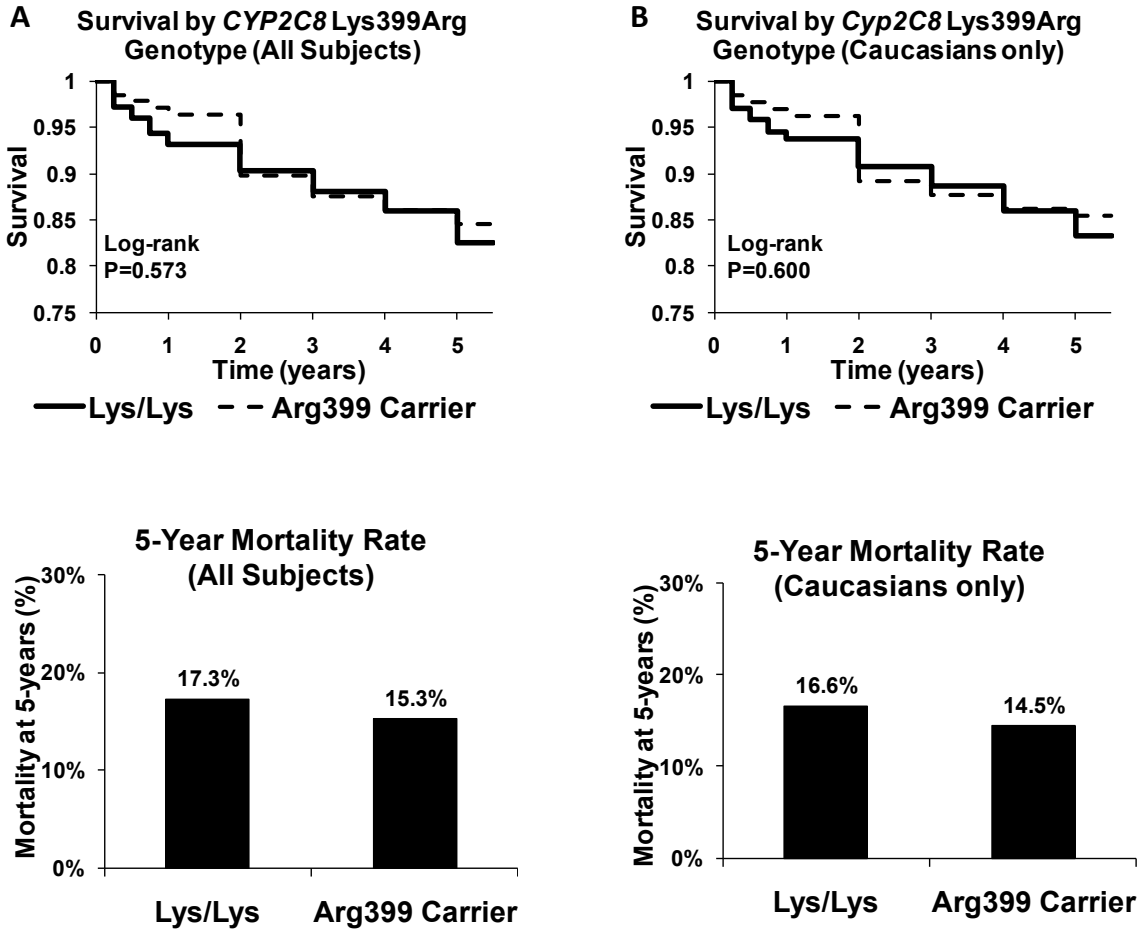

References

1. Roger VL, Go AS, Lloyd-Jones DM, Adams RJ, Berry JD, et al. (2011) Heart disease and stroke statistics--2011 update: a report from the American Heart Association. Circulation 123: e18-e209.

2. Libby P, Ridker PM, Maseri A (2002) Inflammation and atherosclerosis. Circulation 105: 1135-1143.

3. Libby P, Ridker PM (2004) Inflammation and atherosclerosis: role of C-reactive protein in risk assessment. Am J Med 116 Suppl 6A: 9S-16S.

4. Kavsak PA, Ko DT, Newman AM, Palomaki GE, Lustig V, et al. (2008) "Upstream markers" provide for early identification of patients at high risk for myocardial necrosis and adverse outcomes. Clin Chim Acta 387: 133-138.

5. de Lemos JA, Morrow DA, Sabatine MS, Murphy SA, Gibson CM, et al. (2003) Association between plasma levels of monocyte chemoattractant protein-1 and long-term clinical outcomes in patients with acute coronary syndromes. Circulation 107: 690-695.

6. Kavsak PA, Ko DT, Newman AM, Palomaki GE, Lustig V, et al. (2007) Risk stratification for heart failure and death in an acute coronary syndrome population using inflammatory cytokines and N-terminal pro-brain natriuretic peptide. Clin Chem 53: 2112-2118.

7. Ridker PM, Rifai N, Pfeffer M, Sacks F, Lepage S, et al. (2000) Elevation of tumor necrosis factor-alpha and increased risk of recurrent coronary events after myocardial infarction. Circulation 101: 2149-2153.

8. Zeldin DC (2001) Epoxygenase pathways of arachidonic acid metabolism. J Biol Chem 276: 36059-36062.

9. Roman RJ (2002) P-450 metabolites of arachidonic acid in the control of cardiovascular function. Physiol Rev 82: 131-185.

10. Seubert J, Yang B, Bradbury JA, Graves J, Degraff LM, et al. (2004) Enhanced postischemic functional recovery in CYP2J2 transgenic hearts involves mitochondrial ATP-sensitive K+ channels and p42/p44 MAPK pathway. Circ Res 95: 506-514.

11. Seubert JM, Sinal CJ, Graves J, DeGraff LM, Bradbury JA, et al. (2006) Role of soluble epoxide hydrolase in postischemic recovery of heart contractile function. Circ Res 99: 442-450.

12. Motoki A, Merkel MJ, Packwood WH, Cao Z, Liu L, et al. (2008) Soluble epoxide hydrolase inhibition and gene deletion are protective against myocardial ischemia-reperfusion injury in vivo. Am J Physiol Heart Circ Physiol 295: H2128-2134.

13. Nithipatikom K, Gross ER, Endsley MP, Moore JM, Isbell MA, et al. (2004) Inhibition of cytochrome P450omega-hydroxylase: a novel endogenous cardioprotective pathway. Circ Res 95: e65-71.

14. Gross ER, Nithipatikom K, Hsu AK, Peart JN, Falck JR, et al. (2004) Cytochrome P450 omega-hydroxylase inhibition reduces infarct size during reperfusion via the sarcolemmal KATP channel. J Mol Cell Cardiol 37: 1245-1249.

15. Lv X, Wan J, Yang J, Cheng H, Li Y, et al. (2008) Cytochrome P450 omega-hydroxylase inhibition reduces cardiomyocyte apoptosis via activation of ERK1/2 signaling in rat myocardial ischemia-reperfusion. Eur J Pharmacol 596: 118-126.

16. Yousif MH, Benter IF, Roman RJ (2009) Cytochrome P450 metabolites of arachidonic acid play a role in the enhanced cardiac dysfunction in diabetic rats following ischaemic reperfusion injury. Auton Autacoid Pharmacol 29: 33-41.

17. Liu H, Zhao Y, Nie D, Shi J, Fu L, et al. (2008) Association of a functional cytochrome P450 4F2 haplotype with urinary 20-HETE and hypertension. J Am Soc Nephrol 19: 714-721.

18. Fava C, Montagnana M, Almgren P, Rosberg L, Lippi G, et al. (2008) The V433M variant of the CYP4F2 is associated with ischemic stroke in male Swedes beyond its effect on blood pressure. Hypertension 52: 373-380.

19. Ward NC, Tsai IJ, Barden A, van Bockxmeer FM, Puddey IB, et al. (2008) A single nucleotide polymorphism in the CYP4F2 but not CYP4A11 gene is associated with increased 20-HETE excretion and blood pressure. Hypertension 51: 1393-1398.

20. Gainer JV, Bellamine A, Dawson EP, Womble KE, Grant SW, et al. (2005) Functional variant of CYP4A11 20-hydroxyeicosatetraenoic acid synthase is associated with essential hypertension. Circulation 111: 63-69.

21. Lee CR, North KE, Bray MS, Couper DJ, Heiss G, et al. (2007) CYP2J2 and CYP2C8 polymorphisms and coronary heart disease risk: the Atherosclerosis Risk in Communities (ARIC) study. Pharmacogenet Genomics 17: 349-358.

22. Lee CR, North KE, Bray MS, Fornage M, Seubert JM, et al. (2006) Genetic variation in soluble epoxide hydrolase (EPHX2) and risk of coronary heart disease: The Atherosclerosis Risk in Communities (ARIC) study. Hum Mol Genet 15: 1640-1649.

23. Liu PY, Li YH, Chao TH, Wu HL, Lin LJ, et al. (2006) Synergistic effect of cytochrome P450 epoxygenase CYP2J2*7 polymorphism with smoking on the onset of premature myocardial infarction. Atherosclerosis.

24. Spiecker M, Darius H, Hankeln T, Soufi M, Sattler AM, et al. (2004) Risk of coronary artery disease associated with polymorphism of the cytochrome P450 epoxygenase CYP2J2. Circulation 110: 2132-2136.

25. Cresci S, Jones PG, Sucharov CC, Marsh S, Lanfear DE, et al. (2008) Interaction between PPARA genotype and beta-blocker treatment influences clinical outcomes following acute coronary syndromes. Pharmacogenomics 9: 1403-1417.

26. Lanfear DE, Jones PG, Marsh S, Cresci S, McLeod HL, et al. (2005) Beta2-adrenergic receptor genotype and survival among patients receiving beta-blocker therapy after an acute coronary syndrome. Jama 294: 1526-1533.

27. Zineh I, Beitelshees AL, Welder GJ, Hou W, Chegini N, et al. (2008) Epithelial neutrophil-activating peptide (ENA-78), acute coronary syndrome prognosis, and modulatory effect of statins. PLoS ONE 3: e3117.

28. Braunwald E (1989) Unstable angina. A classification. Circulation 80: 410-414.

29. Marsh S, King CR, Garsa AA, McLeod HL (2005) Pyrosequencing of clinically relevant polymorphisms. Methods Mol Biol 311: 97-114.

30. Storey JD, Tibshirani R (2003) Statistical significance for genomewide studies. Proc Natl Acad Sci U S A 100: 9440-9445.

31. Deng Y, Theken KN, Lee CR (2010) Cytochrome P450 epoxygenases, soluble epoxide hydrolase, and the regulation of cardiovascular inflammation. J Mol Cell Cardiol 48: 331-341.

32. Chen D, Whitcomb R, Macintyre E, Tran V, Do ZN, et al. (2011) Pharmacokinetics and Pharmacodynamics of AR9281, an Inhibitor of Soluble Epoxide Hydrolase, in Single- and Multiple-Dose Studies in Healthy Human Subjects. J Clin Pharmacol.

33. Spiecker M, Zeldin DC, Mugge A, Tenderich G, Liao JK, et al. Reduced human myocardial mRNA expression of CYP2J2 in individuals with the G-50T promoter polymorphism; 2006 October 31, 2006; Chicago, USA. Circulation 691, II-117. pp. II-117.

34. King LM, Gainer JV, David GL, Dai D, Goldstein JA, et al. (2005) Single nucleotide polymorphisms in the CYP2J2 and CYP2C8 genes and the risk of hypertension. Pharmacogenet Genomics 15: 7-13.

35. Dai D, Zeldin DC, Blaisdell JA, Chanas B, Coulter SJ, et al. (2001) Polymorphisms in human CYP2C8 decrease metabolism of the anticancer drug paclitaxel and arachidonic acid. Pharmacogenetics 11: 597-607.

36. Lundblad MS, Stark K, Eliasson E, Oliw E, Rane A (2005) Biosynthesis of epoxyeicosatrienoic acids varies between polymorphic CYP2C enzymes. Biochem Biophys Res Commun 327: 1052-1057.

37. Koerner IP, Jacks R, DeBarber AE, Koop D, Mao P, et al. (2007) Polymorphisms in the human soluble epoxide hydrolase gene EPHX2 linked to neuronal survival after ischemic injury. J Neurosci 27: 4642-4649.

38. Przybyla-Zawislak BD, Srivastava PK, Vazquez-Matias J, Mohrenweiser HW, Maxwell JE, et al. (2003) Polymorphisms in human soluble epoxide hydrolase. Mol Pharmacol 64: 482-490.

39. Sandberg M, Hassett C, Adman ET, Meijer J, Omiecinski CJ (2000) Identification and functional characterization of human soluble epoxide hydrolase genetic polymorphisms. J Biol Chem 275: 28873-28881.

40. Stec DE, Roman RJ, Flasch A, Rieder MJ (2007) Functional polymorphism in human CYP4F2 decreases 20-HETE production. Physiol Genomics 30: 74-81.

Chapter VII: Discussion and Perspective

Vascular inflammation is integral to the pathophysiology of atherosclerotic cardiovascular disease, from the initiation of plaque formation to progression to acute coronary syndromes (ACS) [1]. Consequently, novel pharmacologic agents that specifically modulate vascular inflammation may offer therapeutic potential for the treatment of atherosclerosis. Accumulating evidence suggests that cytochrome P450 (CYP)-derived eicosanoids are involved in the regulation of inflammation. CYP epoxygenase-derived epoxyeicosatrienoic acids (EETs) possess potent anti-inflammatory properties by attenuating cytokine-induced leukocyte adhesion to the vascular wall via inhibition of nuclear factor-κB (NF-κB) activation [2]. Conversely, 20-hydroxyeicosatetraenoic acid (20-HETE), the product of ω-hydroxylation of arachidonic acid, induces expression of cellular adhesion molecules and cytokines via NF-κB activation, thereby promoting inflammation [3]. Because of the divergent effects of the CYP epoxygenase and ω-hydroxylase pathways in the regulation of inflammation, alterations in the functional balance between these parallel pathways may contribute to the pathogenesis and progression of inflammatory diseases, including atherosclerosis. The objectives of the work described in this doctoral dissertation were to characterize the effect of inflammation, metabolic dysfunction, and cardiovascular disease on the functional balance between the CYP epoxygenase and ω-hydroxylase pathways, and explore the potential of modulating CYP-mediated eicosanoid metabolism as an anti-inflammatory therapeutic strategy for the treatment of atherosclerotic cardiovascular disease.

It is well established that acute inflammatory stimuli alter hepatic CYP expression *in vitro* and *in vivo* [4,5,6], but the effect on CYP-mediated eicosanoid metabolism across tissues had not been rigorously evaluated. Therefore, we first sought to determine the effect of systemic administration of lipopolysaccharide (LPS), a well-characterized acute inflammatory stimulus, on CYP epoxygenase and ω-hydroxylase expression and metabolic activity in liver, kidney, lung, and heart [7] (Chapter II). Acute activation of the innate immune response altered CYP expression and metabolic activity in a tissue-, isoform-, and time-dependent manner. Moreover, the effect of LPS on the functional balance between the CYP epoxygenase and ω-hydroxylase pathways varied by tissue, highlighting the relative differences in CYP-mediated eicosanoid metabolism across tissues under inflammatory conditions.

These observations suggested that alteration of CYP-mediated eicosanoid metabolism is an important consequence of the acute inflammatory response *in vivo* and that modulating the pathways to increase EETs and decrease 20-HETE may have therapeutic potential, particularly in tissues where inflammatory stimuli tip the functional balance in favor of CYP ω-hydroxylase-mediated 20-HETE biosynthesis, such as liver. We have recently shown that potentiation of the CYP epoxygenase pathway, via enhancement of CYP epoxygenase-mediated EET formation or inhibition of soluble epoxide hydrolase (sEH)-mediated EET hydrolysis, attenuates acute vascular inflammation *in vivo* [8]. Therefore, we sought to determine whether inhibition of the CYP ω-hydroxylase pathway would have a similar anti-inflammatory effect following LPS administration, with the ultimate goal of investigating dual modulation of the pathways as a novel anti-inflammatory therapeutic strategy (Chapter III). In contrast to our hypothesis, inhibition of 20-HETE biosynthesis or the putative 20-HETE receptor did not attenuate LPS-induced inflammatory gene expression, regardless of the tissue evaluated, inhibitor dose, or treatment regimen, demonstrating that the CYP ω-

hydroxylase pathway does not contribute to the acute inflammatory response following LPS administration.

Although it is not a key regulator of LPS-induced acute inflammation *in vivo*, 20-HETE stimulates the production of reactive oxygen species by NADPH oxidase [9] and endothelial nitric oxide synthase uncoupling via NF-κB activation [10,11] in endothelial cells, suggesting that the CYP ω-hydroxylase pathway may be more relevant in the regulation of chronic vascular inflammation in the presence of cardiovascular disease. Consequently, inhibition of the CYP ω-hydroxylase pathway may be an effective anti-inflammatory strategy in models of vascular inflammation driven by overproduction of 20-HETE. For example, inhibition of the putative 20-HETE receptor lowered blood pressure, attenuated NF-κB activation, and improved endothelial function in a model of androgen-induced hypertension, which is mediated by elevated 20-HETE biosynthesis [12]. Thus, future studies investigating the therapeutic effect of inhibiting the CYP ω-hydroxylase pathway in other models of 20-HETE-dependent vascular inflammation are warranted.

Chronic exposure to LPS has been associated with cardiovascular disease risk in humans [13]; however, the doses of LPS used in Chapters II and III are supra-physiologic and stimulate an acute inflammatory response which more closely models septic shock, rather than the chronic inflammatory process that is observed in atherosclerosis. Consequently, we also sought to evaluate the functional balance between the CYP epoxygenase and ω-hydroxylase pathways in a model more relevant to cardiovascular disease, specifically high fat diet-induced metabolic syndrome (Chapter IV). High fat diet-induced metabolic dysfunction suppressed hepatic CYP epoxygenase metabolic activity and induced renal CYP ω-hydroxylase metabolic activity, thereby shifting the functional balance in favor of 20-HETE in both tissues. Of note, alterations in CYP-mediated eicosanoid metabolism were apparent after only two

weeks of high fat diet, suggesting that the shift in the functional balance toward the CYP ω-hydroxylase pathway contributes to the pathophysiologic consequences of long-term high fat diet feeding, such as insulin resistance, steatohepatitis, hypertension, and renal injury [14,15,16,17]. Thus, studies seeking to evaluate the therapeutic utility of modulating the CYP epoxygenase and ω-hydroxylase pathways to increase EETs or decrease 20-HETE are warranted.

Interestingly, enalapril reversed the high fat diet-induced alterations in hepatic CYP epoxygenase and renal CYP ω-hydroxylase metabolic activity and restored the functional balance between the pathways, suggesting that the renin-angiotensin system regulates CYP-mediated eicosanoid metabolism in the presence of metabolic syndrome. Although we did not directly demonstrate that angiotensin II suppresses hepatic CYP epoxygenase metabolic activity and induces renal CYP ω-hydroxylase metabolic activity, our findings, taken together with prior observations that angiotensin II regulates CYP-mediated eicosanoid metabolism [18,19,20], strongly implicate angiotensin II in mediating the observed high fat diet-induced alterations in CYP-mediated eicosanoid metabolism. A recent study has demonstrated that 20-HETE stimulates expression of ACE and the angiotensin II receptor [21], suggesting that 20-HETE may promote chronic vascular inflammation via renin-angiotensin system activation. Further investigation of the interplay between the renin-angiotensin system and CYP-mediated eicosanoid metabolism is warranted.

The studies described in Chapters II and IV demonstrate that systemic inflammation and high fat diet-induced metabolic syndrome alter CYP-mediated eicosanoid metabolism in mice. However, few studies have directly measured CYP-derived eicosanoids in humans, and the clinical factors that are associated with CYP epoxygenase, sEH, and CYP ω-hydroxylase function in patients with established coronary artery disease (CAD) have not been described. Therefore, we quantified

plasma levels of EETs, DHETs, and 20-HETE in a well-treated cohort of CAD patients and healthy individuals without risk factors for cardiovascular disease (Chapter V). Compared to healthy volunteers, CAD patients exhibited higher plasma EETs, lower plasma DHETs, and higher epoxide:diol ratios, indicative of lower sEH activity. Further studies are needed to elucidate the mechanism underlying the observed suppression of sEH activity in CAD patients.

Understanding the clinical factors that influence CYP-mediated eicosanoid metabolism may help identify subsets of the population that would derive the greatest benefit from therapies that modulate these pathways. Although we identified several covariates that were associated with CYP epoxygenase and ω-hydroxylase pathway function in CAD patients, our analysis was not comprehensive. For example, we were unable to evaluate the effects of aspirin, statins, and beta-blockers on CYP-mediated eicosanoid metabolism due to the high use of these medications in CAD patients. Moreover, many of the clinical characteristics in CAD patients, such as serum lipid levels and blood pressure values, were influenced by drug therapy. Future studies designed to characterize the effects of these clinical factors on CYP epoxygenase and ω-hydroxylase pathway function remain necessary.

Although preclinical studies suggest that potentiation of CYP epoxygenase-derived EETs and inhibition of CYP ω-hydroxylase-derived 20-HETE may attenuate vascular inflammation and improve outcomes in CAD patients, investigation of this therapeutic strategy in humans has been limited by the lack of approved pharmacologic agents that specifically modulate CYP-mediated eicosanoid metabolism. Therefore, we evaluated the association between functional genetic variants in the CYP epoxygenases (*CYP2J2*, *CYP2C8*), sEH (*EPHX2*), and the CYP ω-hydroxylases (*CYP4A11*, *CYP4F2*) and survival in ACS patients in order to explore the effect of alterations in CYP-mediated eicosanoid metabolism on outcomes in patients with established CAD (Chapter VI).

Consistent with our hypothesis, the *EPHX2* Arg55 and *CYP4F2* Met433 polymorphisms were associated with higher mortality in ACS patients. In contrast, the *CYP2J2 -50T* variant allele was associated with lower mortality. Additional studies are necessary to validate these relationships, as well as characterize the mechanism(s) underlying the observed associations. Our results suggest that alterations in CYP-mediated eicosanoid metabolism influence prognosis in patients with established CAD, and support the development of drugs which specifically target the CYP epoxygenase and ω-hydroxylase pathways as a treatment strategy for atherosclerosis.

References

1. Libby P, Ridker PM, Maseri A (2002) Inflammation and atherosclerosis. Circulation 105: 1135-1143.

2. Node K, Huo Y, Ruan X, Yang B, Spiecker M, et al. (1999) Anti-inflammatory properties of cytochrome P450 epoxygenase-derived eicosanoids. Science 285: 1276-1279.

3. Ishizuka T, Cheng J, Singh H, Vitto MD, Manthati VL, et al. (2008) 20-Hydroxyeicosatetraenoic acid stimulates nuclear factor-kappaB activation and the production of inflammatory cytokines in human endothelial cells. J Pharmacol Exp Ther 324: 103-110.

4. Morgan ET (2001) Regulation of cytochrome p450 by inflammatory mediators: why and how? Drug Metab Dispos 29: 207-212.

5. Riddick DS, Lee C, Bhathena A, Timsit YE, Cheng PY, et al. (2004) Transcriptional suppression of cytochrome P450 genes by endogenous and exogenous chemicals. Drug Metab Dispos 32: 367-375.

6. Morgan ET, Li-Masters T, Cheng PY (2002) Mechanisms of cytochrome P450 regulation by inflammatory mediators. Toxicology 181-182: 207-210.

7. Theken KN, Deng Y, Kannon MA, Miller TM, Poloyac SM, et al. (2011) Activation of the acute inflammatory response alters cytochrome P450 expression and eicosanoid metabolism. Drug Metab Dispos 39: 22-29.

8. Deng Y, Edin ML, Theken KN, Schuck RN, Flake GP, et al. (2011) Endothelial CYP epoxygenase overexpression and soluble epoxide hydrolase disruption attenuate acute vascular inflammatory responses in mice. FASEB J 25: 703-713.

9. Medhora M, Chen Y, Gruenloh S, Harland D, Bodiga S, et al. (2008) 20-HETE increases superoxide production and activates NAPDH oxidase in pulmonary artery endothelial cells. Am J Physiol Lung Cell Mol Physiol 294: L902-911.

10. Cheng J, Ou JS, Singh H, Falck JR, Narsimhaswamy D, et al. (2008) 20-hydroxyeicosatetraenoic acid causes endothelial dysfunction via eNOS uncoupling. Am J Physiol Heart Circ Physiol 294: H1018-1026.

11. Cheng J, Wu CC, Gotlinger KH, Zhang F, Falck JR, et al. (2010) 20-hydroxy-5,8,11,14-eicosatetraenoic acid mediates endothelial dysfunction via IkappaB kinase-dependent endothelial nitric-oxide synthase uncoupling. J Pharmacol Exp Ther 332: 57-65.

12. Wu CC, Cheng J, Zhang FF, Gotlinger KH, Kelkar M, et al. (2011) Androgen-dependent hypertension is mediated by 20-hydroxy-5,8,11,14-eicosatetraenoic acid-induced vascular dysfunction: role of inhibitor of kappaB Kinase. Hypertension 57: 788-794.

13. Stoll LL, Denning GM, Weintraub NL (2004) Potential role of endotoxin as a proinflammatory mediator of atherosclerosis. Arterioscler Thromb Vasc Biol 24: 2227-2236.

14. Buettner R, Scholmerich J, Bollheimer LC (2007) High-fat diets: modeling the metabolic disorders of human obesity in rodents. Obesity (Silver Spring) 15: 798-808.

15. Gomez-Lechon MJ, Jover R, Donato MT (2009) Cytochrome p450 and steatosis. Curr Drug Metab 10: 692-699.

16. Dobrian AD, Davies MJ, Prewitt RL, Lauterio TJ (2000) Development of hypertension in a rat model of diet-induced obesity. Hypertension 35: 1009-1015.

17. Zhou Y, Lin S, Chang HH, Du J, Dong Z, et al. (2005) Gender differences of renal CYP-derived eicosanoid synthesis in rats fed a high-fat diet. Am J Hypertens 18: 530-537.

18. Carroll MA, Balazy M, Margiotta P, Huang DD, Falck JR, et al. (1996) Cytochrome P-450-dependent HETEs: profile of biological activity and stimulation by vasoactive peptides. Am J Physiol 271: R863-869.

19. Croft KD, McGiff JC, Sanchez-Mendoza A, Carroll MA (2000) Angiotensin II releases 20-HETE from rat renal microvessels. Am J Physiol Renal Physiol 279: F544-551.

20. Kaergel E, Muller DN, Honeck H, Theuer J, Shagdarsuren E, et al. (2002) P450-dependent arachidonic acid metabolism and angiotensin II-induced renal damage. Hypertension 40: 273-279.

21. Sodhi K, Wu CC, Cheng J, Gotlinger K, Inoue K, et al. (2010) CYP4A2-induced hypertension is 20-hydroxyeicosatetraenoic acid- and angiotensin II-dependent. Hypertension 56: 871-878.